Chemoselective bioconjugation reactions of tyrosine residues for application in PET radiochemistry

by

Samantha Leier

A thesis submitted in partial fulfillment of the requirements for the degree of

Master of Science

in

Cancer Sciences

Department of Oncology
University of Alberta

ABSTRACT

Achieving chemoselectivity while maintaining bioorthogonality are among some of the major challenges in bioconjugation chemistry. Bioconjugation chemistry has important applications in PET radiochemistry. While modern bioconjugation techniques rely predominantly on lysine and cysteine residues as targets for bioconjugation, other bioconjugation techniques that selectively target other amino acids would contribute greatly to the development of new PET radiotracers. Although only modestly prevalent and often buried within the protein structure, tyrosine represents an attractive target for bioconjugation. Tyrosine residues can be selectively targeted by both luminol derivatives and aryl diazonium salts. Luminol derivatives react via an ene-like reaction where as diazonium compounds react via electrophilic aromatic substitution to produce a stable conjugate. Recently, luminol derivatives have been reported for the introduction of fluorescent probes into proteins and diazonium salts have been reported for the introduction of radiometals into tyrosinamide-containing polymers. To the best of our knowledge, neither technique has been applied to PET radiotracer synthesis. Therefore, the aim of this project is the chemoselective introduction of radionuclides onto tyrosine residues under mild conditions. Specifically, we describe the preparation of ^{18}F-labeled luminol derivatives as well as ^{64}Cu- and ^{68}Ga-labeled diazonium salts as novel building blocks for subsequent coupling with tyrosine residues under mild conditions. Luminol derivative *N*-(4-[^{18}F]fluorobenzyl)-2-methyl-1,4-dioxo-1,2,3,4-tetrahydro-phthalazine-6-carboxamide (**29**) was synthesized in 48% radiochemical yield. The use of H_2O_2 in the presence of hemin as an oxidizing agent resulted in improved oxidation when compared with 1,3-dibromo-5,5-dimethylhydantoin, *N*-bromosuccinimide, 1,3,4,6-tetrachloro-3α,6α-diphenyl-glucoluril coated iodination tubes and *N*-chloro-benzenesulfonamide coated iodination beads. Tyrosine-click chemistry of compound **29** with acetyl-L-tyrosine methyl amide afforded the expected conjugate in 27% radiochemical yield. As well, ^{68}Ga- and ^{64}Cu-labeled NOTA-diazonium salts were synthesized from 20 µg of macrocyclic chelator 2-S-(4-aminobenzyl)-1,4,7-triazacyclononane-1,4,7-triacetic acid (*p*-NH_2-Bn-NOTA). ^{68}Ga- and ^{64}Cu-labeled NOTA complexes were prepared in high radiochemical yields >80% and *in situ* conversion of ^{68}Ga- and ^{64}Cu-labeled *p*-NH_2-Bn-NOTA complexes into corresponding diazonium salts was carried out with $NaNO_2$ under acidic conditions. Azo coupling with L-tyrosine, neurotensin NT(8-13), human serum albumin (HSA) and tobacco mosaic virus (TMV) afforded the expected conjugates in radiochemical yields upwards of 80%, 45%, 20% and 9%, respectively. Coupling

reactions proceeded under mild, aqueous conditions within 60 min. The described luminol-based tyrosine-click chemistry technique and azo coupling technique provide innovative bioconjugation strategies for the chemoselective introduction of various radionuclides onto tyrosine residues under mild and aqueous reaction conditions. The applied mild reaction conditions make these novel bioconjugation strategies also compatible with delicate tyrosine-based biomolecules such as proteins and may be expanded to antibodies.

PREFACE

This thesis describes original work by Samantha Leier. Radiosynthesis and purification of ^{64}Cu-labeled tobacco mosaic virus (TMV) described in sections **2.3** and **3.3** was carried out with the help of Dr. Susan Richter. IC_{50} determination described in sections **2.4** and **3.3** was performed by Dr. Ralf Bergmann at Helmholtz-Zentrum Dresden-Rossendorf. PET studies described in sections **2.6** and **3.3** were performed by Dr. Melinda Wuest and were in compliance with the Canadian Council of Animal Care (Cross Cancer Institute, University of Alberta, Protocol number: AC13203).

ACKNOWLEDGMENTS

First and foremost, I would like to thank my supervisor Dr. Frank Wuest for his encouragement, guidance and support throughout my Master's research. I would also like to thank my committee members, Dr. Ralf Schirrmacher and Dr. Carlos Velazquez, for their continued support.

I would like to extend a special thank you to Dr. Atul Bhardwaj and Dr. Jatinder Kaur for their mentorship and unconditional support. Thank you to Dr. Melinda Wuest for performing the PET studies, Dr. Ralf Bergmann at Helmholtz-Zentrum Dresden-Rossendorf for performing the IC_{50} determination and Dr. Susan Richter for her expertise and help with the radiosynthesis and purification of ^{64}Cu-labeled TMV. Last but not least, thank you to the entire Wuest lab group for providing insight and support over the course of my time as a graduate student.

TABLE OF CONTENTS

LIST OF TABLES

LIST OF FIGURES

LIST OF SCHEMES

LIST OF ABBREVIATIONS

ºC – Degrees celsius

µg – Microgram

µL – Microliter

[^{18}F]F-PTAD) – [^{18}F]4-(4-Fluorophenyl)-1,2,4-triazole-3,5-dione

[^{18}F]FS-PTAD – 4-(*p*-[^{18}F]Fluorosulfonyl)phenyl)-1,2,4-triazoline-3,5-dione

[^{18}F]F-Py-TFP – [^{18}F]2,3,5,6-Tetrafluorophenyl 6-fluoronicotinate

[^{18}F]SFB – *N*-Succinimidyl 4-[^{18}F]fluorobenzoate

^{18}F – Fluorine-18

^{64}Cu – Copper-64

^{68}Ga – Gallium-68

Boc – *tert*-Butyloxycarbonyl

BSA – Bovine serum albumin

DCM – Dichloromethane

DIPEA – *N,N*-Diisopropylethylamine

DMAP – 4-Dimethylaminopyridine

DMF – Dimethylformamide

DMSO – Dimethyl sulfoxide

DOTA – 1,4,7,10-Tetraazacyclododecane-1,4,7,10tetraaceticacid

DTPA – Diethylenetriaminopentaaceticacid

EDCI – 1-Ethyl-3-(3-dimethylaminopropyl)carbodiimide

EDTA – Ethylenediaminetetraacetic acid

HPLC – High performance liquid chromatography

HSA – Human serum albumin

kDa – Kilodalton

MBq – Megabecquerels

MS – Mass spectrometry

NBS – *N*-Bromosuccinimide

NMR – Nuclear magnetic resonance

NOTA – 1,4,7-Triazacyclononane-1,4,7-triaceticacid

PBS – Phosphate buffered saline

PET – Positron emission tomography

p-NH_2-Bn-DTPA – 2-S-(4-Aminobenzyl)-diethylenetriamine pentaacetic acid

p-NH_2-Bn-NOTA – 2-S-(4-Aminobenzyl)-1,4,7-triazacyclononane-1,4,7-triacetic acid

PTAD – 4-Phenyl-1,2,4-triazole-3,5-dione

radio-HPLC – High performance liquid radiochromatography

radio-TLC – Thin layer radiochromatography

R_f – Retention factor

RSA – Rat serum albumin

SDS-PAGE – Sodium dodecyl sulfate polyacrylamide gel electrophoresis

SEC – Size exclusion chromatography

SUV – Standardized uptake value

TEA – Triethylamine

THF – Tetrahydrofuran

TLC – Thin layer chromatography

TMV – Tobacco mosaic virus

1.0 INTRODUCTION

1.1 A Brief History of Nuclear Medicine

Early nuclear medicine was significantly influenced by radioiodine chemistry. Some of the first applications included the use of various radioisotopes of iodine for thyroid cancer imaging and therapy. Following its discovery in 1938, ^{131}I was used for both therapy and diagnostic imaging as it has a half-life of 8 days and decays primarily by beta emission but also produces an easily detectable gamma ray with an energy of 367 keV [1-3]. Initially produced by deuteron bombardment of a tellurium target in a cyclotron, the first application in humans included the assessment of iodine uptake and metabolism by the thyroid of patients with thyroid dysfunction [4, 5]. Tumour uptake was first demonstrated shortly thereafter in patients with metastatic thyroid cancer [6]. Other radioisotopes of iodine were later used for imaging, particularly ^{123}I due to its shorter half-life of 13.2 hours and more favourable mode of decay. Rather than decaying by beta emission, ^{123}I decays by electron capture and produces a gamma ray with an energy of 159 keV [7]. Later, ^{125}I was used for brachytherapy due to its longer half-life of 59.5 days in combination with its low energy gamma ray with an energy of 28.5 keV [8, 9].

As the application of radioactivity in medical imaging expanded, the role of bioconjugation chemistry became more prominent. Proteins were labeled with ^{131}I via radioiodination techniques targeting tyrosine residues (Figure 1.1). As early as 1944, ^{131}I-labeled bovine serum albumin (BSA) was used to image the movement of serum proteins in traumatic shock [10]. By 1950, ^{131}I-labeled human serum albumin (HSA) was used for blood pool imaging in humans [11, 12]. In 1959, radioimmunoassay was developed [13]. This *in vitro* assay was initially used to determine the concentration of serum antigens based on the ratio of free and bound radiolabeled antigens to their corresponding antibodies in the presence of competing serum antigens and often used ^{125}I-labeled proteins labeled via tyrosine [14].

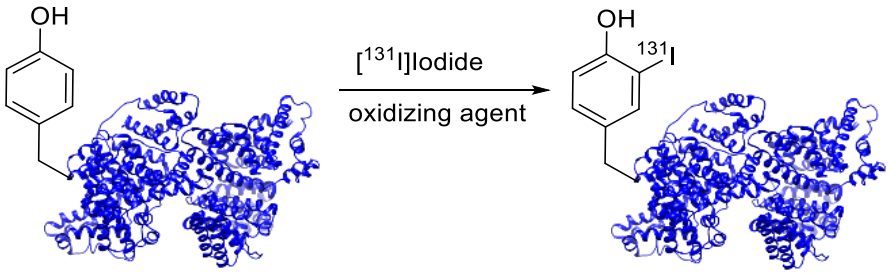

Figure 1.1. Radioiodination of tyrosine-containing proteins.

Today, bioconjugation techniques targeting other amino acids such as lysine and cysteine are employed to incorporate other radionuclides, such as ^{18}F, ^{68}Ga, ^{64}Cu and many others. Though ^{18}F is a positron emitter with an ideal half-life of 109.8 minutes, direct fluorination requires harsh conditions that are incompatible with delicate biomolecules such as proteins. This is overcome by the use of prosthetic groups, which are fluorinated prior to bioconjugation with proteins [15]. One of the most popular examples is *N*-succinimidyl 4-[^{18}F]fluorobenzoate ([^{18}F]SFB), which can be synthesised from trimethylammonium precursors, which exploit the nucleophilic nature of [^{18}F]fluoride (Figure 1.2) [16]. Such bifunctional labeling agents undergo bioconjugation reactions with the α- or ε-amino groups of peptides or proteins. These bifunctional labeling agents are not just limited to ^{18}F chemistry and can also be functionalized with chelators to include radiometals. Bifunctional chelating agents commonly include active esters, isothiocyanates and maleimides for bioconjugation with amino or thiol groups in peptides and proteins [17]. Macrocyclic chelators such as 1,4,7,10-tetraazacyclododecane-1,4,7,10tetraaceticacid (DOTA) and 1,4,7-triazacyclononane-1,4,7-triaceticacid (NOTA) have largely replaced acyclic chelators like diethylenetriaminopentaaceticacid (DTPA) and ethylenediaminotetraaceticacid (EDTA) due to their improved coordination chemistry with a variety of metals to form stable chelates (Figure 1.3) [18].

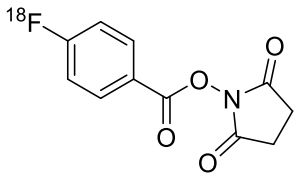

Figure 1.2. Bifunctional labeling agent [^{18}F]SFB.

Figure 1.3. Macrocyclic chelators, DOTA and NOTA.

1.2 Bioconjugation of Tyrosine Residues

Tyrosine is an attractive alternative target for the chemoselective incorporation of radionuclides into peptides and proteins. Bioconjugation techniques targeting tyrosine include azo coupling, tyrosine-click chemistry, mannich-type reactions, Pd-mediated cross coupling and oxidative coupling (Figure 1.4) [19, 20]. Some of these techniques have already been applied to radiochemistry.

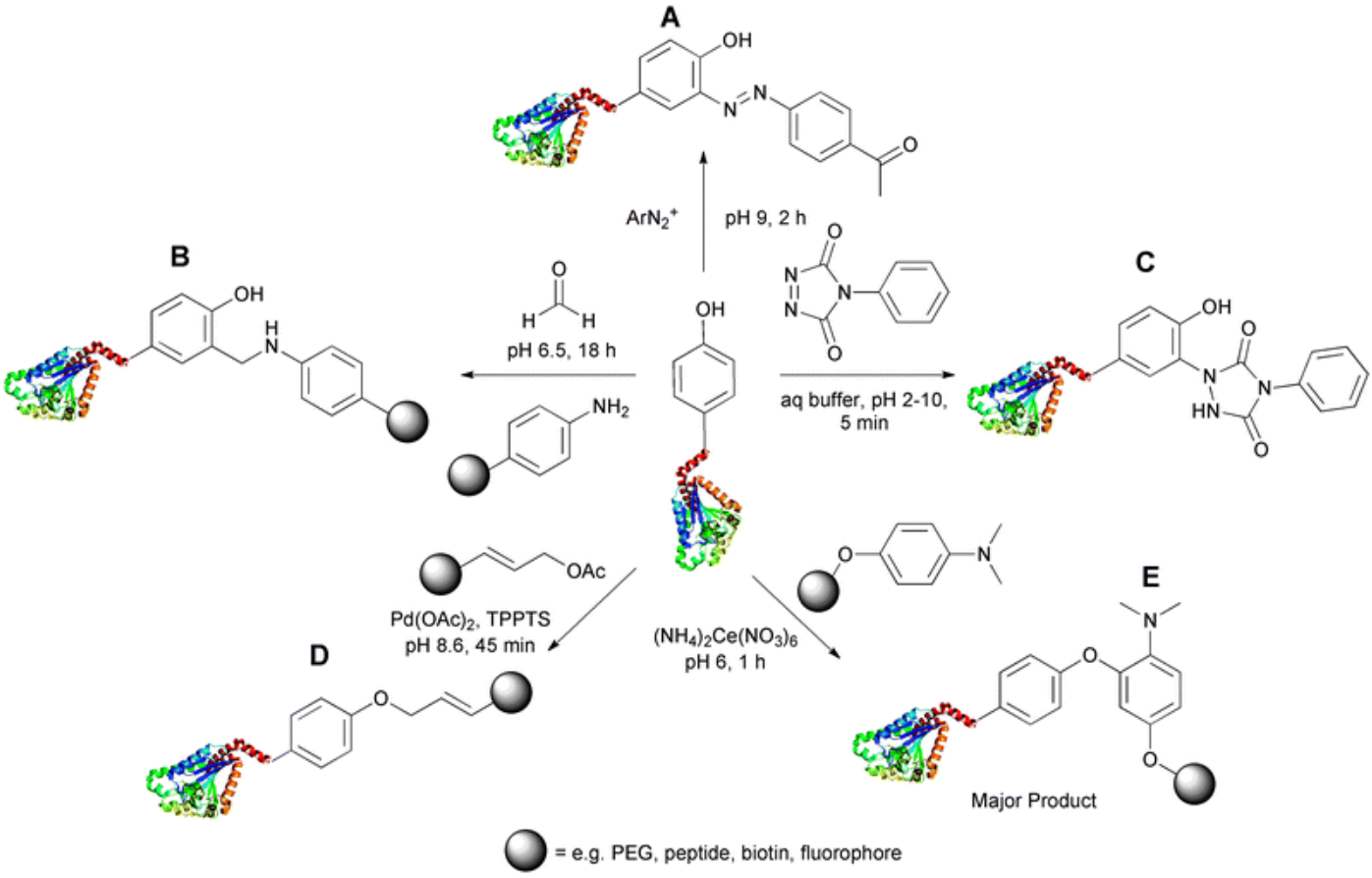

Figure 1.4. Bioconjugation techniques targeting tyrosine. A) Azo coupling. B) Mannich-type reactions. C) Tyrosine-click chemistry. D) Pd-mediated cross-coupling. E) Oxidative coupling [20].

The application of azo coupling in radiochemistry was initially explored for bioconjugation of acyclic chelators like ethylenediaminetetraacetic acid (EDTA) with proteins for post-labeling with radiometals such as ^{111}In for *in vivo* scintillation studies [21]. Azo coupling is a bioconjugation strategy that utilizes diazonium compounds, which react via electrophilic aromatic substitution to produce a diazo conjugate (Figure 1.5). More recently, azo coupling has been applied to radiochemistry for the incorporation of ^{111}In and ^{125}I into tyrosinamide-containing polymers, for future pharmacokinetic studies [22]. Incorporation of ^{111}In was carried out using a post-labeling approach in which bifunctional chelator 2-S-(4-Aminobenzyl)-diethylenetriamine

pentaacetic acid (*p*-NH_2-Bn-DTPA) was diazotized and coupled with tyrosinamide-containing polymers prior to ^{111}In-labeling (Figure 1.6).

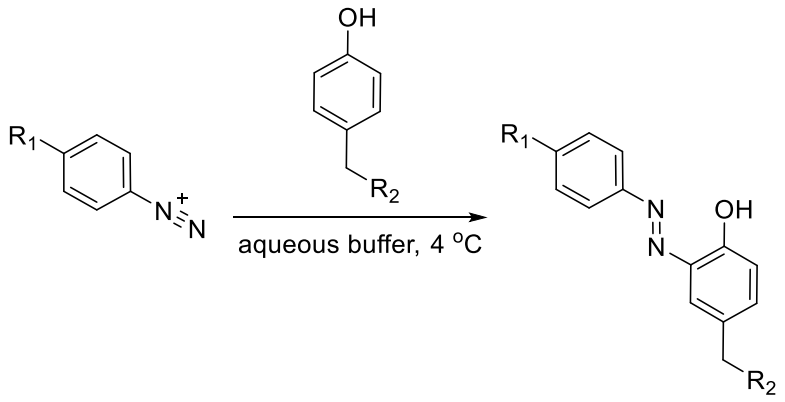

Figure 1.5. Azo coupling with aryl diazonium salts.

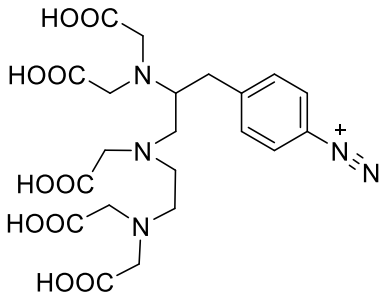

Figure 1.6. Diazotized bifunctional chelator *p*-NH_2-Bn-DTPA for azo coupling and post-labeling with ^{111}In.

Tyrosine-click chemistry has also been applied to radiochemistry through the synthesis of 'clickable' prosthetic groups for ^{18}F. Tyrosine-click chemistry is an emerging strategy in which cyclic diazodicarboxamide derivatives react via an ene-like reaction to produce a heteroatom bond (Figure 1.7) [23, 24]. PTAD-derived prosthetic group [^{18}F]4-(4-fluorophenyl)-1,2,4-triazole-3,5-dione ([^{18}F]F-PTAD) was synthesized and clicked with tyrosine derivative acetyl-L-tyrosine methyl amide [25]. Similarly, prosthetic group 4-(*p*-[^{18}F]fluorosulfonyl)phenyl)-1,2,4-triazoline-3,5-dione ([^{18}F]FS-PTAD) was synthesized and clicked with L-tyrosine (Figure 1.8) [26].

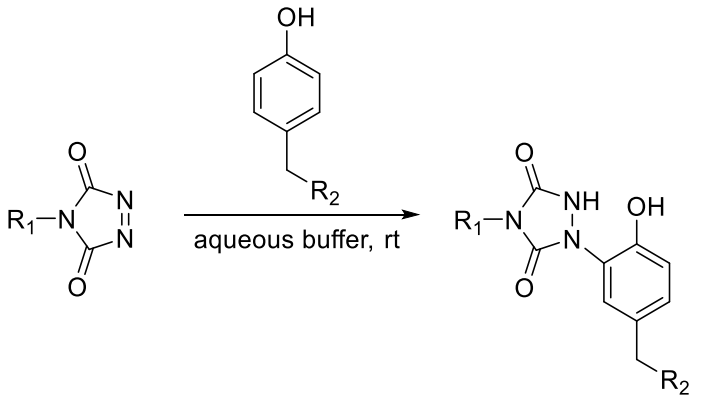

Figure 1.7. Tyrosine-click with cyclic diazodicarboxamides, according to an ene-like reaction.

Figure 1.8. 'Clickable' prosthetic groups for tyrosine-click with ^{18}F: [^{18}F]F-PTAD and [^{18}F]FS-PTAD.

Chemiluminescent compound 3-aminophthalhydrazide, commonly known as luminol, emits blue light with a wavelength of 425 nm after oxidation (Figure 1. 9) [27]. Specifically, luminescence occurs when degradation of the oxidized intermediate results in an excited phthalate, which transitions to ground state emitting a photon [28]. Recently, luminol derivatives have been reported as a more stable alternative to traditional cyclic diazodicarboxamide derivatives, as they do not produce the electrophilic isocyanate degradation product following oxidation (Figure 1.10 and Figure 1.11) [29]. To the best of our knowledge, this modified tyrosine-click strategy has not yet been applied to radiochemistry.

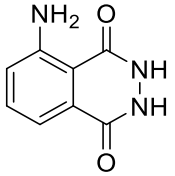

Figure 1. 9. Structure of chemiluminescent compound, luminol.

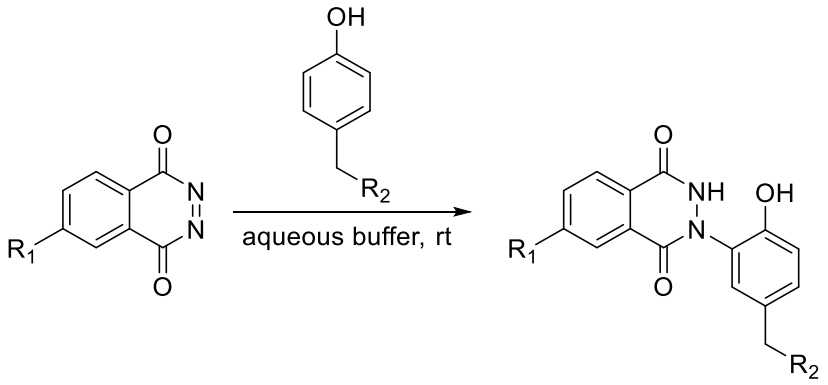

Figure 1.10. Tyrosine-click with luminol derivatives, according to an ene-like reaction.

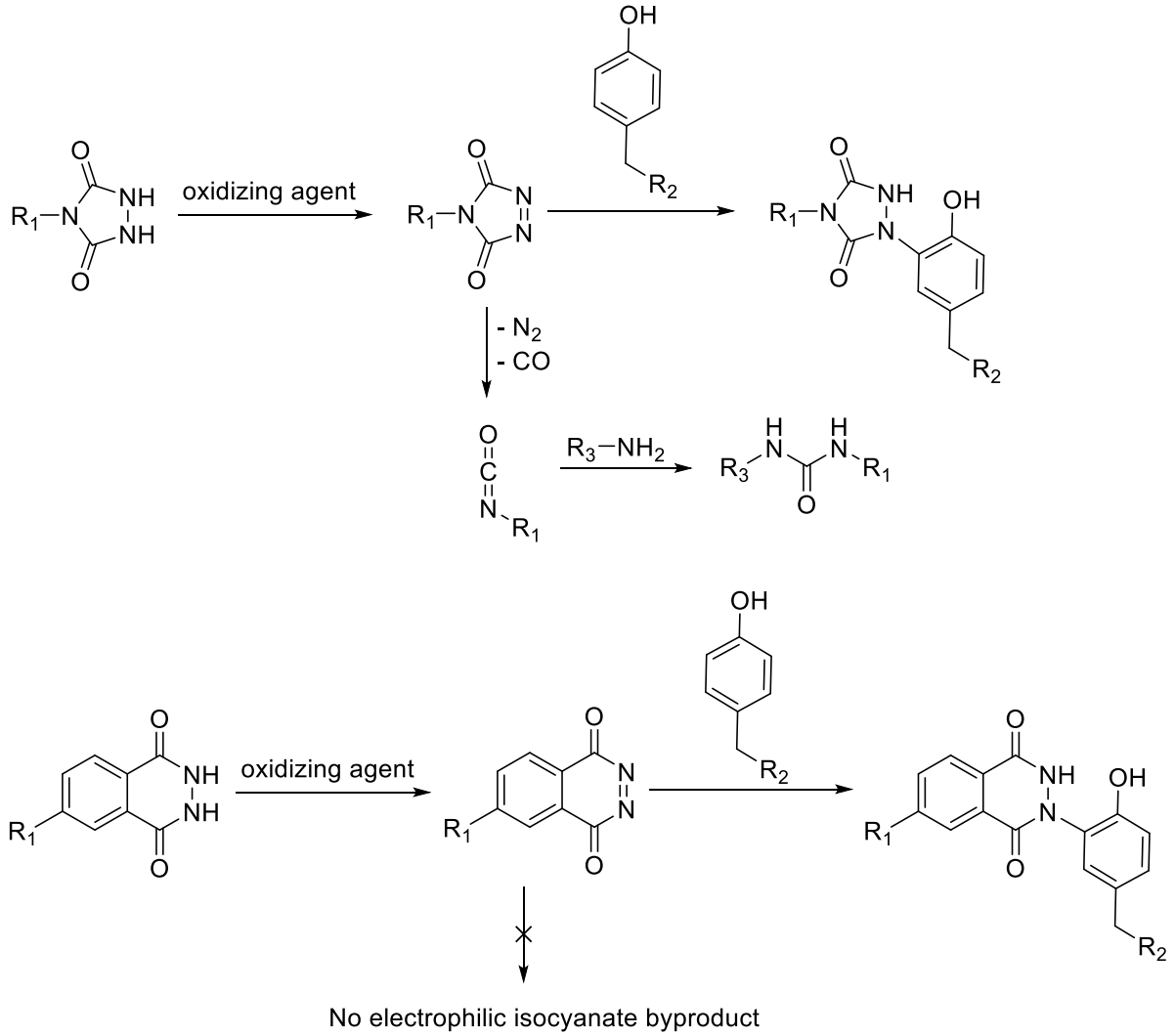

Figure 1.11. Stability of cyclic diazodicarboxamides in comparison with luminol derivatives, post-oxidation.

1.3 Hypothesis and Aim of the Thesis

This thesis hypothesizes that the application of tyrosine-click and azo coupling chemistry to PET radiochemistry is a versatile bioconjugation technique for the chemoselective incorporation of radionuclides onto tyrosine residues under mild conditions. To test and verify this hypothesis, the following two major project goals were proposed.

1) The radiosynthesis and application of ^{18}F-labeled luminol derivatives as novel tyrosine-click building blocks.

2) The preparation of ^{64}Cu- and ^{68}Ga-labeled diazonium salts and their subsequent azo coupling with tyrosine residues on the amino acid, peptide, protein and nanoparticle level.

2.0 MATERIALS AND METHODS

2.1 General

^{1}HNMR and ^{13}CNMR spectra were recorded on a Bruker AM 600 NMR spectrometer. Chemical shifts are given in parts per million with tetramethylsilane (TMS) as an internal reference. MS data were recorded on a Waters Micromass ZQ 4000 mass spectrometer, an Agilent 6220 oaTOF mass spectrometer or an AB Sciex Voyager Elite MALDI mass spectrometer. LCMS data were recorded on Agilent 6130 mass spectrometer with Agilent 1260 HPLC. Flash column chromatography was performed on a Combiflash R_f system using a gold silica column. HPLC was performed on a Gilson system with a 321 pump and 155 UV detector. Automated radiosynthesis of 4-[^{18}F]fluorobenzylamine was performed on a GE TRACERlab™ FX. All chemicals were obtained from Sigma-Aldrich and used without further purification, with the exception of neurotensin (8-13) which was obtained from Bachem and *p*-NH_2-Bn-NOTA which was obtained from Macrocyclics.

2.2 Chemical Syntheses

2.2.1 Ethyl *N*,*N*-[(4-nitrophenoxy)carbonylamino]carbamate (1)

A solution of ethyl carbazate and dry trimethylamine in dry tetrahydrofuran was added dropwise to 1.1 equivalents of 4-nitrophenylchloroformate in tetrahydrofuran, under nitrogen. The reaction was stirred at room temperature for three hours and monitored by TLC using a 50% ethyl acetate in hexane solvent system. The reaction was filtered and the filtrate was concentrated *in vacuo*. The product was purified by column chromatography using an ethyl acetate/hexane gradient. The product had an R_f value of 0.30 and was characterized by ^{1}H NMR and MS. The yield was 45%. ^{1}H NMR (600 MHz, MeOD): δ 8.32 (d, 2H), 7.46 (d, 2H), 4.22 (m, 2H), 1.26 (t, J = 6.6 Hz, 3H).

2.2.2 Ethyl 2-[(4-{[(*tert*-butoxycarbonyl)amino]methyl}phenyl)carbamoyl] hydrazinecarboxylate (2)

A solution of 4-[(*N*-Boc)aminomethyl]aniline and trimethylamine in acetonitrile was added dropwise to 1.2 equivalents of compound **1** in acetonitrile. The reaction was stirred at room temperature for eighteen hours and monitored by TLC using a 75% ethyl acetate in hexane solvent system. The reaction was concentrated *in vacuo* and the product was purified by column chromatography using an ethyl acetate/hexane solvent system. The product had an R_f value of 0.20 and was characterized by ^{1}H NMR. The yield was 30%. ^{1}H NMR (600 MHz, DMSO-d_6): δ 8.82 (s, 1H), 8.61 (s, 2H), 8.01 (s, 1H), 7.30-7.42 (m, 4H), 4.01-4.30 (m, 4H), 1.39 (s, 9H), 1.25 (t, J = 9 Hz, 3H).

2.2.3 *tert*-Butyl [4-(3,5-dioxo-1,2,4-triazolidin-4-yl)benzyl]carbamate (3)

To a solution of compound **2** in ethanol, 1.5 equivalents of sodium ethoxide were added in portions. The reaction was stirred at room temperature for eighteen hours and monitored by TLC using a 10% methanol in dichloromethane solvent system. The reaction was acidified with acetic acid, concentrated *in vacuo*, filtered and washed with distilled water. The remaining solid product had an R_f value of 0.10 and was characterized by ^{1}H NMR and ^{13}C NMR. The yield was 73%. ^{1}H NMR (600 MHz, DMSO-d_6): δ 10.43 (s, 2H), 7.36 (d, J = 12 Hz, 2H), 7.32 (d, J = 6 Hz, 2H), 4.15 (d, J = 6 Hz, 2H), 1.39 (s, 9H). ^{13}C NMR (150 MHz, $CDCl_3$): δ 155.69, 153.36, 139.70, 130.19, 127.09, 125.81, 77.78, 42.89, 28.14.

2.2.4 4-[4-(Aminomethyl)phenyl]-1,2,4-triazoline-3,5-dione (4)

An excess of trifluoroacetic acid was added to compound **3**. The reaction was stirred at room temperature for one hour and monitored by TLC using a 10% methanol in dichloromethane solvent system. The reaction was concentrated *in vacuo*. The product had an R_f value of 0.03 and was characterized by ^{1}H NMR. The yield was 79%. ^{1}H NMR (600 MHz, DMSO-d_6): δ 10.53 (s, 2H), 8.19 (s, 3H), 7.55 (d, J = 12 Hz, 2H), 7.51 (d, J = 12 Hz, 2H), 4.09 (d, J = 6 Hz, 2H).

2.2.5 Ethyl 2-[(4-fluorobenzyl)carbamoyl]hydrazinecarboxylate (6)

To a solution of compound **1** in acetonitrile, 1.1 equivalents of 4-fluorobenzylamine and *N*,*N*-diisopropylethylamine in acetonitrile were added dropwise. The reaction was stirred at room temperature for eighteen hours and monitored by TLC using a 75% ethyl acetate in hexane solvent system. The reaction was concentrated *in vacuo* and the product was purified by column chromatography using an ethyl acetate/hexane solvent system. The product had an R_f value of 0.24 and was characterized by ^{1}H NMR and ^{13}C NMR. The yield was 40%. ^{1}H NMR (600 MHz, DMSO-d_6): δ 8.82 (s, 1H), 7.83 (s, 1H), 7.29-7.26 (m, 2H), 7.13-7.09 (m, 2H), 6.96 (s, 1H), 4.19 (d, J = 6 Hz, 2H), 4.03 (q, J = 8.0 Hz, 2H), 1.17 (t, J = 6 Hz, 3H). ^{13}C NMR (150 MHz, DMSO-d_6): δ 162.29, 160.69, 158.85, 157.38, 137.33, 129.34, 115.28, 115.15, 60.89, 42.36, 15.00.

2.2.6 4-(3,5-Dioxo-1,2,4-triazolidin-4-yl)benzenesulfonyl chloride (8)

To 4-phenylurazole, 7 equivalents of chlorosulfonic acid were added. The reaction was stirred at 60 ºC for two hours. It was cooled to room temperature and added dropwise to 40 mL of crushed ice. The solution was filtered several times and the remaining solid was dissolved in hot ethyl acetate, concentrated *in vacuo* and cooled in an ice bath. Cold hexane was added and the solution was filtered. The remaining solid product was characterized by ^{1}H NMR, ^{13}C NMR and MS. The yield was 44%. ^{1}H NMR (600 MHz, DMSO-d_6): δ 7.67 (d, J = 8.4 Hz, 2H), 7.41 (d, J = 9.6 Hz, 2H). ^{13}C NMR (150 MHz, $(CD_3)_2CO$): δ 153.29, 141.62, 139.34, 127.74, 125.47.

2.2.7 4-{[(E)-(4-Fluorophenyl)methylidene]amino}-1,2,4-triazolidine-3,5-dione (10)

To a solution of urazine in distilled water, 10 equivalents of 4-fluorobenzaldehyde were added. The reaction was stirred under reflux for 45 minutes and monitored by TLC using a 50% methanol in dichloromethane solvent system. The reaction was concentrated *in vacuo,* dried by lyophilization and washed with ether. The product had an R_f value of 0.83 and was characterized by ^{1}H NMR and MS. The yield was 17%. ^{1}H NMR (600 MHz, DMSO-d_6): δ 9.40 (s, 1H), 7.93-7.84 (m, 2H), 7.42-7.29 (m, 2H).

2.2.8 Di-*tert*-butyl [(4-nitrobenzyl)oxy]imidodicarbonate (11)

To a solution of *O*-(4-nitrobenzyl)hydroxylamine hydrochloride and triethylamine in acetonitrile, 2 equivalents of BOC anhydride and 2 equivalents of 4-dimethylaminopyridine were added. The reaction was stirred at 45 ºC for 3 hours and monitored by TLC using a 30% ethyl acetate in hexane solvent system. The reaction was concentrated *in vacuo* and purified by flash column chromatography using an ethyl acetate/hexane solvent system. The product had an R_f value of 0.60 and was characterized by ^{1}H NMR, ^{13}C NMR and MS. The yield was 88%. ^{1}H NMR (600 MHz, $CDCl_3$): δ 8.16 (d, J = 8.4 Hz, 2H), 7.57 (d, 2H), 4.95 (s, 2H), 1.48 (s, 18H). ^{13}C NMR (150 MHz, $CDCl_3$): δ 150.04, 148.07, 141.66, 129.73, 123.64, 84.34, 53.43, 34.01, 28.39, 28.10.

2.2.9 Di-*tert*-butyl [(4-aminobenzyl)oxy]imidodicarbonate (12)

To a solution of compound **11** in 10% water in acetonitrile, 0.2 equivalents of nickel acetate tetrahydrate were added. The mixture was stirred for 5 minutes before 4 equivalents of sodium borohydride were added. The reaction was stirred at room temperature for 15 minutes and monitored by TLC using a 30% ethyl acetate in hexane solvent system. The reaction was washed with water and brine, extracted with dichloromethane, dried over sodium sulfate and purified by flash column chromatography using an ethyl acetate/hexane solvent system. The product had an R_f value of 0.24 and was purified using flash column chromatography and characterized by ^{1}H NMR, ^{13}C NMR and MS. The yield was 45%. ^{1}H NMR (600 MHz, MeOD): δ 7.16 (d, J = 8.4 Hz, 2H), 6.70 (d, J = 8.4 Hz, 2H), 4.77 (s, 2H), 1.54 (s, 18H). ^{13}C NMR (150 MHz, MeOD): δ 150.55, 148.63, 131.23, 123.09, 114.44, 77.87, 26.85.

2.2.10 Ethyl 2-{[4-{[(di-*tert*-butoxycarbonyl)amino]oxy}methyl)phenyl]carbamoyl} hydrazine carboxylate (13)

To a solution of compound **12** and triethylamine in acetonitrile, 1.5 equivalents of compound **1** were added dropwise. The reaction was stirred at 45 ºC for 6 hours and monitored by TLC using a 75% ethyl acetate in hexane solvent system. The reaction was concentrated *in*

vacuo, washed with water and brine, extracted with ethyl acetate, dried over sodium sulfate and purified by flash column chromatography using an ethyl acetate/hexane solvent system. The product had an R_f value of 0.52 and was characterized by ^{1}H NMR, ^{13}C NMR and MS. The yield was 49%. ^{1}H NMR (600 MHz, MeOD): δ 7.48 (d, *J* = 8.4 Hz, 2H), 7.36 (d, *J* = 8.4 Hz, 2H), 4.86 (s, 2H), 4.20 (q, *J* = 7.6 Hz, 2H), 1.55 (s, 18H), 1.30 (t, *J* = 7.2 Hz, 3H). ^{13}C NMR (150 MHz, MeOD): δ 152.46, 141.64, 132.42, 130.80, 121.01, 85.82, 79.42, 63.48, 29.02, 15.45.

2.2.11 2-Methyl-1,4-dioxo-1,2,3,4-tetrahydrophthalazine-6-carboxylic acid (20)

To a solution of 1,2,4-benzenetricarboxylic anhydride in acetic acid, 2 equivalents of 1-Boc-1-methylhydrazine were added. The reaction was stirred under reflux for five hours and monitored by TLC using an 80% ethyl acetate in hexane solvent system. The reaction was filtered and the solid was washed with water, dried under vacuum and washed with ether. The product had an R_f value of 0.28 and was characterized by ^{1}H NMR, ^{13}C NMR and LCMS. The yield was 69%. ^{1}H NMR (600 MHz, DMSO-d_6): Pair of isomers δ 8.72 (d, 1H), 8.47 (s, 1H), 8.31-8.37 (m, 3H), 8.06 (d, 1H), 3.59 (s, 3H), 3.58 (s, 3H). ^{13}C NMR (150 MHz, DMSO-d_6): Pair of isomers δ 166.62, 166.59, 157.49, 157.21, 135.03, 134.31, 133.29, 132.50, 131.84, 129.21, 127.97, 127.82, 127.53, 125.94, 125.36, 38.25.

2.2.12 6-{[(2,5-Dioxopyrrolidin-1-yl)oxy]carbonyl}2-methyl-2,3-dihydrophthalazine-1,4-dione (21)

To a solution of compound **20** in tetrahydrofuran, 2 equivalents of *N*-hydroxysuccinimide and 2 equivalents of 1-ethyl-3-(3-dimethylaminopropyl) carbodiimide were added. The reaction was stirred at room temperature for eighteen hours under argon and monitored by TLC using a 10% methanol in dichloromethane solvent system. The reaction was concentrated *in vacuo*, washed with water, extracted with dichloromethane and dried over sodium sulfate. The product had an R_f value of 0.44.

2.2.13 2-Methyl-1,4-dioxo-1,2,3,4-tetrahydrophthalazine-6-carbonyl chloride (22)

A large excess of thionyl chloride was added to compound **20**. The reaction was stirred at room temperature for 30 minutes, then heated to 80 ºC and stirred for an additional thirty minutes. The reaction was monitored by TLC using a 10% methanol in dichloromethane solvent system. Following completion, the excess thionyl chloride was evaporated by heating to 85 ºC and the remaining solid was washed with ether. The product had an R_f value of 0.42 and was characterized by ^{1}H NMR. The yield was 98%. ^{1}H NMR (600 MHz, DMSO-d_6): Pair of isomers δ 8.49 (d, 1H), 8.34 (d, 1H), 8.09-8.14 (m, 3H), 7.83 (d, 1H), 3.36 (s, 3H), 3.35 (s, 3H).

2.2.14 *N*-(4-Fluorobenzyl)-2-methyl-1,4-dioxo-1,2,3,4-tetrahydrophthalazine-6-carboxamide (23)

To a solution of compound **22** in dichloromethane, 2 equivalents of 4-fluorobenzylamine were added in portions. The reaction was stirred at room temperature for eighteen hours and monitored by TLC using a 10% methanol in dichloromethane solvent system. The reaction was concentrated *in vacuo*, washed with 10% citric acid, extracted with ethyl acetate and purified by flash column chromatography, using a methanol/dichloromethane gradient. The product had an R_f value of 0.39 and was characterized by ^{1}H NMR, ^{13}C NMR and LCMS. The yield was 10%. ^{1}H NMR (600 MHz, DMSO-d_6): Pair of isomers δ 8.73 (d, 1H), 8.33 (dd, 1H), 8.05 (d, 1H), 7.39-7.41 (m, 2H), 7.16-7.18 (m, 2H), 4.50 (d, 2H), 3.58 (s, 3H). ^{13}C NMR (150 MHz, DMSO-d_6): Pair of isomers δ 165.40, 165.38, 162.47, 160.88, 137.62, 136.03, 136.00, 131.96, 131.93, 129.90, 129.85, 129.17, 125.70, 125.67, 125.18, 125.10, 115.59, 115.45, 115.09, 42.67, 38.28. LC-MS: 328.1 [M+H].

2.2.15 Conjugation of compound 23 with acetyl-L-tyrosine methylamide

To 3 equivalents of compound **23**, 1 equivalent of acetyl-L-tyrosine methyl amide and 0.01 equivalents of hemin in dimethyl sulfoxide, 10 equivalents of hydrogen peroxide were added dropwise. The reaction was stirred at room temperature for thirty minutes and monitored by TLC using a 10% methanol in dichloromethane solvent system. The reaction was diluted

with ethyl acetate, washed with water and purified by HPLC. The product had an R_f value of 0.09 and was characterized by ^{1}H NMR and LCMS. The yield was 42%. ^{1}H NMR (600 MHz, DMSO-d_6): δ 8.63-8.67 (m, 1H), 8.20-8.22 (m, 2H), 7.31-7.34 (m, 2H), 7.10-7.20 (m, 2H), 6.88-7.00 (m, 2H), 6.86-6.88 (m, 1H), 4.50 (d, J = 9.0 Hz, 2H), 4.43-4.44 (m, 1H), 3.30 (s, 3H), 2.73-2.99 (m, 2H), 2.59 (d, J = 7.2 Hz, 3H), 1.84 (s, 3H).

2.2.16 Chelation of *p*-NH_2-Bn-NOTA with ^{nat}Cu

An excess of copper (II) chloride dihydrate and EDTA in 1 M ammonium acetate buffer pH 6 was shaken at room temperature for thirty minutes before it was added to a solution of *p*-NH_2-Bn-NOTA in 1 M ammonium acetate buffer pH 6. The reaction was shaken on a thermoshaker at 60 ºC for one hour before being shaken at room temperature for twenty-four hours. The reaction was purified by HPLC and characterized by LCMS. LC-MS: 469.1 [M+H].

2.2.17 Chelation of *p*-NH_2-Bn-NOTA with ^{nat}Ga

An excess of gallium trichloride and EDTA in 1 M sodium acetate buffer pH 4.5 was shaken at room temperature for five minutes before it was added to a solution of *p*-NH_2-Bn-NOTA in 1 M sodium acetate buffer pH 4.5. The reaction was shaken on a thermoshaker at room temperature for twenty-four hours. The reaction was purified by HPLC and characterized by LCMS. LC-MS: 475.1 [M+H].

2.2.18 Diazotization of ^{nat}Cu-NOTA-NH_2

To a solution of compound **31** in 1 M hydrochloric acid, 1 equivalent of sodium nitrite was added. The reaction was periodically shaken at 4 ºC for two minutes. The product was used, *in situ*, for the next step without purification.

2.2.19 Diazotization of ^{nat}Ga-NOTA-NH$_2$

To a solution of compound **32** in 1 M hydrochloric acid, 1 equivalent of sodium nitrite was added. The reaction was periodically shaken at 4 ºC for two minutes. The product was used, *in situ*, for the next step without purification.

2.2.20 Conjugation of ^{nat}Cu-NOTA-N$_2$ with L-tyrosine

To 1 equivalent of L-tyrosine in 1 x PBS pH 7.2, the diazotized compound **33** was added. The pH was adjusted to 9 with the addition of 4 M sodium hydroxide and the reaction was periodically shaken at 4 ºC for thirty minutes. The product was purified by HPLC and characterized by LCMS. The yield was 28%. LC-MS: 662.1 [M+H].

2.2.21 Conjugation of ^{nat}Ga-NOTA-N$_2$ with L-tyrosine

To 1 equivalent of L-tyrosine in 1 x PBS pH 7.2, the diazotized compound **34** was added. The pH was adjusted to 9 with the addition of 4 M sodium hydroxide and the reaction was periodically shaken at 4 ºC for thirty minutes. The product was purified by HPLC and characterized by LCMS. The yield was 7%. LC-MS: 667.2 [M+H].

2.2.22 Conjugation of ^{nat}Cu-NOTA-N$_2$ with neurotensin NT(8-13)

To 1 equivalent of neurotensin NT(8-13) in 1 x PBS pH 7.2, the diazotized compound **33** was added. The pH was adjusted to 9 with the addition of 4 M sodium hydroxide and the reaction was periodically shaken at 4 ºC for thirty minutes. The product was purified by HPLC and characterized by LCMS. The yield was 76%.

2.2.23 Conjugation of ^{nat}Ga-NOTA-N$_2$ with neurotensin NT(8-13)

To 1 equivalent of neurotensin NT(8-13) in 1 x PBS pH 7.2, the diazotized compound **34** was added. The pH was adjusted to 9 with the addition of 4 M sodium hydroxide and the reaction

was periodically shaken at 4 ºC for thirty minutes. The product was purified by HPLC and characterized by LCMS. The yield was 66%.

2.3 Radiochemical Syntheses

2.3.1 [^{18}F]Fluorobenzaldehyde (18)

To 500-1000 MBq of azeotropically dried [^{18}F]fluoride, 5-10 mg of 4-(trimethylammonium triflate)benzaldehyde in acetonitrile was added. The sealed reaction was vortexed and reacted at 100 ºC for 10 minutes and monitored by radio-TLC using a 75% ethyl acetate in hexane solvent system. The product had an R_f value of 0.60 and characterized based on the R_f value of cold 4-fluorobenzaldehyde. The decay corrected yield was 71%, and the radiochemical purity was >95%.

2.3.2 4-{[(E)-(4-[^{18}F]-Fluorophenyl)methylidene]amino}-1,2,4-triazolidine-3,5-dione (19)

To a 0.03 M solution of urazine in 25% 0.1 M HCl in acetonitrile, 3 MBq of 4-[^{18}F]fluorobenzaldehyde (**18**) were added. The reaction was shaken on a thermoshaker at 45 ºC for 15 minutes and monitored by radio-TLC using a 20% ethyl acetate in hexane solvent system. The product had an R_f value of 0.04 and was characterized by radio-TLC based on the R_f value of the cold reference. The product was obtained without purification, with a radiochemical purity of 92%.

2.3.3 4-[^{18}F]Fluorobenzylamine (28)

[^{18}F]Fluorobenzylamine (**28**) was prepared according to literature [30]. To 500-1000 MBq of azeotropically dried [^{18}F]fluoride, 5-10 mg of 4-cyano-*N,N,N*-trimethylanilinium trifluoromethansulfonate in dimethyl sulfoxide was added. The sealed reaction was vortexed and reacted at 95 ºC for 15 minutes. Following cartridge purification, 4-[^{18}F]fluorobenzylnitrile (**27**) was obtained. Reduction of compound **5** using 50 mg of sodium borohydride with 25 mg of nickel chloride as a catalyst at 25 ºC for 15 minutes, followed by cartridge purification, afforded 4-

[^{18}F]fluorobenzylamine (**28**). The product was characterized by radio-TLC based on the R_f value of cold 4-fluorobenazylamine. The product had an R_f value of 0.10, using a 50% ethyl acetate in hexane solvent system. The decay corrected yield was 24% and the radiochemical purity was >98%.

2.3.4 *N*-(4-[^{18}F]Fluorobenzyl)-2-methyl-1,4-dioxo-1,2,3,4-tetrahydrophthalazine-6-carboxamide (29)

To a solution of compound **22** in tetrahydrofuran, 6 MBq of 4-[^{18}F]fluorobenzylamine (**28**) were added. The reaction was shaken on a thermoshaker at 25 ºC for fifteen minutes and monitored by radio-TLC using a 10% methanol in dichloromethane solvent system. The product had an R_f value of 0.69, was purified by radio-HPLC and characterized based on the retention time of the cold reference. The decay corrected radiochemical yield was 48% and the radiochemical purity was >97%.

2.3.5 Conjugation of compound 29 with acetyl-L-tyrosine methylamide

To 2 MBq of compound **29** in a 50% acetonitrile in 0.2% trifluoroacetic acid water solution, 100 µg of acetyl-L-tyrosine methylamide, 10 µg of hemin and 3 µL of hydrogen peroxide were added. The reaction was shaken on a thermoshaker at 25 ºC for 30 minutes and monitored by radio-TLC, using a 10% methanol in dichloromethane solvent system. The product had an R_f value of 0.09, was purified by radio-HPLC and characterized based on the retention time of the cold reference. The decay corrected radiochemical yield was 27%, with a radiochemical purity >81%.

2.3.6 Chelation of *p*-NH_2-Bn-NOTA with ^{64}Cu

To a solution of *p*-NH_2-Bn-NOTA in 0.25 M ammonium acetate buffer pH 5.5, 10 MBq of ^{64}Cu were added. The reaction was shaken on a thermoshaker at 37 ºC for fifteen minutes and monitored by radio-TLC using a 10% 1 M ammonium acetate in methanol solvent system. The

product had an R_f value of 0.30 and was used in the next step without purification. The radiochemical purity was >98%.

2.3.7 Chelation of *p*-NH_2-Bn-NOTA with ^{68}Ga

To a solution of *p*-NH_2-Bn-NOTA in 0.25 M ammonium acetate buffer pH 5.5, 5 MBq of ^{68}Ga were added. The reaction was shaken on a thermoshaker at 37 ºC for fifteen minutes and monitored by radio-TLC using a 10% 1 M ammonium acetate in methanol solvent system. The product had an R_f value of 0.30 and was used in the next step without purification. The radiochemical purity was >94%.

2.3.8 Diazotization of ^{64}Cu-NOTA-NH_2

To a solution of compound **39** in 0.1 M ammonium acetate buffer pH 5.5100 µL of 1 M hydrochloric acid and 10 µL of a 2 M sodium nitrite solution were added. The reaction was periodically shaken at 4 ºC for ten minutes. The product was used, *in situ*, for the next step without purification.

2.3.9 Diazotization of ^{68}Ga-NOTA-NH_2

To a solution of compound **40** in 0.1 M ammonium acetate buffer pH 5.5100 µL of 1 M hydrochloric acid and 10 µL of a 2 M sodium nitrite solution were added. The reaction was periodically shaken at 4 ºC for ten minutes. The product was used, *in situ*, for the next step without purification.

2.3.10 Conjugation of ^{64}Cu-NOTA-N_2 with L-tyrosine

To 500 µg of L-tyrosine in 0.1 M borate buffer pH 8.8, the diazotized compound **41** was added. The pH was adjusted to 9 with the addition of 4 M sodium hydroxide and the reaction was periodically shaken at 4 ºC for thirty minutes. The product was purified by HPLC and

characterized based on the retention time of the cold reference. The radiochemical yield was 56%.

2.3.11 Conjugation of ^{68}Ga-NOTA-N$_2$ with L-tyrosine

To 500 µg of L-tyrosine in 0.1 M borate buffer pH 8.8, the diazotized compound **42** was added. The pH was adjusted to 9 with the addition of 4 M sodium hydroxide and the reaction was periodically shaken at 4 ºC for thirty minutes. The product was purified by HPLC and characterized based on the retention time of the cold reference. The radiochemical yield was 80%.

2.3.12 Conjugation of ^{64}Cu-NOTA-N$_2$ with neurotensin NT(8-13)

To 200 µg of neurotensin NT(8-13) in 0.1 M borate buffer pH 8.8, the diazotized compound **41** was added. The pH was adjusted to 9 with the addition of 4 M sodium hydroxide and the reaction was periodically shaken at 4 ºC for thirty minutes. The product was purified by HPLC and characterized based on the retention time of the cold reference. The radiochemical yield was 45%.

2.3.13 Conjugation of ^{68}Ga-NOTA-N$_2$ with neurotensin NT(8-13)

To 200 µg of neurotensin NT(8-13) in 0.1 M borate buffer pH 8.8, the diazotized compound **42** was added. The pH was adjusted to 9 with the addition of 4 M sodium hydroxide and the reaction was periodically shaken at 4 ºC for thirty minutes. The product was purified by HPLC and characterized based on the retention time of the cold reference. The radiochemical yield was 11%.

2.3.14 Conjugation of ^{64}Cu-NOTA-N$_2$ with HSA

To 100 µg of HSA in 0.1 M borate buffer pH 8.8, the diazotized compound **41** was added. The pH was adjusted to 9 with the addition of 1 M sodium hydroxide and the reaction was periodically shaken at 4 ºC for thirty minutes. The product was purified by SEC and characterized

by SDS-PAGE with Coomassie staining and radioactive scan. The decay corrected radiochemical yield was 20%.

2.3.15 Diazotization of ^{64}Cu-NOTA-N_2 with TMV

To 234 µg of TMV in 0.1 M borate buffer pH 8.8, the diazotized compound **41** was added. The pH was adjusted to 9 with the addition of 1 M sodium hydroxide and the reaction was periodically shaken at 4 ºC for thirty minutes. The product was purified by SEC and characterized by SDS-PAGE with Coomassie staining and radioactive scan. The decay corrected radiochemical yield was 9%.

2.4 IC_{50} Determination

IC_{50} values were determined using a radiometric competitive binding assay. [^{125}I]tyr^3-neurotensin, with a specific activity of 81.4 GBq/µmol from PerkinElmer, was used as a radiotracer. HT-29 cells plated on tissue culture T-25/75 flasks were incubated in culture media in humidified 5% CO / 95% air at 37 ºC for three to five days. Cells were washed three times with Tris buffer, suspended in 8 mL of Tris buffer and homogenized. Cell densities ranged from 4 x 10^6 and 7 x 10^6 cells/mL. A 100 µM peptide stock solution was prepared using water and serial dilutions were prepared using Tris buffer (50 mM Tris–HCl, 1 mM EDTA, 0.1% BSA, and 0.5 mM *o*-phenanthroline, cOmplete™, EDTA-free Protease Inhibitor Cocktail, pH 7.4), with concentrations ranging from 10^{-5} M and 10^{-12} M. A 100 µL aliquot of peptide solution was combined with 200 µL of cell homogenate, 500 µL of Tris buffer and 200 µL of radiotracer. The solution was incubated at room temperature for thirty minutes. Free and bound ligand were separated by filtration, using Whatman GF/B glass fiber filters and a Brandel cell harvester (Gaithersburg, MD, USA). Filters were washed three times with Tris buffer and quantified using a gamma counter (Wizard-2, PerkinElmer). IC_{50} values were calculated by nonlinear regression, using sigmoidal dose-response curves from GraphPad Prism 7 software.

2.5 SDS-PAGE

Sodium dodecyl sulfate-polyacrylamide gel electrophoresis (SDS-PAGE) was used to characterize ^{64}Cu-labeled HSA (**47**). Radiolabeled proteins were visualized with a combination of Coomassie staining and a radioactive scan of the gel. To a 30 µL aliquot of each sample, 6 µL of 5X Laemmli stain with dithiothreitol (DTT) was added before incubation at 95 ºC for five minutes. Samples were run, along with a protein ladder, on a Bio-Rad Mini-PROTEAN® TGX™ precast gel (10% Tris buffer) in a Bio-Rad Mini-PROTEAN® Tetra Cell with 1X running buffer at 200 V (35 mA) for 40 minutes. The gel was imprinted on a Fujifilm BAS 5000 phosphor imager for 45 minutes and scanned. The gel was then incubated in Coomassie® Brilliant Blue R-250 (Bio-Rad) for 20 minutes at room temperature before de-staining with de-staining solution.

2.6 PET Studies

One PET experiment using a normal BALB/c mouse was carried out to determine the biodistribution and metabolic profile of ^{64}Cu-labeled HSA (**47**). Isoflurane in 100% oxygen (gas flow, 1 L/min) was used as a general anesthetic. Body temperature was kept constant at 37 ºC. Following anesthetization, the mouse was immobilized in the prone position in the center field of view of an Inveon® preclinical PET scanner (Siemens Preclinical Solutions, Knoxville, TN, USA). Radioactivity of the injection solution in a 0.5 mL syringe was measured using a dose calibrator (AtomlabTM 300, Biodex Medical Systems, New York, U.S.A.) prior to injection. The emission scan of a 120 min dynamic PET acquisition was initiated. Following a 15 second delay, ~5 MBq of radiochemically pure ^{64}Cu-labeled HSA (**47**) in 200 µL of phosphate buffered saline (PBS) was injected into the tail vein. Data acquisition continued for 120 min in 3D list mode. After the experiment list mode data were sorted into sinograms with 61 time frames (10×2, 8×5, 6×10, 6×20, 8×60, 10×120 and 9×300 s). In addition to the dynamic 120 min scan another static scan was measured after 24 h p.i. with a scan duration time of 60 min. Image files were reconstructed using maximum a posteriori (MAP) reconstruction mode. Correction for partial volume effects was not performed. Image files were further processed using ROVER v2.0.21 software (ABX GmbH, Radeberg, Germany). Masks defining 3D regions of interest (ROI) were set and the ROIs were defined by 50% thresholding. Mean standardized uptake values [SUVmean = (activity/mL

tissue)/(injected activity/body weight), mL/g] were calculated for each ROI and time-activity curves were generated using GraphPad Prism 5.0 (GraphPad Software Inc., La Jolla, CA, U.S.A.).

3.0 RESULTS

3.1 Synthesis of cyclic diazodicarboxamides and their application in tyrosine-click chemistry

To evaluate the application of tyrosine-click chemistry to PET radiochemistry as a bioconjugation technique, ^{18}F-lableled cyclic diazodicarboxamide derivatives were designed. Cold reference compounds were synthesized, oxidation chemistry was explored and bioconjugation with tyrosine-containing compounds was attempted in preliminary experiments. Once these preliminary insights had been established, radiochemistry with fluorine-18 was carried out.

3.1.1 Synthesis of cyclic diazodicarboxamides as cold reference compounds

The structures of five cyclic diazodicarboxamide derivatives were proposed for chemical synthesis and subsequent tyrosine click (Figure 3. 1).

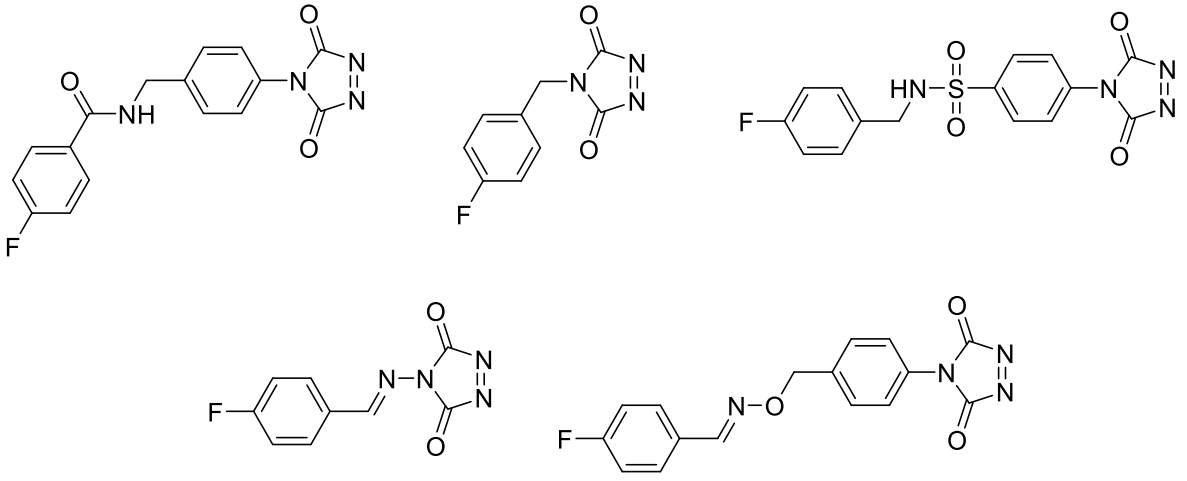

Figure 3. 1. Proposed cyclic diazodicarboxamide derivatives.

The synthesis of cold reference compound *N*-[4-(3,5-dioxo-1,2,4-triazolin-4-yl)benzyl]-4-fluorobenzamide (**5**) was attempted using two different synthesis strategies (Scheme 3.1 and Scheme 3.2).

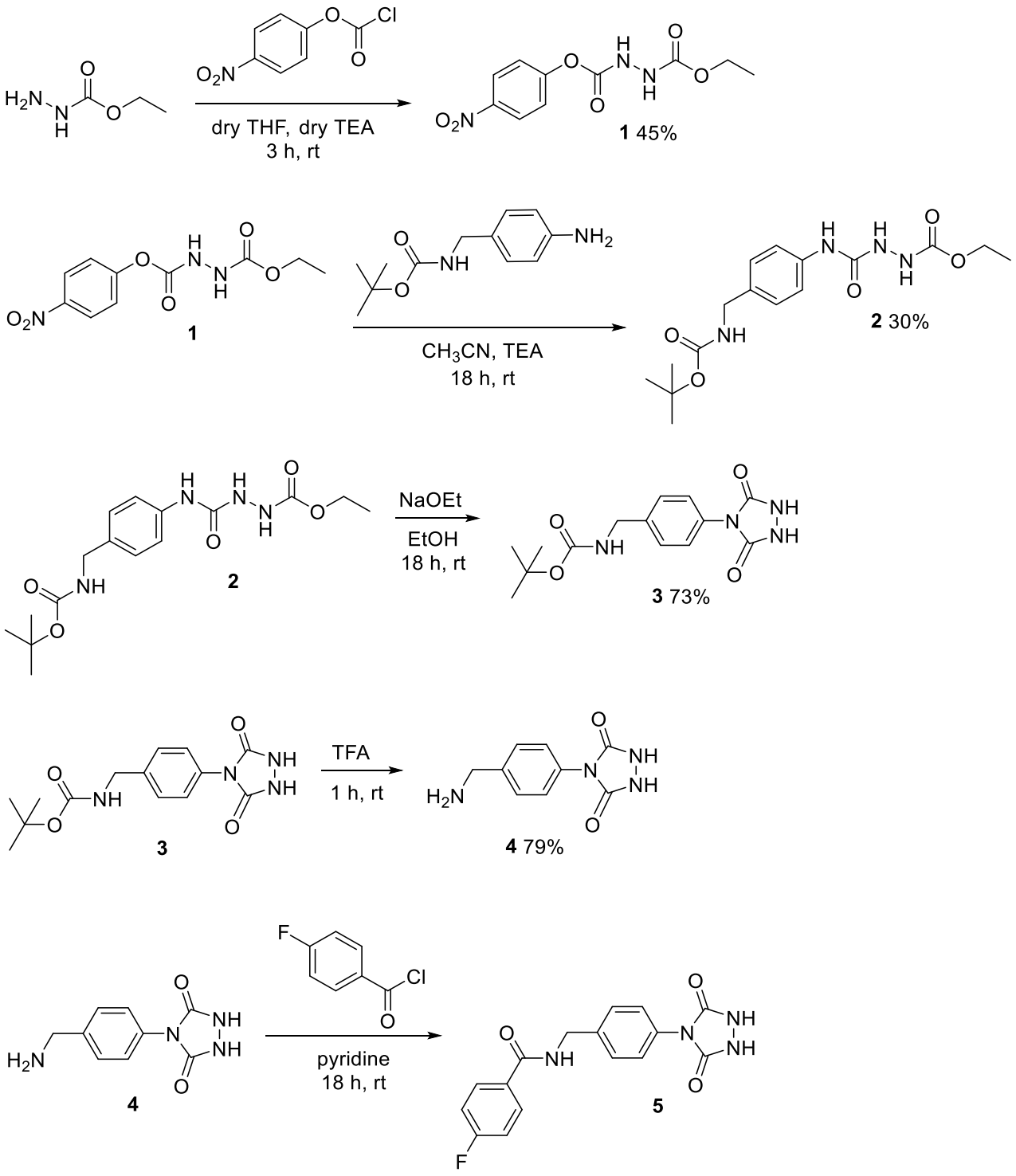

Scheme 3.1. Synthesis of *N*-[4-(3,5-dioxo-1,2,4-triazolin-4-yl)benzyl]-4-fluorobenzamide (**5**), using an acid chloride.

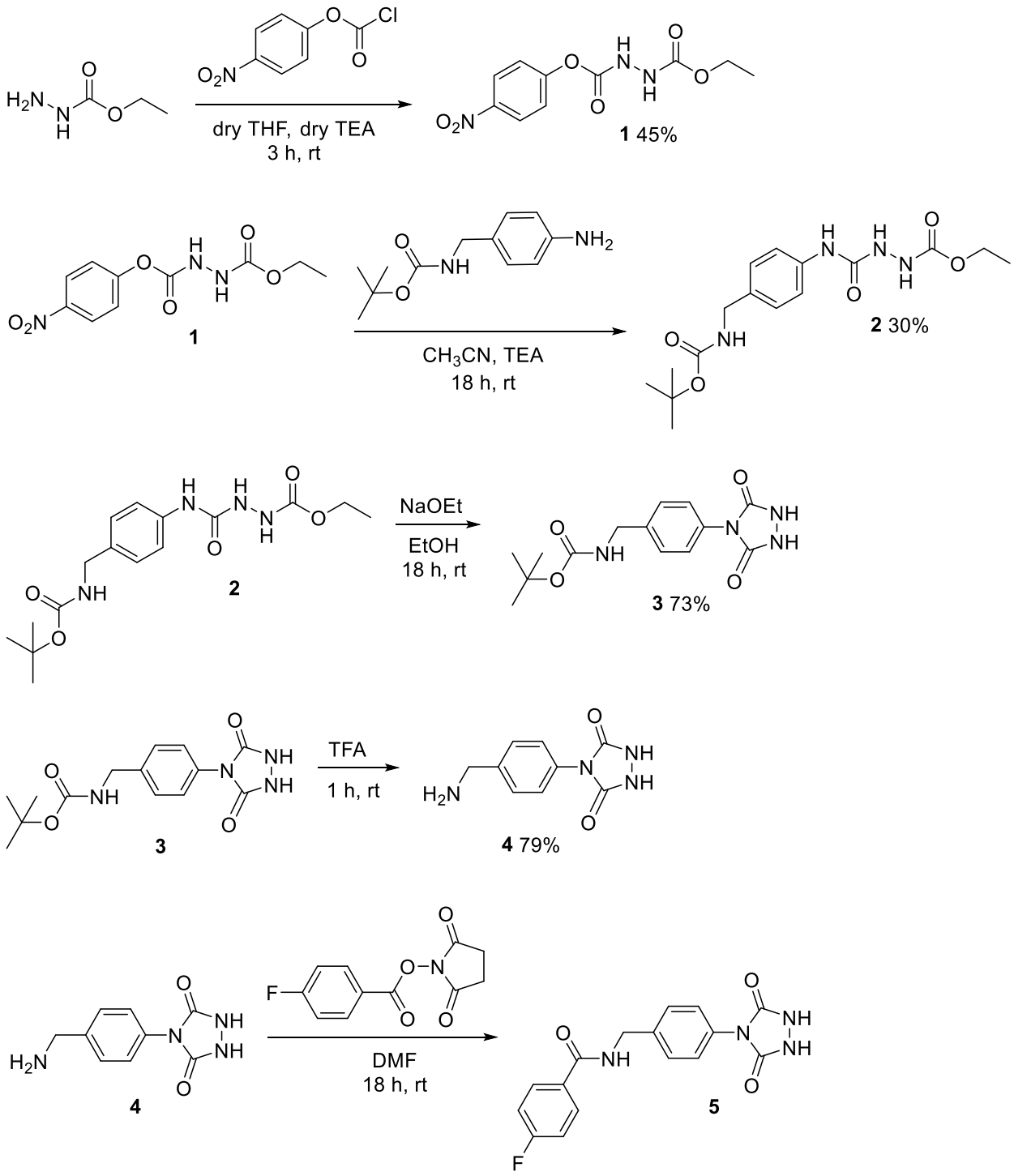

Scheme 3.2. Synthesis of *N*-[4-(3,5-dioxo-1,2,4-triazolin-4-yl)benzyl]-4-fluorobenzamide (**5**), using an active ester.

First, compound **1** was synthesized from commercially available ethyl carbazate (**1**) and 4-nitrophenylchloroformate (**2**), using triethylamine as an auxiliary base to deprotonate the amine group. After purification by column chromatography, compound **1** was obtained in 45% yield. Compound **1** was then reacted with 4-[(*N*-Boc)aminomethyl]aniline and purified by column chromatography to yield compound **2** in 30% yield. Cyclization of compound **2** with sodium ethoxide followed by purification by filtration produced compound **3** in 73% yield and subsequent BOC deprotection with trifluoroacetic acid produced compound **4** in 79% yield. Finally, synthesis of compound **5** was attempted using both 4-fluorobenzyol chloride and succinimidyl 4-fluorobenzoate. Following purification by column chromatography, it was determined that the expected product was not formed in either reaction.

With the unsuccessful synthesis of this first cyclic diazodicarboxamide derivative, the synthesis of cold reference compound 4-(4-fluorobenzyl)-1,2,4-triazoline-3,5-dione (**7**) was attempted in just two steps (Scheme 3.3).

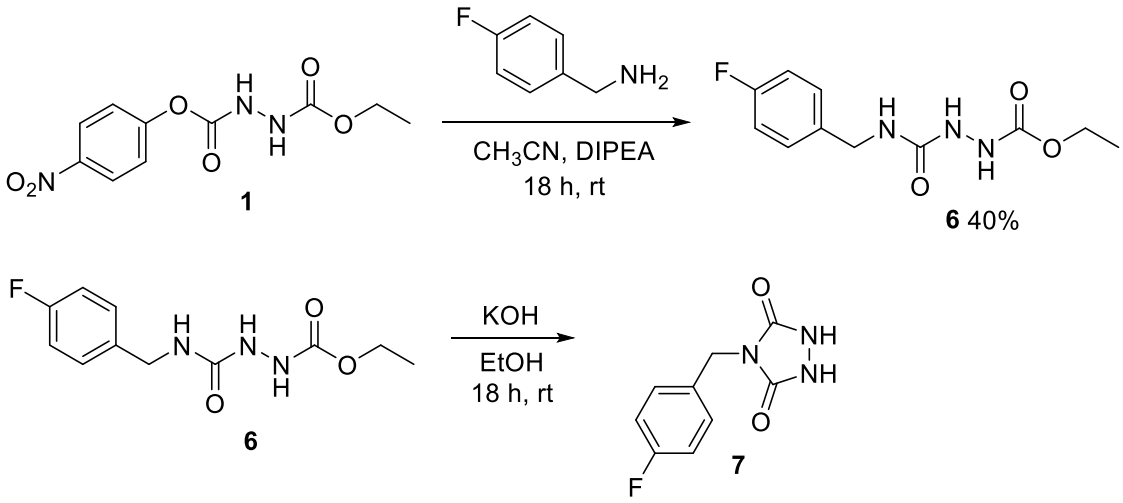

Scheme 3.3. Synthesis of 4-(4-fluorobenzyl)-1,2,4-triazoline-3,5-dione (**7**).

Reaction of previously synthesized compound **1** with 4-fluorobenzylamine was carried out, using *N,N*-diisopropylethylamine as an auxiliary base. After purification by column chromatography, compound **6** was obtained in 40% yield. Cyclization of compound **6** with potassium hydroxide was attempted however it was determined that the cyclized product was not formed.

Next, the synthesis of cold reference compound 4-(3,5-dioxo-1,2,4-triazolidin-4-yl)-*N*-(4-fluorobenzyl) benzene sulfonamide (**9**) was attempted in two steps (Scheme 3.4).

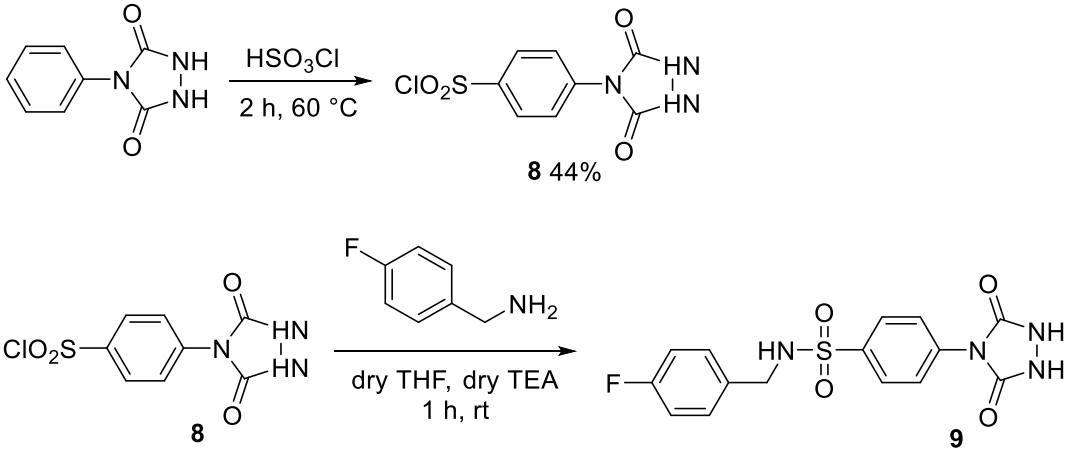

Scheme 3.4. Synthesis of 4-(3,5-dioxo-1,2,4-triazolidin-4-yl)-*N*-(4-fluorobenzyl) benzene sulfonamide (**9**).

Compound **8** was synthesized from commercially available 4-phenylurazole and chlorosulfonic acid according to literature and was obtained in 44% yield [31]. Subsequent reaction of compound **8** with 4-fluorobenylamine formed the expected product however, HPLC purification resulted only in degradation of the product.

Synthesis of cold reference compound 4-{[(E)-(4-fluorophenyl)methylidene]amino}-1,2,4-triazolidine-3,5-dione (**10**) was carried out in a single step (Scheme 3.5).

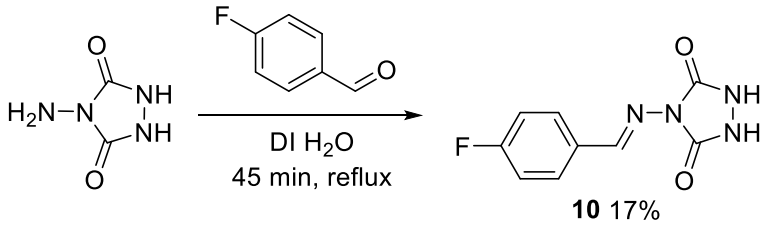

Scheme 3.5. Synthesis of 4-{[(E)-(4-fluorophenyl)methylidene]amino}-1,2,4-triazolidine-3,5-dione (**10**).

Compound **10** was synthesized from commercially available urazine and 4-fluorobenzaldehyde. After purification by washing with ether, compound **10** was obtained in 17% yield.

Synthesis of the final cold reference compound di-*tert*-butyl {[4-(3,5-dioxo-1,2,4-triazolidin-4-yl)benzyl]oxy} carbamate (**14**) was attempted in five steps (Scheme 3.6).

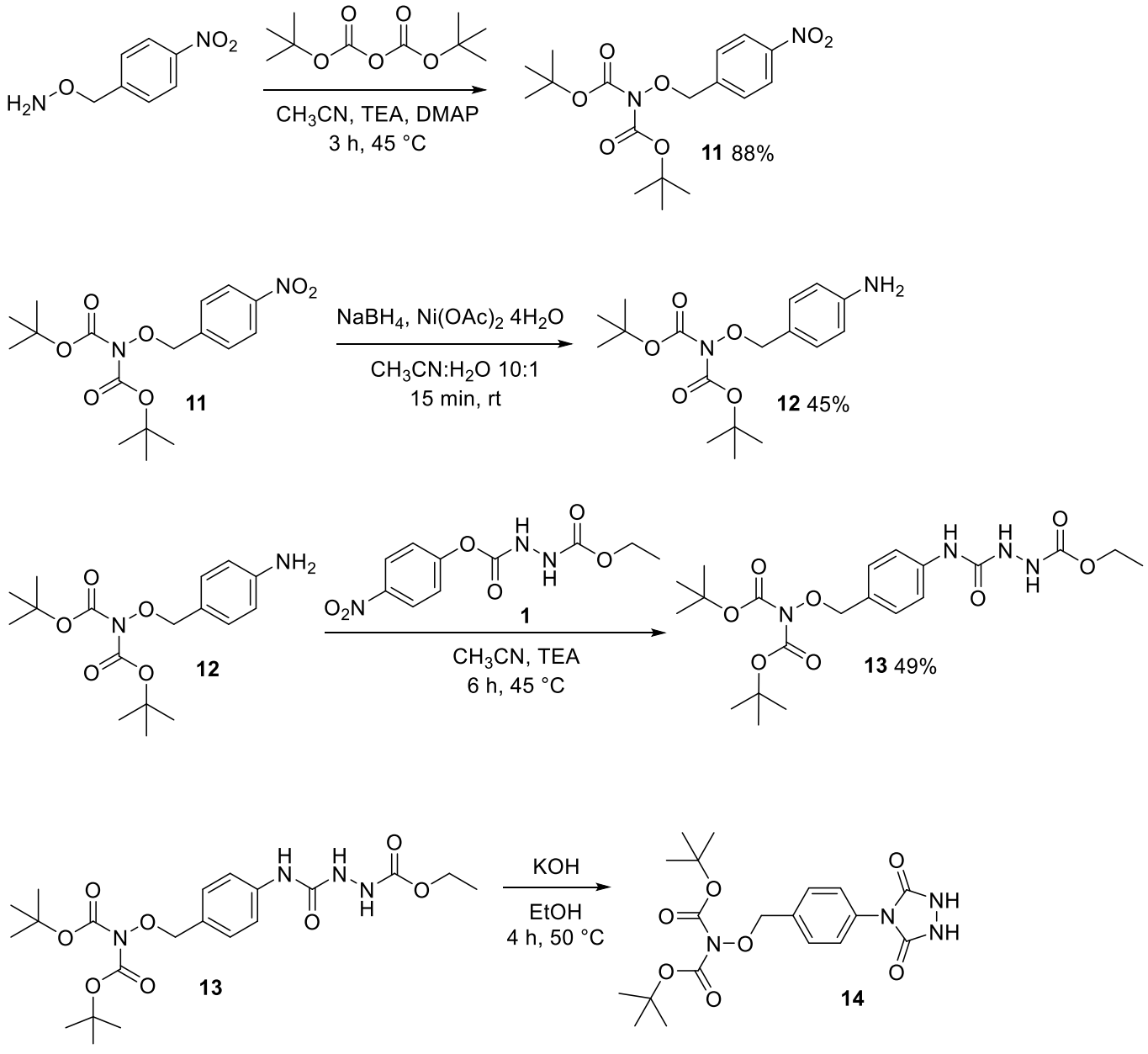

Scheme 3.6. Synthesis of di-*tert*-butyl {[4-(3,5-dioxo-1,2,4-triazolidin-4-yl)benzyl]oxy} carbamate (**14**).

Beginning with commercially available O-(4-Nitrobenzyl)hydroxylamine hydrochloride, BOC protection of the amine group with BOC anhydride and purification by flash column chromatography produced the BOC protected compound **11** in 88% yield. The nitro group was then reduced to an amine with the use of sodium borohydride as a reducing agent in the presence of a nickel acetate tetrahydrate catalyst. After purification by flash column chromatography, compound **12** was obtained in 45% yield. Reaction of compound **12** with previously synthesized compound **1** and purification by flash column chromatography produced compound **13** in 49% yield. Cyclization of compound **13** with potassium hydroxide formed the cyclized compound **14** however, both flash column chromatography and preparative TLC failed to separate the cyclized product from the impurities similar in retention factor.

3.1.2 Oxidation chemistry

The oxidation of urazoles to triazolinediones is a critical step in the synthesis of clickable cyclic diazodicarboxamide precursors and can be accomplished using a variety of oxidants[32, 33]. Oxidants were tested using commercially available 4-phenylurazole as a precursor to produce the cyclic diazodicarboxamide 4-phenyl-1,2,4-triazole-3,5-dione (PTAD) (Table 3.1). Oxidation is indicated by a characteristic red colour change, except in the case of H_2O_2 with hemin where the colour change cannot be observed due to the dark colour of hemin. In this case, oxidation is confirmed by characterization of the final clicked product. Following oxidation testing, *N*-bromosuccinimide with pyridine, sodium nitrite with either acetic acid or trifluoroacetic acid and 1,3-dibromo-5,5-dimethylhydantoin were selected for use in cyclic diazodicarboxamide cold synthesis. Iodination tubes and iodination beads may be more useful for radiosynthesis, as they are intended for small scale use with proteins and contain mild oxidizing agents compatible with delicate biomolecules.

Oxidizing Agent	Colour Change
Potassium peroxymonosulfate	No colour change
m-Chloroperbenzoic acid	No colour change
N-bromosuccinimide, pyridine	Red colour change
Sodium nitrite, acetic acid or trifluoroacetic acid	Red colour change
1,3-dibromo-5,5-dimethylhydantoin	Red colour change
1,3,4,6-tetrachloro-3α,6α-diphenylglucoluril (iodination tubes)	Red colour change
N-chloro-benzenesulfonamide (iodination beads)	Red colour change
H_2O_2, hemin	*N/A

Table 3.1. Oxidation of 4-phenylurazole to produce cyclic diazodicarboxamide PTAD, indicated by a red colour change. *Not applicable; colour change cannot be observed due to the dark colour of hemin. Oxidation was confirmed by LCMS characterization of final clicked product.

3.1.3 Bioconjugation with tyrosine-containing compounds via tyrosine-click chemistry

Following oxidation testing, the oxidation and subsequent conjugation of compound **10** with phenol, L-tyrosine and tyrosine-containing peptide neurotensin NT(8-13) was attempted.

The conjugation of compound **10** with phenol was attempted using 1,3-dibromo-5,5-dimethylhydantoin as an oxidant (Scheme 3.7). Following purification by HPLC, the expected conjugate was produced in poor yields <5%.

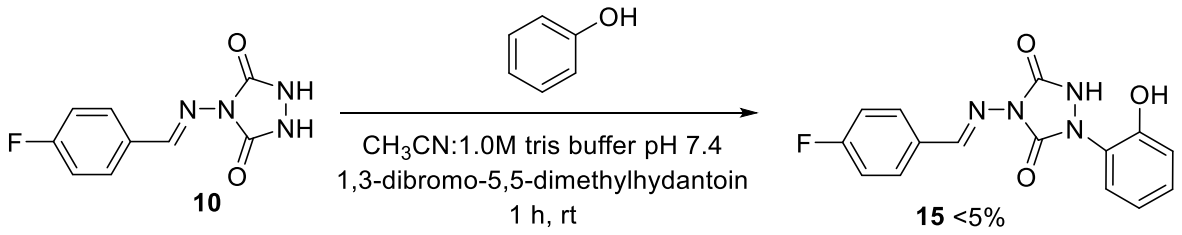

Scheme 3.7. Conjugation of compound **10** with phenol.

The conjugation of compound **10** with L-tyrosine was attempted using sodium nitrite as an oxidant in the presence of acetic acid (Scheme 3.8). Following purification by HPLC, the expected conjugate was produced in poor yields <5%.

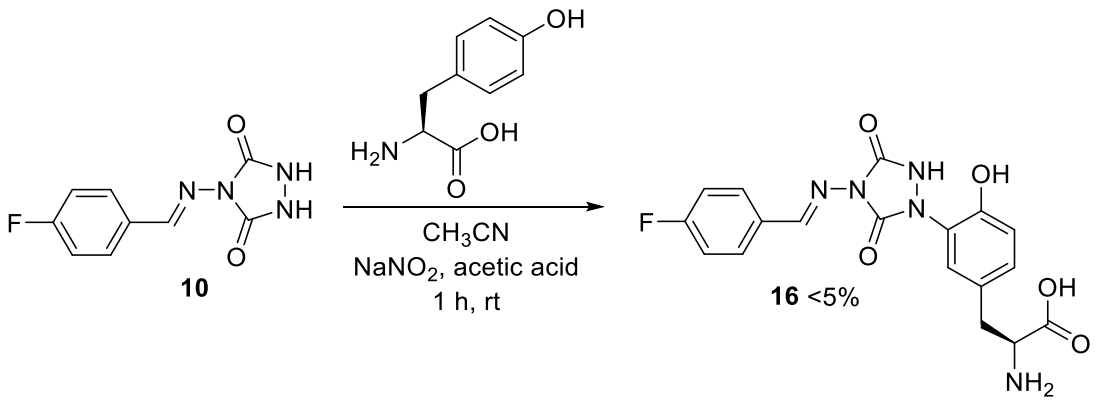

Scheme 3.8. Conjugation of compound **10** with L-tyrosine.

The conjugation of compound **10** with neurotensin NT(8-13) was attempted using *N*-bromosuccinimide as an oxidant in the presence of pyridine (Scheme 3.9). Following purification by HPLC, it was determined that the expected conjugate was not formed. It is important to note that repeating the reaction using 1,3-dibromo-5,5-dimethylhydantoin as an oxidant did not improve yields.

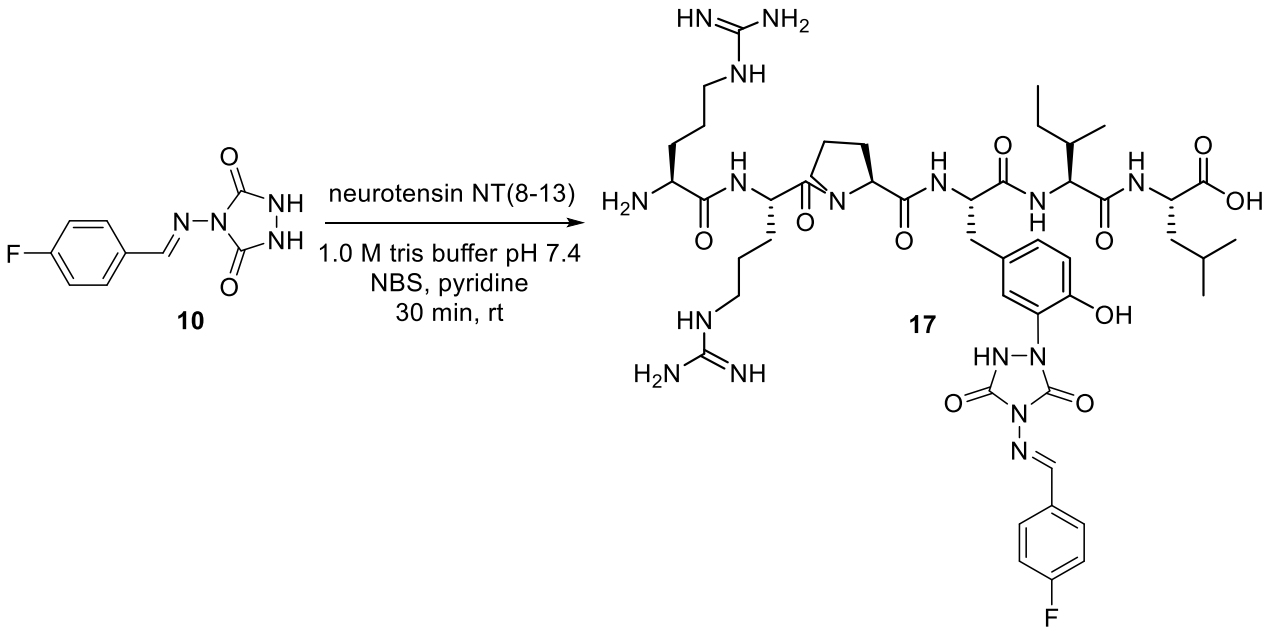

Scheme 3.9. Conjugation of compound **10** with neurotensin NT(8-13).

3.1.4 Radiochemistry with fluorine-18

With compound **10** as a cold reference, radiosynthesis was carried out using 4-[^{18}F]fluorobenzaldehyde as a prosthetic group for fluorine-18.

4-[^{18}F]fluorobenzaldehyde (**18**) can be easily prepared from a 4-(trimethylammonium triflate)benzaldehyde precursor [16]. 4-(trimethylammonium triflate)benzaldehyde, prepared from 4-(dimethylamino)benzaldehyde, provides a good leaving group for subsequent radiofluorination. Radiofluorination can be accomplished using [^{18}F]fluoride, which was prepared from [^{18}O]H_2O in a cyclotron and dried azeotropically. Dry [^{18}F]fluoride was then reacted with 4-(trimethylammonium triflate)benzaldehyde to produce 4-[^{18}F]fluorobenzaldehyde (**18**). Following purification by C18-U cartridge, compound **18** was obtained in 71% radiochemical yield (Scheme 3.10).

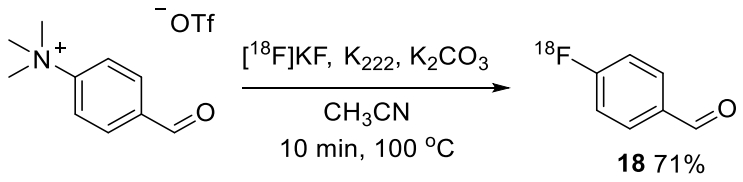

Scheme 3.10. Radiosynthesis of [^{18}F]fluorobenzyaldehyde (**18**).

The radiosynthesis of 4-{[(E)-(4-[^{18}F]fluorophenyl)methylidene]amino}-1,2,4-triazolidine-3,5-dione (**19**) was carried out with urazine and 4-[^{18}F]fluorobenzaldehyde (**18**). Without purification, compound **19** in 92% radiochemical purity (Scheme 3.11).

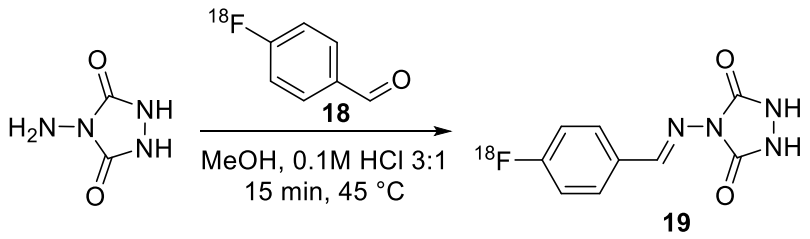

Scheme 3.11. Radiosynthesis of 4-{[(E)-(4-[^{18}F]-fluorophenyl)methylidene]amino}-1,2,4-triazolidine-3,5-dione (**19**).

3.2 Synthesis of luminol derivatives and their application in tyrosine-click chemistry

To further evaluate the application of tyrosine-click chemistry to PET radiochemistry as a bioconjugation technique, ^{18}F-lableled luminol derivatives were designed for comparison with the previously designed cyclic diazodicarboxamides. Cold reference compounds were synthesized, oxidation of luminol derivatives was explored and bioconjugation with tyrosine-containing compounds was attempted in preliminary experiments. Once these preliminary insights had been established, radiochemistry with fluorine-18 was carried out.

3.2.1.1 Synthesis of luminol derivatives as cold reference compounds

The synthesis of cold reference compound *N*-(4-fluorobenzyl)-2-methyl-1,4-dioxo-1,2,3,4-tetrahydrophthalazine-6-carboxamide (**23**) was carried out in three steps: synthesis of an *N*-substituted luminol derivative functionalized with a carboxylic acid group, activation of the carboxylic acid group as either an active ester or an acid chloride and nucleophilic attack by 4-fluorobenzylamine (Scheme 3.12 and Scheme 3.13).

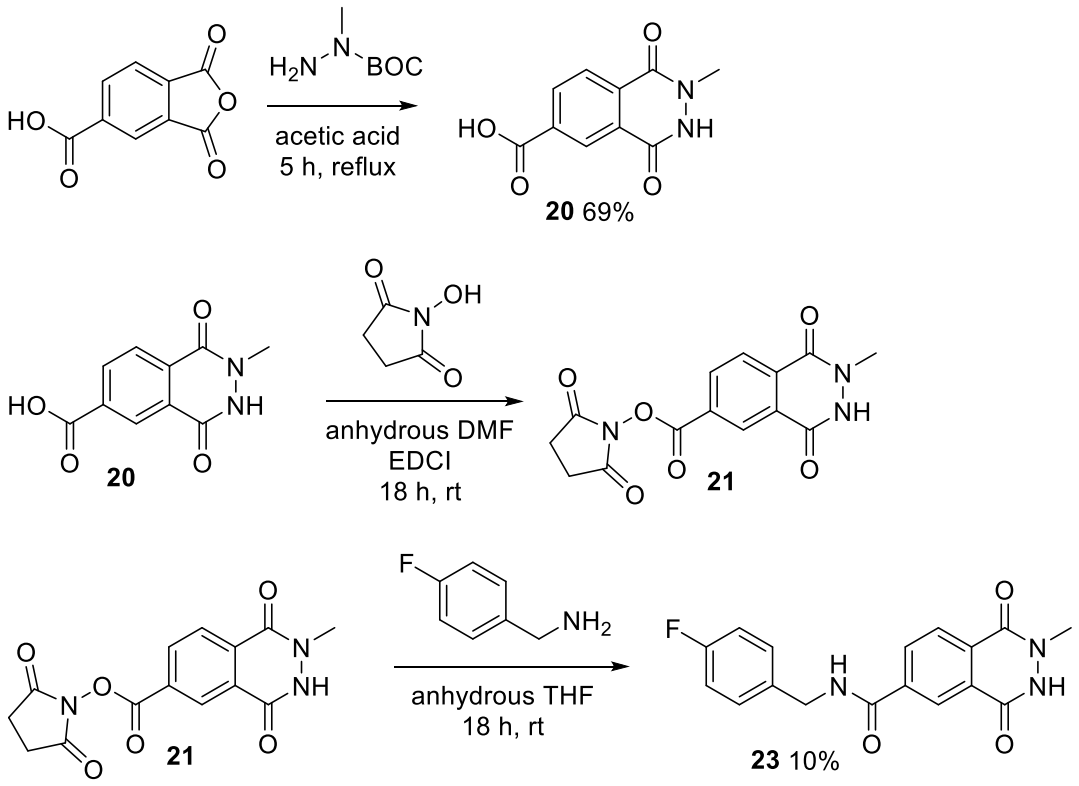

Scheme 3.12. Synthesis of *N*-(4-fluorobenzyl)-2-methyl-1,4-dioxo-1,2,3,4-tetrahydrophthalazine-6-carboxamide (**23**), using an active ester.

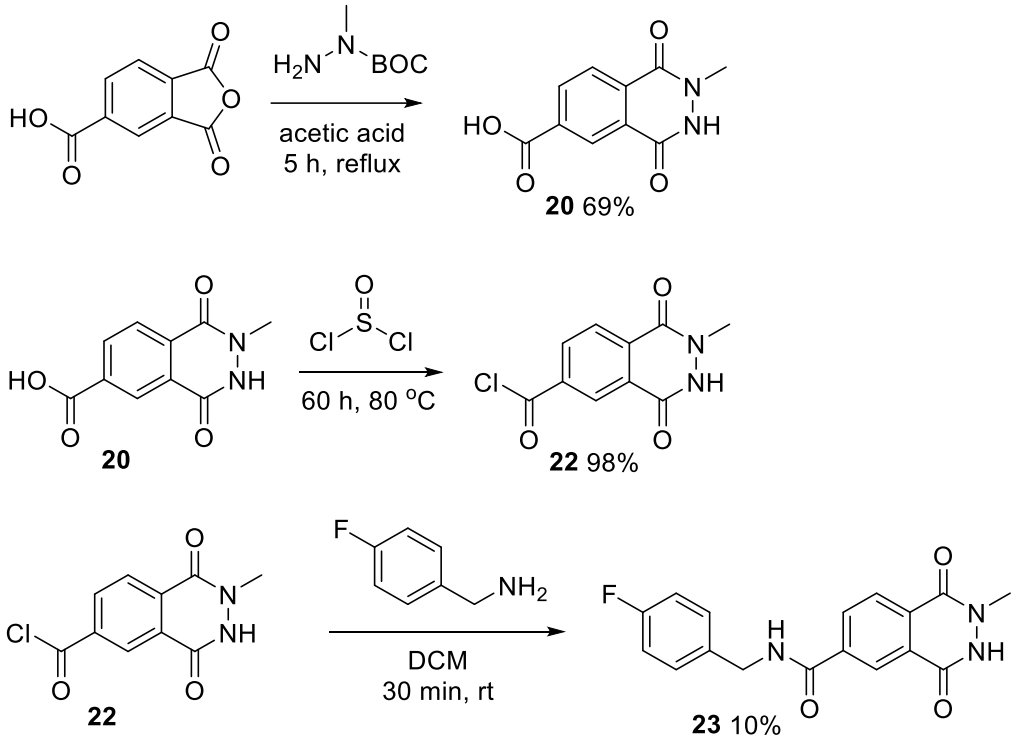

Scheme 3.13. Synthesis of *N*-(4-fluorobenzyl)-2-methyl-1,4-dioxo-1,2,3,4-tetrahydrophthalazine-6-carboxamide (**23**), using an acid chloride.

In the initial step, compound **20** was synthesized from commercially available 1,2,4-benzenetricarboxylic anhydride and 1-Boc-1-methylhydrazine, using glacial acetic acid as a reaction solvent and for removal of the Boc protecting group. After purification by washing with ether, compound **20** was obtained in 69% yield.

Next, compound **20** was reacted with *N*-hydroxysuccinimide, using EDCI as the activating carbodiimide, to yield compound **21**. However, yield could not be determined due to the presence of an impurity, despite purification by silica plug filtration and washing with ether. Similarly, compound **22** was synthesized by reaction of compound **20** with thionyl chloride, which was also used as the reaction solvent. After washing with ether, compound **22** was obtained in 98% yield.

Finally, compound **23** was synthesized using both an active ester and an acid chloride. Compound **23** was synthesized by reaction of compound **21** with 4-fluorobenzylamine. Following purification by flash column chromatography, compound **23** was obtained in 10% yield. Similarly,

compound **23** was synthesized by reaction of compound **22** with 4-fluorobenzylamine. Following purification by flash column chromatography, compound **23** was obtained in 10% yield.

3.2.2 Oxidation of luminol derivatives

Just as with urazoles, the oxidation of luminol derivatives to cyclic diazodicarboxamides is a critical preliminary step for the tyrosine-click reaction. The oxidation capacity of a variety of oxidizing agents was evaluated based on the oxidation of compound **23** and subsequent conjugation with acetyl-L-tyrosine methyl amide (Table 3.1). Oxidizing agents tested included oxidizing agents for iodination (1,3,4,6-tetrachloro-3α,6α-diphenylglucoluril and *N*-chloro-benzenesulfonamide), traditional oxidizing agents (1,3-dibromo-5,5-dimethylhydantoin and *N*-bromosuccinimide in the presence of pyridine) and hydrogen peroxide in the presence of hemin, which has been previously used for the oxidation of luminol derivatives[27, 34]. The iodination tubes and iodination beads failed to oxidize compound **23** while traditional oxidizing agents partially oxidized compound **23**, resulting in poor yields < 5%. Hydrogen peroxide in the presence of hemin demonstrated improved oxidation, resulting in 42% yield.

Oxidizing Agent	**Yield (%)**
1,3,4,6-tetrachloro-3α,6α-diphenylglucoluril (iodination tubes)	No product
N-chloro-benzenesulfonamide (iodination beads)	No product
1,3-dibromo-5,5-dimethylhydantoin	< 5%
N-bromosuccinimide, pyridine	< 5%
H_2O_2, hemin	42%

Table 3.2. Oxidation of *N*-(4-fluorobenzyl)-2-methyl-1,4-dioxo-1,2,3,4-tetrahydrophthalazine-6-carboxamide (**23**) and conjugation with acetyl-L-tyrosine methyl amide.

3.2.3 Bioconjugation of luminol derivatives with tyrosine-containing compounds via tyrosine-click chemistry

Following the synthesis and optimization of oxidation of luminol derivatives, conjugation with various tyrosine derivatives were attempted.

The conjugation of compound **23** with L-tyrosine was attempted using hydrogen peroxide in the presence of hemin as an oxidant (Scheme 3.14). Following purification by HPLC, it was determined that the expected conjugate was not formed.

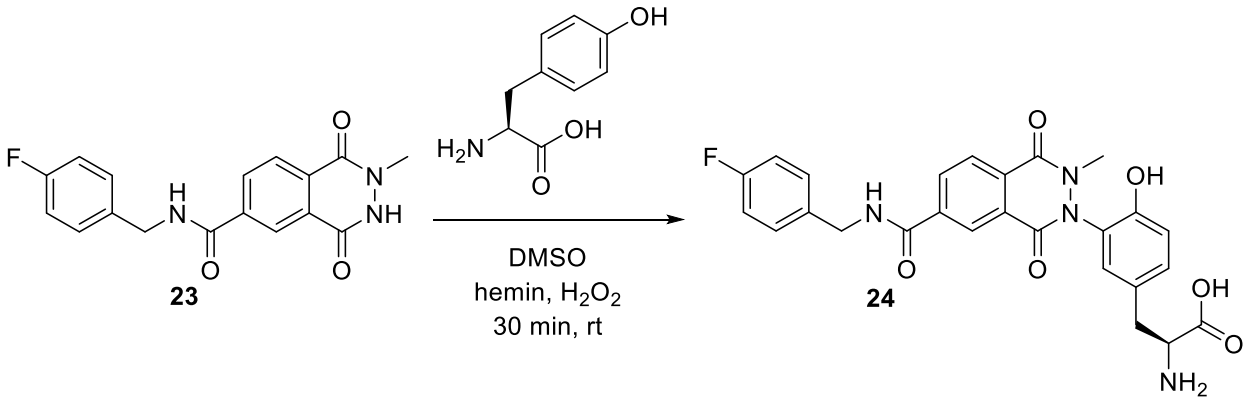

Scheme 3.14. Conjugation of compound **23** with L-tyrosine.

Similarly, the conjugation of compound **23** with acetyl-L-tyrosine methyl amide was attempted using hydrogen peroxide in the presence of hemin as an oxidant (Scheme 3.15). Following purification by HPLC, compound **25** was obtained in 42% yield.

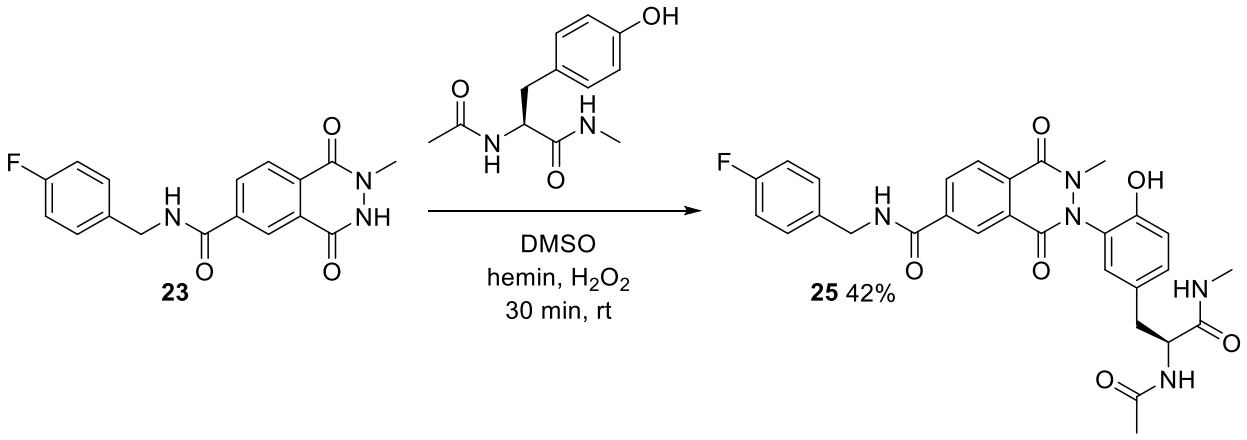

Scheme 3.15. Conjugation of compound **23** with acetyl-L-tyrosine methyl amide.

Finally, the conjugation of compound **23** with neurotensin (8-13) was attempted using hydrogen peroxide in the presence of hemin as an oxidant (Scheme 3.16). Following purification by HPLC, it was determined that the expected conjugate was not formed.

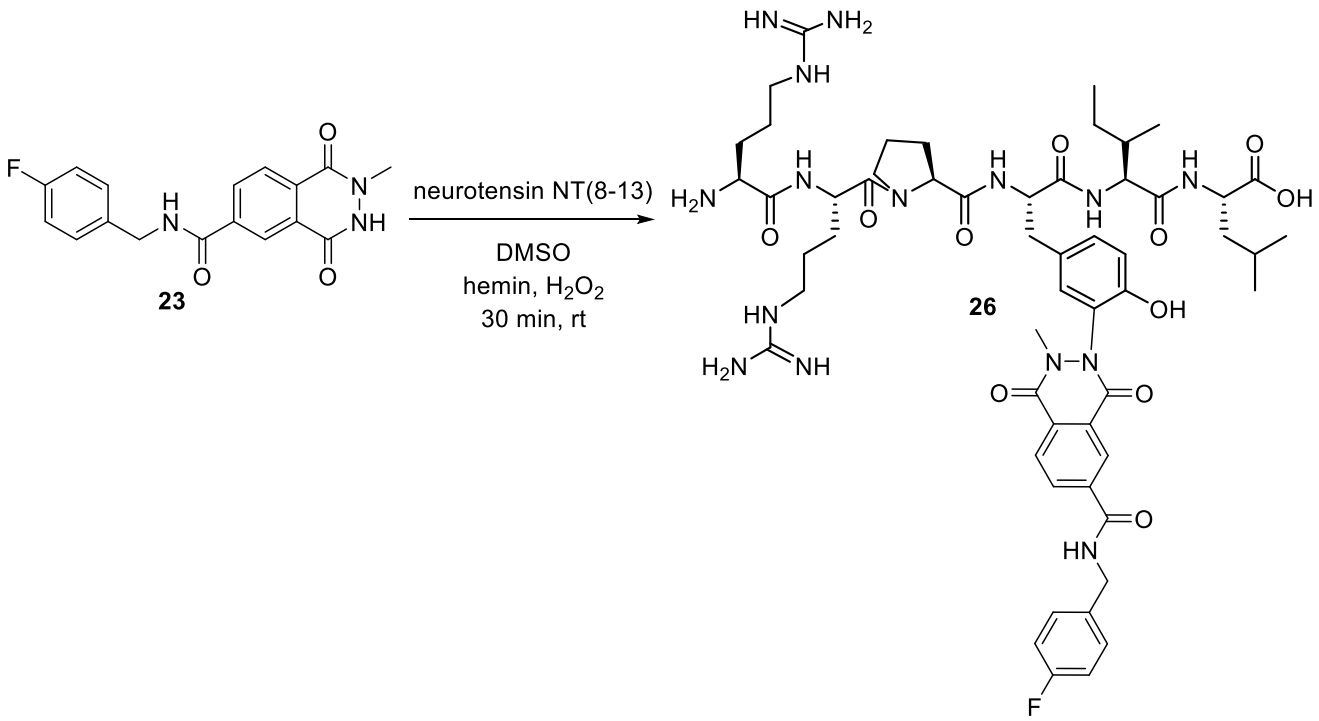

Scheme 3.16. Conjugation of compound **23** with neurotensin (8-13).

3.2.4 Radiochemistry with fluorine-18

With compound **25** as a cold reference, radiosynthesis was carried out using 4-[^{18}F]fluorobenzylamine as a prosthetic group for fluorine-18.

4-[^{18}F]fluorobenzylamine (**28**) can be easily prepared, both manually or using an automated synthesis unit, from a 4-cyano-*N,N,N*-trimethylanilinium trifluoromethansulfonate precursor, which provides a good leaving group for subsequent radiofluorination. [^{18}F]fluoride was prepared from [^{18}O]H_2O in a cyclotron and dried azeotropically. Dry [^{18}F]fluoride was then reacted with 4-cyano-*N,N,N*-trimethylanilinium trifluoromethansulfonate to produce 4-[^{18}F]fluorobenzonitrile (**27**). 4-[^{18}F]fluorobenzonitrile (**27**) was reduced to 4-[^{18}F]fluorobenzylamine (**28**), using sodium borohydride as a reducing agent in the presence of a nickel chloride catalyst. Following purification by C18-U cartridge, compound **28** was obtained in 24% radiochemical yield (Scheme 3.17) [30].

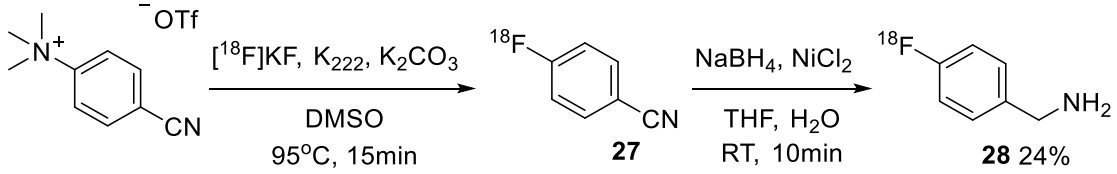

Scheme 3.17. Radiosynthesis of [^{18}F]fluorobenzylamine (**28**).

Radiosynthesis of compound **29** was carried out using both an active ester and an acid chloride. The radiosynthesis of compound **29** was first carried out with compound **21** and 4-[^{18}F]fluorobenzylamine (**28**). Compound **29** was produced in 78% radiochemical purity (Scheme 3.18). The radiosynthesis of compound **29** was then carried out with compound **22** and 4-[^{18}F]fluorobenzylamine (**28**). Compound **29** was produced in 82% radiochemical purity and following purification by radio-HPLC, compound **29** was obtained in 48% radiochemical yield (Scheme 3.19).

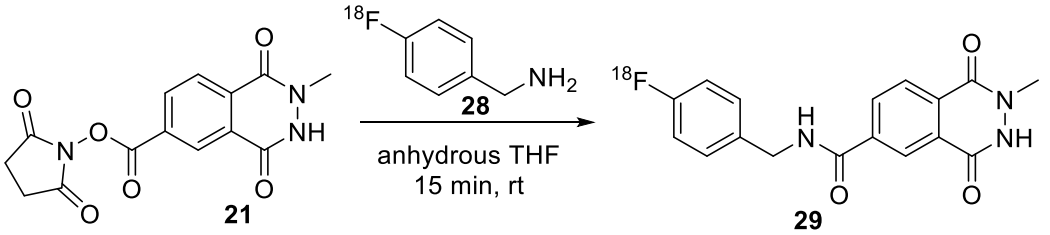

Scheme 3.18. Radiosynthesis of *N*-(4-[^{18}F]fluorobenzyl)-2-methyl-1,4-dioxo-1,2,3,4-tetrahydrophthalazine-6-carboxamide (**29**), using an active ester.

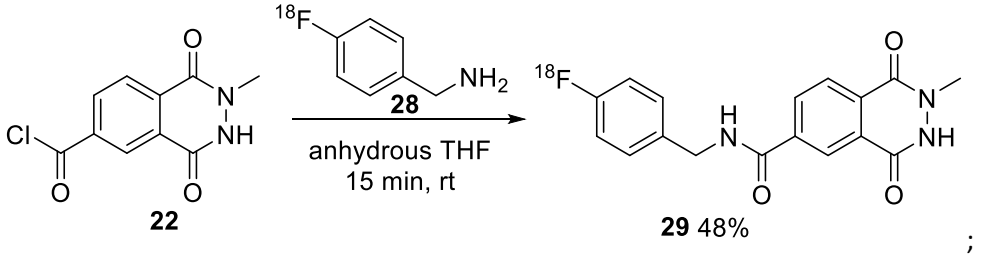

;

Scheme 3.19. Radiosynthesis of *N*-(4-[^{18}F]fluorobenzyl)-2-methyl-1,4-dioxo-1,2,3,4-tetrahydrophthalazine-6-carboxamide (**29**), using an acid chloride.

Conjugation of compound **29** with acetyl-L-tyrosine methyl amide was carried out using hydrogen peroxide in the presence of hemin as an oxidant. Following purification by radio-HPLC, compound **30** was obtained in 27% radiochemical yield (Scheme 3.20).

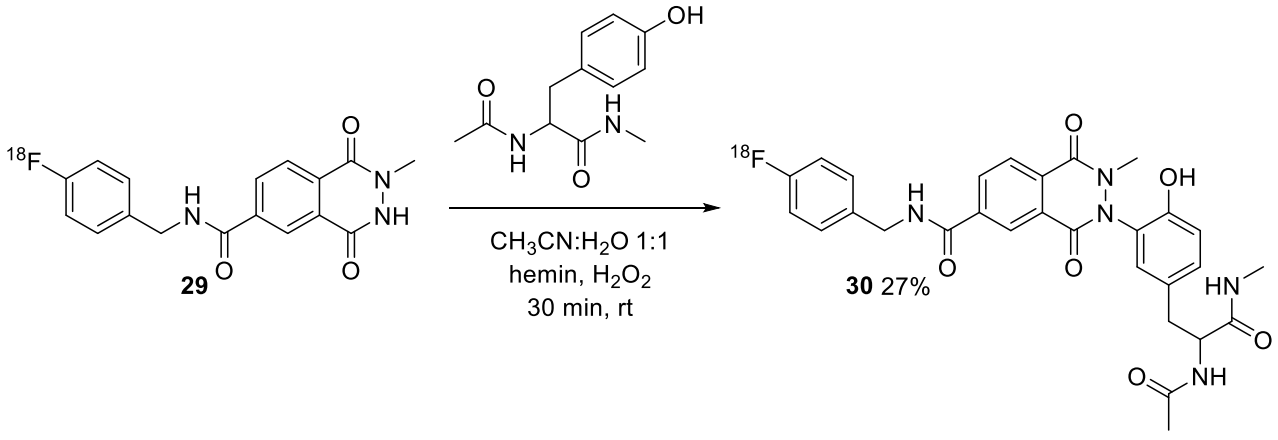

Scheme 3.20. Conjugation of compound **29** with acetyl-L-tyrosine methyl amide.

3.3 Synthesis of aryl diazonium salts and their application in tyrosine labeling chemistry

To evaluate the application of azo coupling to PET radiochemistry as a bioconjugation technique, ^{64}Cu- and ^{68}Ga-labeled aryl diazonium salts were designed. Cold reference compounds were synthesized and bioconjugation with tyrosine residues was attempted in preliminary experiments. Once these preliminary insights had been established, radiochemistry with copper-64 and gallium-68 was carried out and bioconjugation with tyrosine-containing biomolecules was attempted.

3.3.1 Synthesis of aryl diazonium salts as cold reference compounds

The synthesis of cold reference compounds **35**, **36**, **37** and **38** were carried out in three steps: chelation, diazotization and azo coupling with L-tyrosine and neurotensin NT(8-13).

2-S-(4-Aminobenzyl)-1,4,7-triazacyclononane-1,4,7-triacetic acid (*p*-NH_2-Bn-NOTA) was used as a chelator. Copper and gallium chelates were prepared from [^{nat}Cu]copper chloride and [^{nat}Ga]gallium chloride. Following purification by HPLC, products were obtained in quantitative yields and used for the next step (Scheme 3.21 and Scheme 3.22).

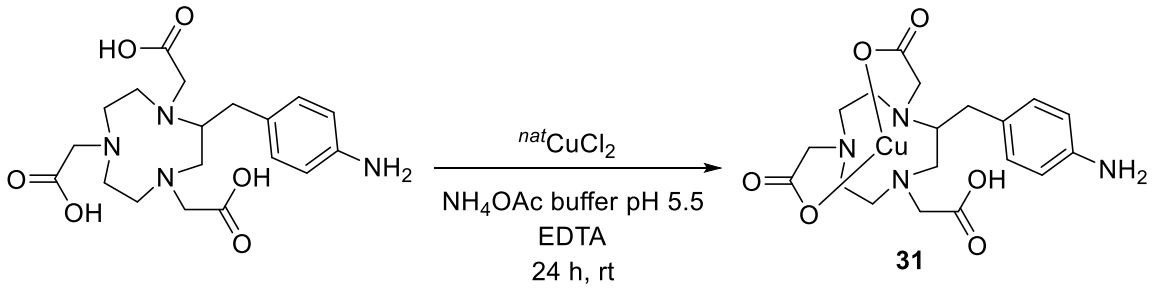

Scheme 3.21. Chelation of [^{nat}Cu]copper chloride with *p*-NH_2-Bn-NOTA.

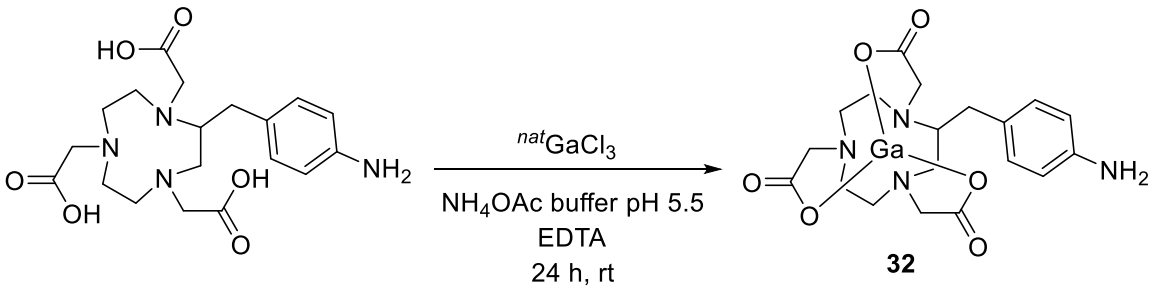

Scheme 3.22. Chelation of [^{nat}Ga]gallium chloride with *p*-NH_2-Bn-NOTA.

Diazotization of compound **31** and compound **32** was carried out using sodium nitrite under acidic conditions. The respective diazonium salts were formed *in situ* and used without purification (Scheme 3.23 and Scheme 3.24).

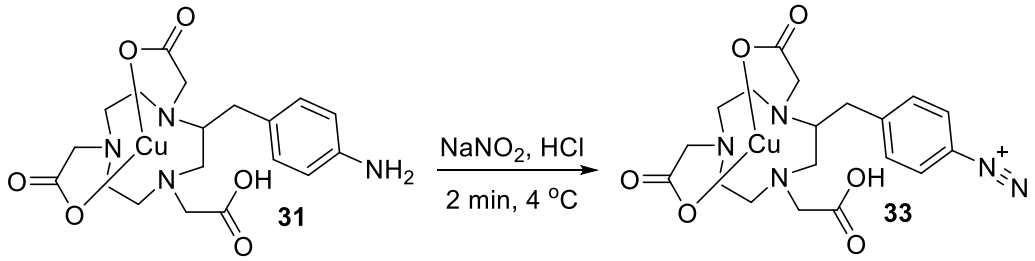

Scheme 3.23. Diazotization of ^{nat}Cu-NOTA chelate.

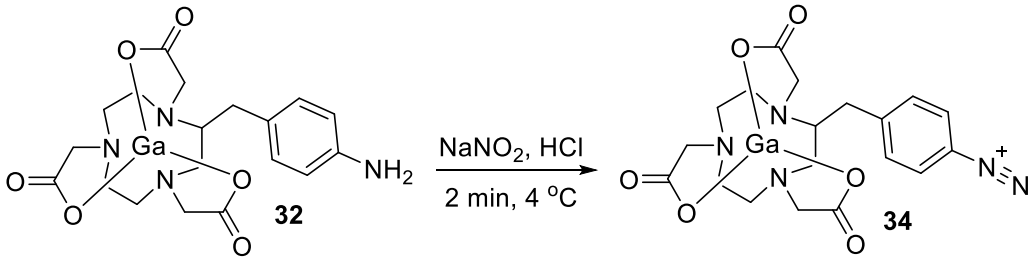

Scheme 3.24. Diazotization of ^{nat}Ga-NOTA chelate.

3.3.2 Azo coupling of aryl diazonium salts with tyrosine-containing biomolecules

Compounds **33** and **34** were then coupled with L-tyrosine. Coupling was carried out at pH 8-9 under mild, aqueous conditions. Following purification by HPLC, compounds **35** and **36** were obtained in 28% and 7% yields, respectively (Scheme 3.25 and Scheme 3.26).

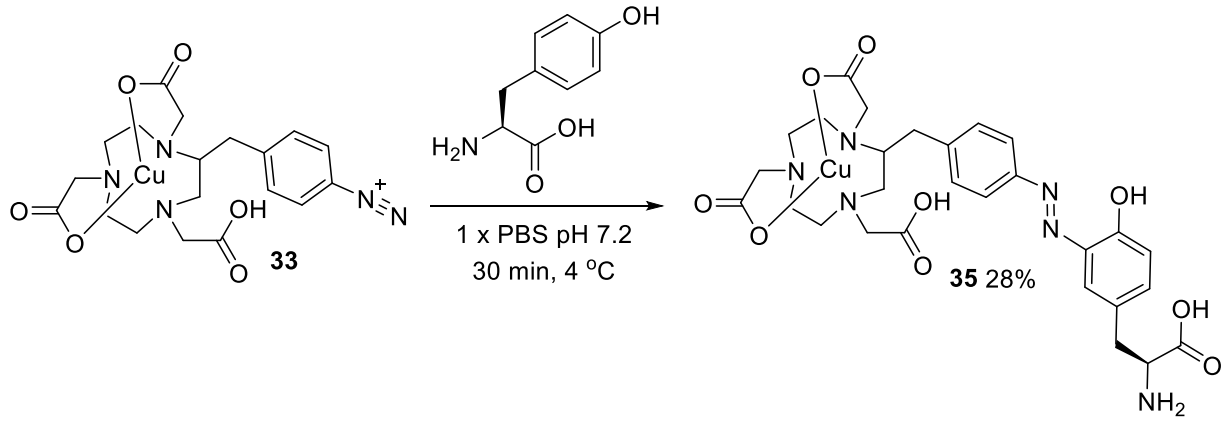

33

Scheme 3.25. Conjugation of compound **33** with L-tyrosine.

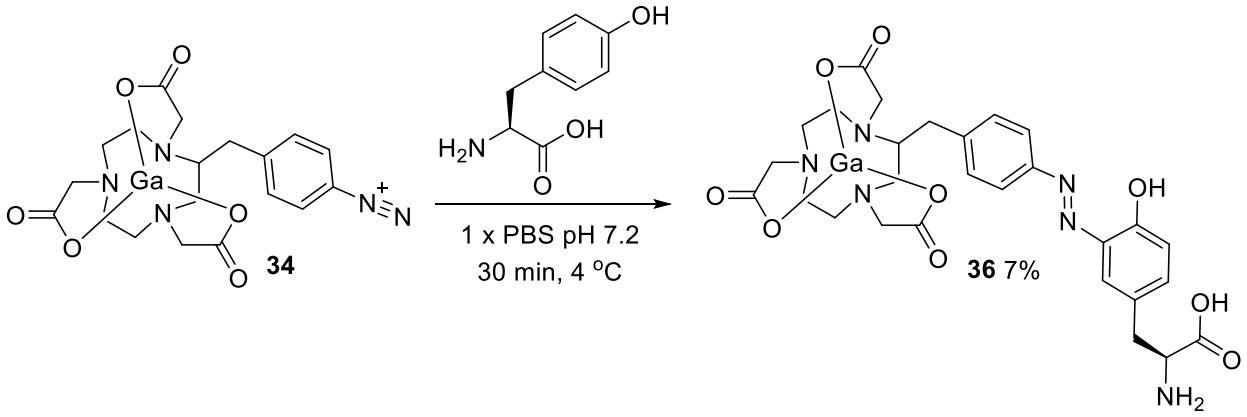

34

Scheme 3.26. Conjugation of compound **34** with L-tyrosine.

Compounds **33** and **34** were also coupled with neurotensin NT(8-13). Similarly, coupling was carried out at pH 8-9 under mild, aqueous conditions. Following purification by HPLC, compounds **37** and **38** were obtained in 76% and 66% yields, respectively (Scheme 3.27 and Scheme 3.28).

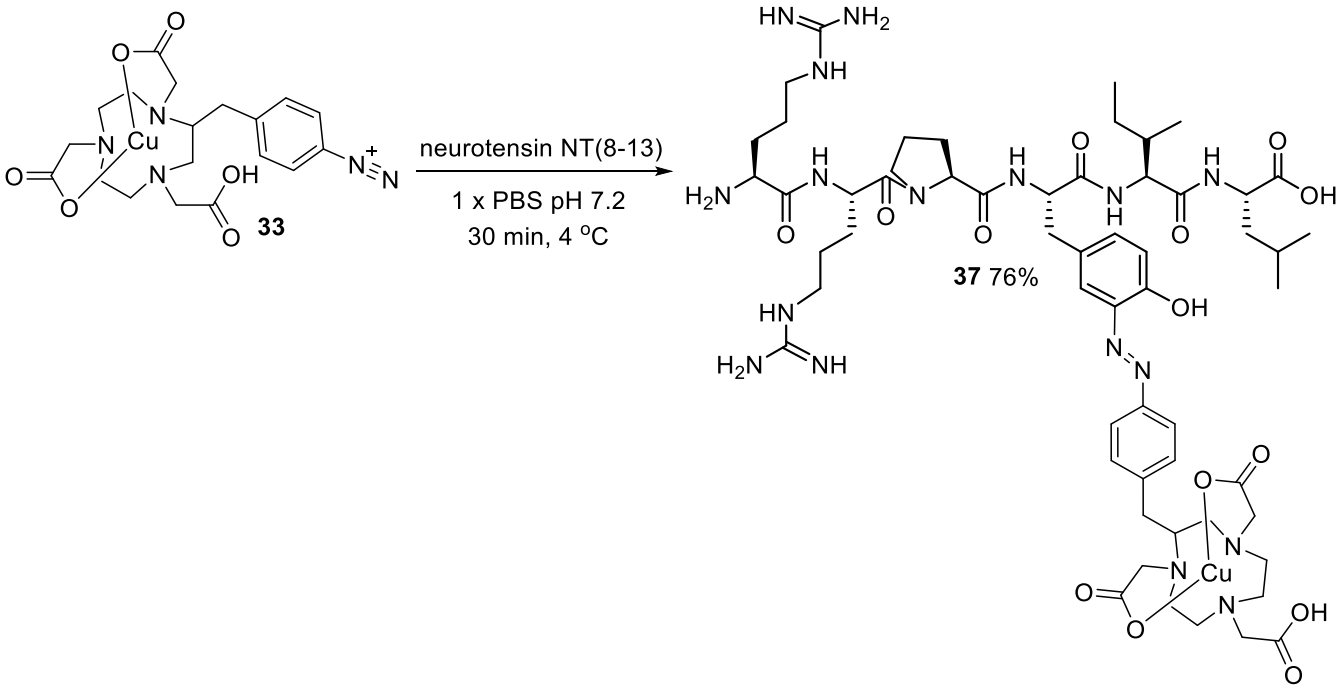

Scheme 3.27. Conjugation of compound **33** with neurotensin NT(8-13).

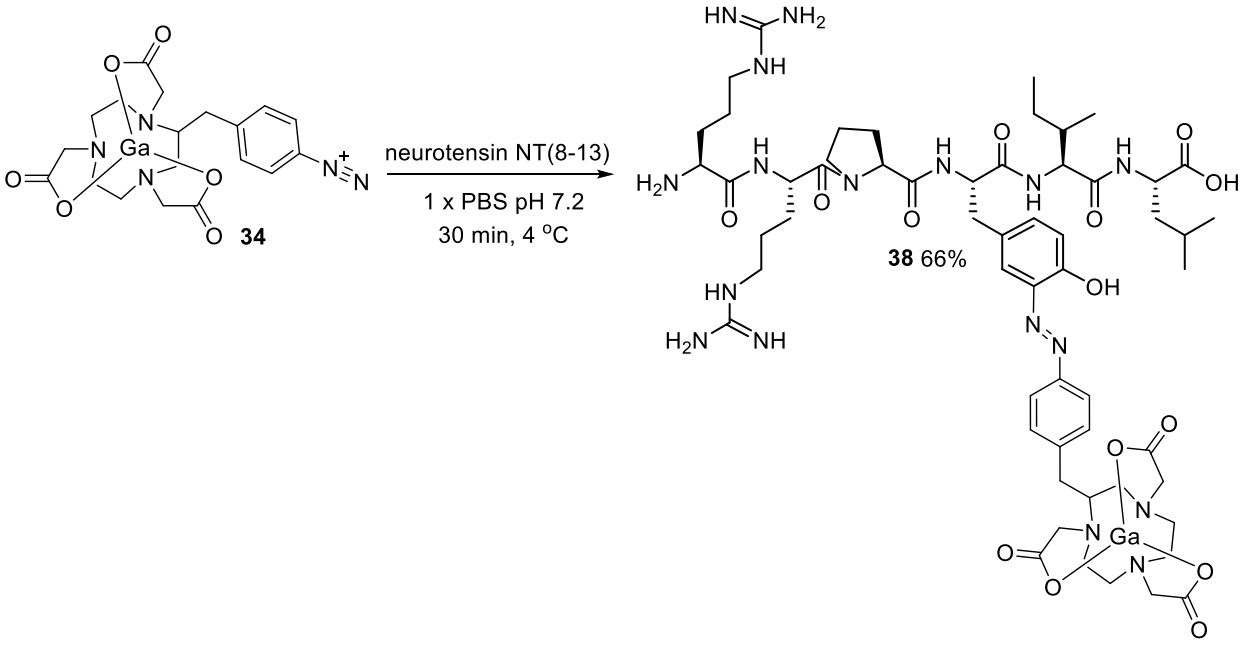

Scheme 3.28. Conjugation of compound **34** with neurotensin NT(8-13).

Following isolation of compounds **37** and **38**, IC_{50} determination was carried out via a radiometric competitive binding assay in neurotensin receptor 1 expressing HT-29 cells (Helmholtz-Zentrum Dresden-Rossendorf). When compared to unmodified neurotensin NT(8-13), ^{nat}Ga and ^{nat}Cu-labeled neurotensin NT(8-13) demonstrated comparable binding affinity, with IC_{50} values of 42 picomolar and 163 picomolar, respectively (Table 3.3, Figure 3.2).

Peptide	**IC_{50} value (pM)**
NT(8-13)	33
Cu-NOTA-NT(8-13)	163
Ga-NOTA-NT(8-13)	42

Table 3.3. IC_{50} values of neurotensin NT(8-13), ^{nat}Cu-labeled neurotensin NT(8-13) (**37**) and ^{nat}Ga-labeled neurotensin NT(8-13) (**38**).

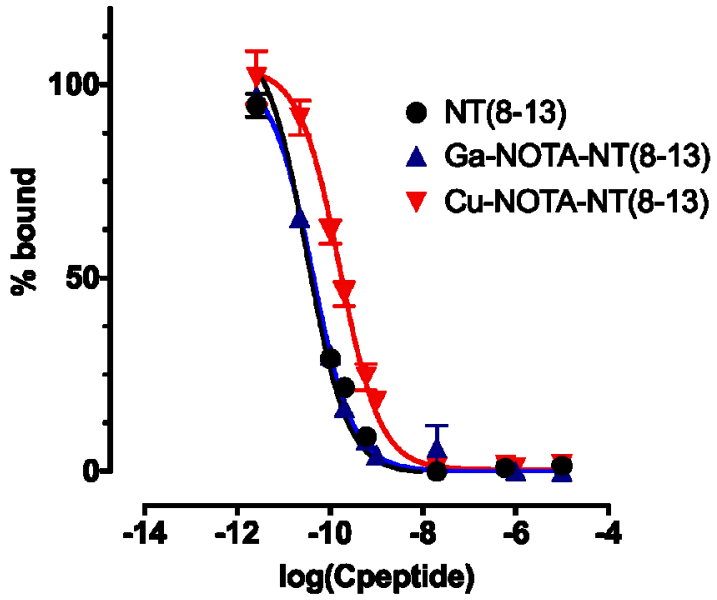

Figure 3.2. Competitive binding curve of compound **37** and compound **38** compared to neurotensin NT(8-13).

3.3.3 Radiochemistry with copper-64 and gallium-68

Radiosynthesis of aryl diazonium salts was carried out using [^{64}Cu]copper chloride and [^{68}Ga]gallium chloride for chelation with *p*-NH_2-Bn-NOTA, followed by *in situ* diazotization of chelates. [^{64}Cu]copper chloride was obtained from Washington University (St. Louis, MO, U.S.A), where it was prepared from ^{64}Ni in a cyclotron. Chelation with *p*-NH_2-Bn-NOTA produced the expected chelate (**39**) in >98% radiochemical purity and was used without further purification (Scheme 3.29). [^{68}Ga]gallium chloride was eluted from a [^{68}Ga]gallium germanium-68/gallium-68 generator using 0.6 M HCl. Chelation with *p*-NH_2-Bn-NOTA produced the expected chelate (**40**) in >94% radiochemical purity and was used without further purification (Scheme 3.30).

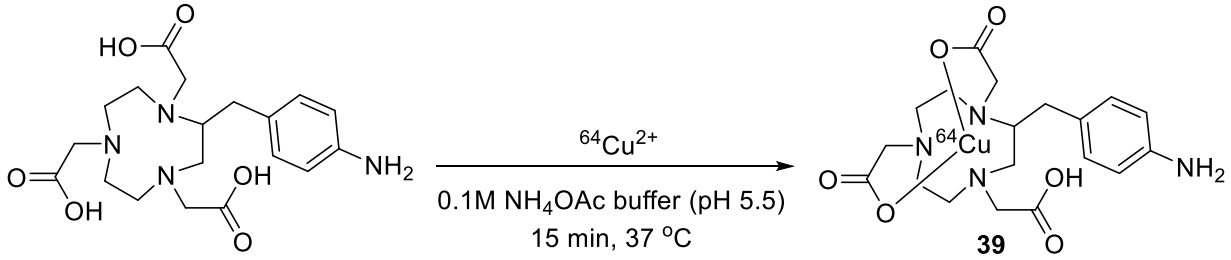

Scheme 3.29. Chelation of [^{64}Cu]copper chloride with *p*-NH_2-Bn-NOTA.

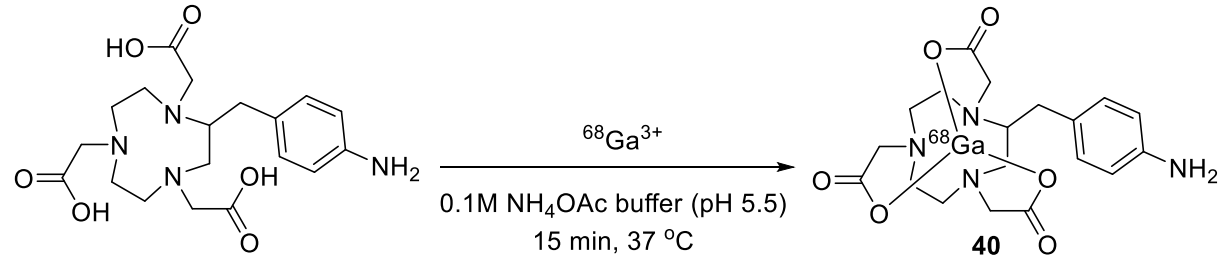

Scheme 3.30. Chelation of [^{68}Ga]gallium chloride with *p*-NH_2-Bn-NOTA.

Diazotization of compound **39** and compound **40** was carried out using sodium nitrite under acidic conditions. The respective diazonium salts were formed *in situ* and used without purification (Scheme 3.31 and Scheme 3.32). Radiochemical purity could not be determined due to instability of diazonium salts on TLC however, complete conversion is expected.

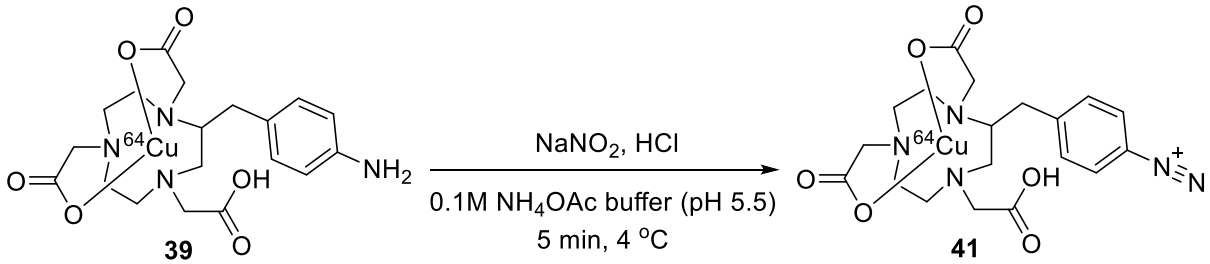

Scheme 3.31. Diazotization of ^{64}Cu-NOTA chelate.

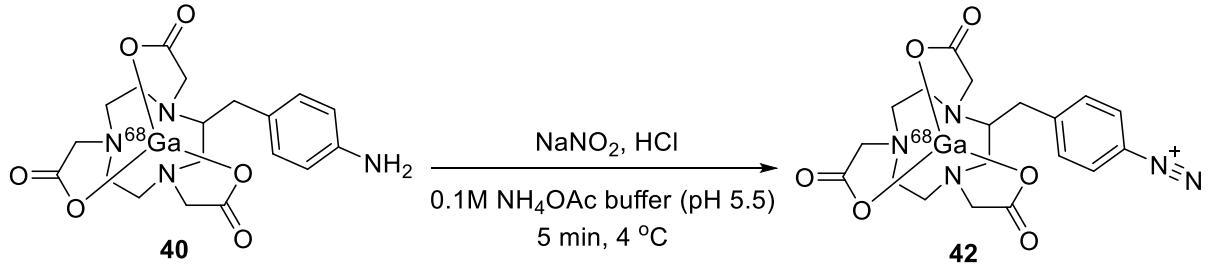

Scheme 3.32. Diazotization of ^{68}Ga-NOTA chelate.

3.3.4 Azo coupling of radiolabeled aryl diazonium salts with tyrosine-containing biomolecules

Following radiosynthesis, the utility of these radiometal-containing aryl diazonium salts was evaluated via coupling with tyrosine residues on the amino acid, peptide, protein and nanoparticle level.

^{64}Cu and ^{68}Ga-labeled diazonium salts were first tested in a coupling reaction with L-tyrosine. With compound **35** and compound **36** as cold references, coupling of compound **41** and compound **42** with L-tyrosine was carried out at pH 8-9 under mild, aqueous conditions. Following purification by radio-HPLC, compound **43** and compound **44** were obtained in 56% and 80% radiochemical yields, respectively (Scheme 3.33 and Scheme 3.34).

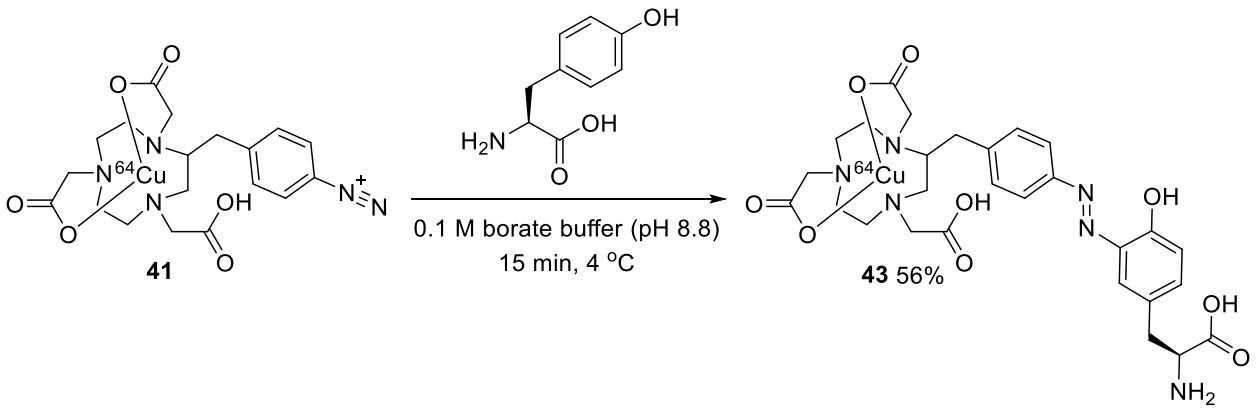

Scheme 3.33. Conjugation of compound **41** with L-tyrosine.

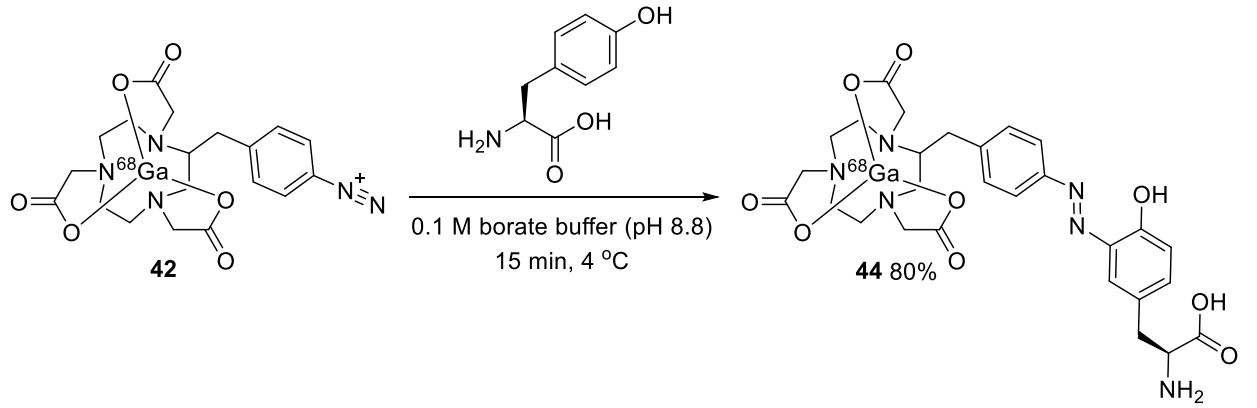

Scheme 3.34. Conjugation of compound **42** with L-tyrosine.

Next, the ability of ^{64}Cu and ^{68}Ga-labeled diazonium salts to couple with model peptide neurotensin NT(8-13) was evaluated. Neurotensin NT(8-13) is a hexapeptide which contains a single tyrosine residue, which is preceded by two arginine residues and a proline residue and followed by an isoleucine and a leucine residue. With compound **37** and compound **38** as cold references, coupling of compound **41** and compound **42** with neurotensin NT(8-13) was carried out at pH 8-9 under mild, aqueous conditions. Following purification by radio-HPLC, compound **45** and compound **46** were obtained in 19% and 45% radiochemical yields, respectively (Scheme 3.35 and Scheme 3.36).

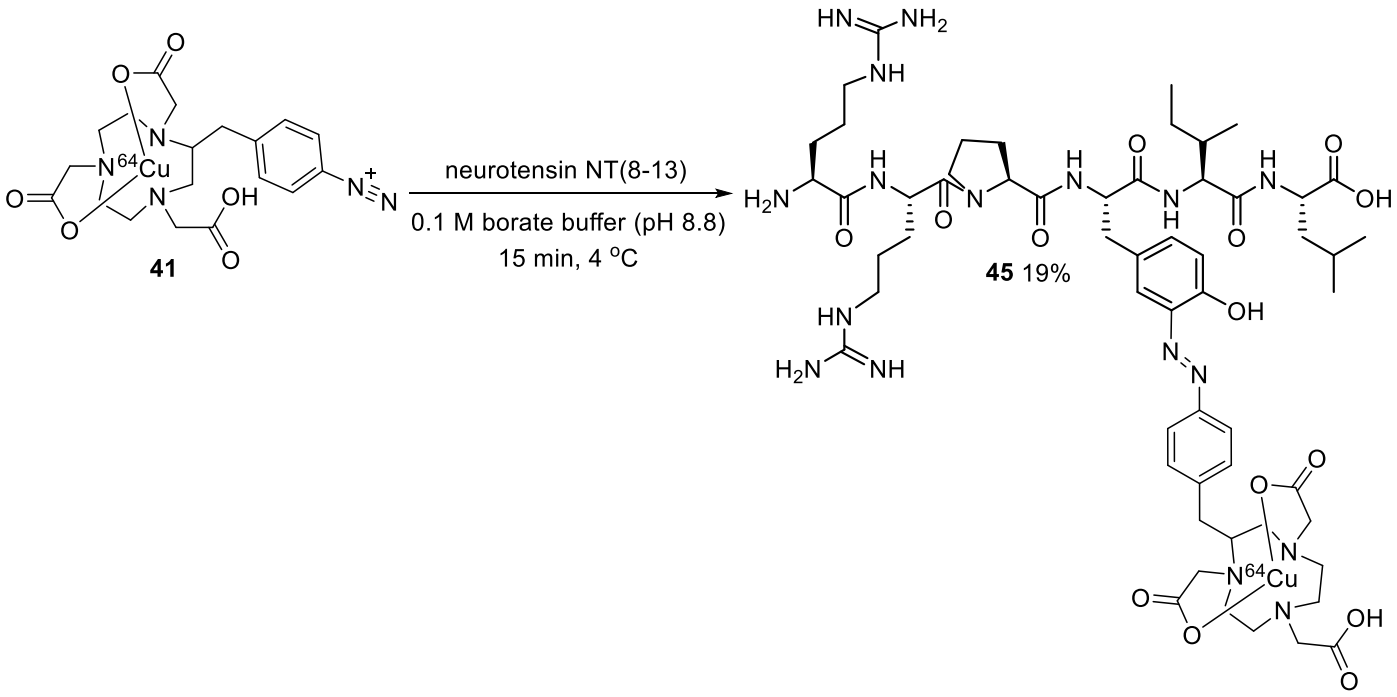

Scheme 3.35. Conjugation of compound **41** with neurotensin NT(8-13).

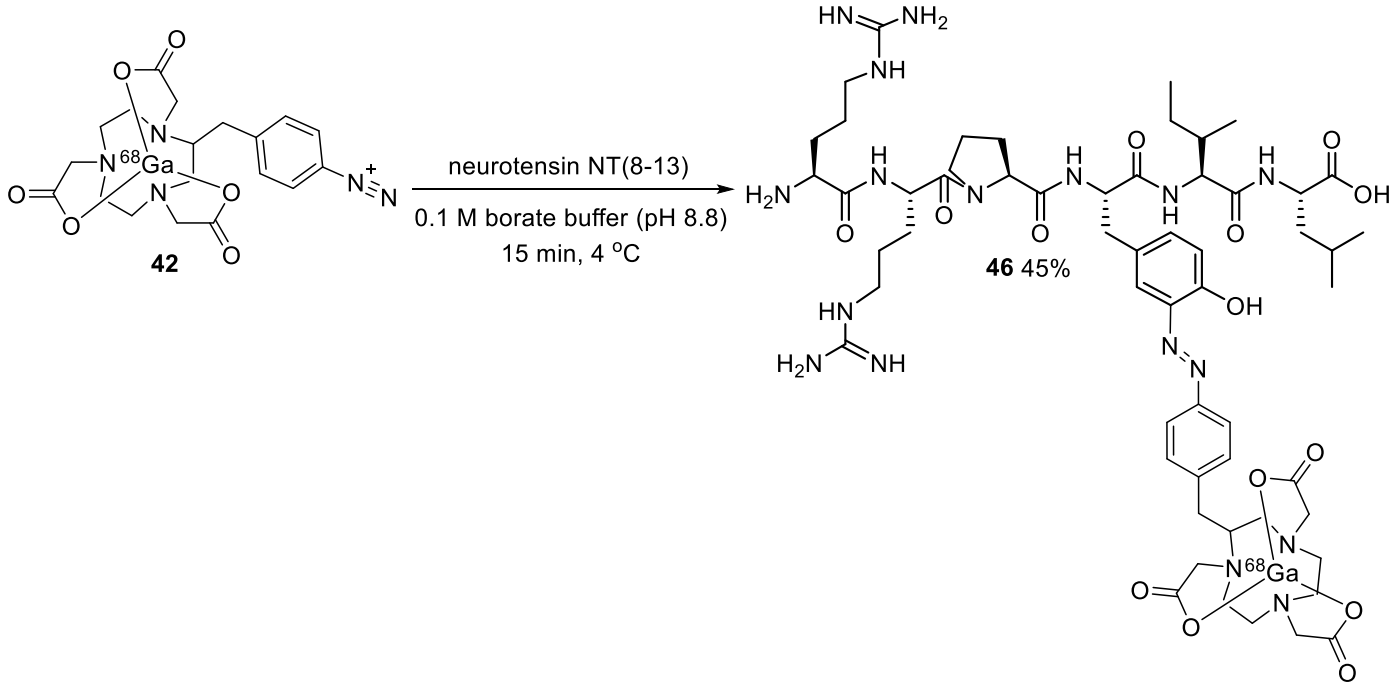

Scheme 3.36. Conjugation of compound **42** with neurotensin NT(8-13).

While labeling of amino acids and peptides does not necessarily require mild reaction conditions, labeling of delicate proteins requires mild aqueous conditions and for this reason is often more challenging. To demonstrate the value of this technique in protein labeling chemistry, ^{64}Cu-labeled compound **41** was used to label model protein human serum albumin (HSA). HSA contains 18 tyrosine residues and is a common blood pool marker, which makes it a good candidate for PET studies. For this reason, the ^{68}Ga-labeled compound **42** was not used due to the short half-life of ^{68}Ga (67.7 minutes), which is not useful for monitoring later time points *in vivo*. Coupling of compound **41** with HSA was carried out at pH 8-9 under mild, aqueous conditions. Following purification by size exclusion chromatography (SEC), compound **47** was obtained in 20% radiochemical yield, and >95% radiochemical purity (Scheme 3.37).

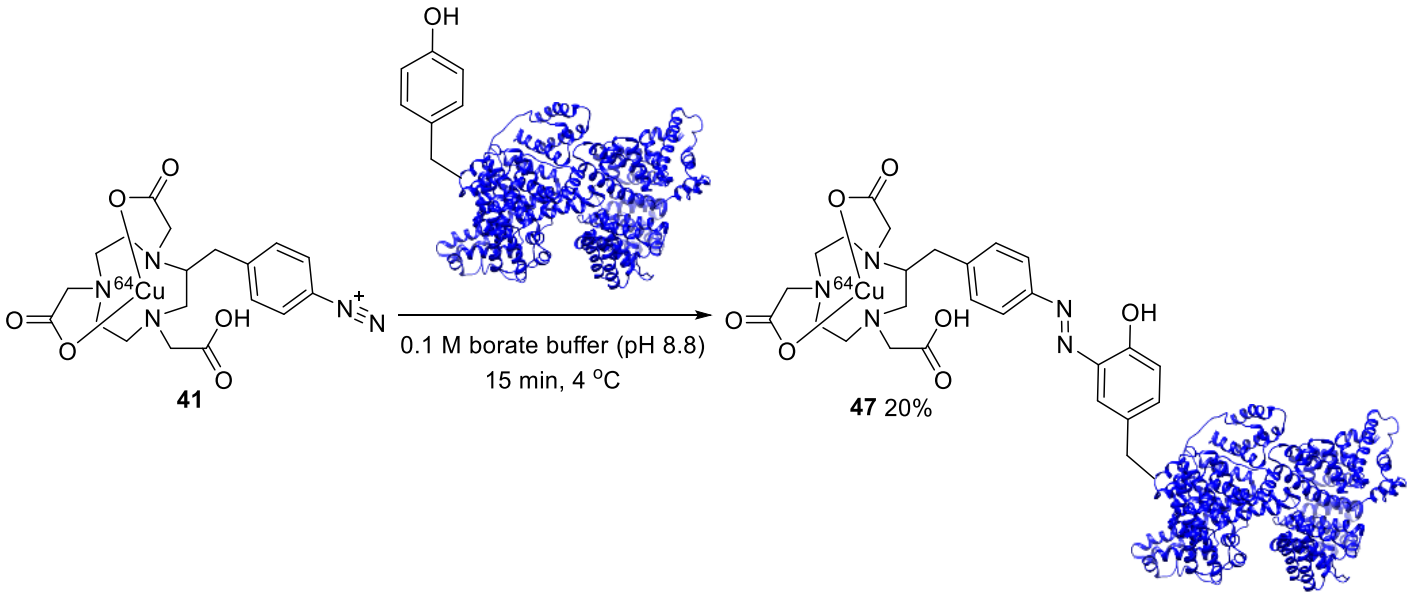

Scheme 3.37. Conjugation of compound **41** with HSA.

To further characterize the ^{64}Cu-labeled HSA (**47**) after SEC purification, an aliquot was taken for SDS-PAGE analysis. Coomassie staining and the corresponding radioactive scan of the gel clearly shows the expected 66 kDa band, indicating radiolabeled HSA in the radiochemically pure fractions isolated by SEC purification (lanes 3 – 6) as well as in the crude reaction mixture prior to SEC purification (lane 9) (Figure 3.3).

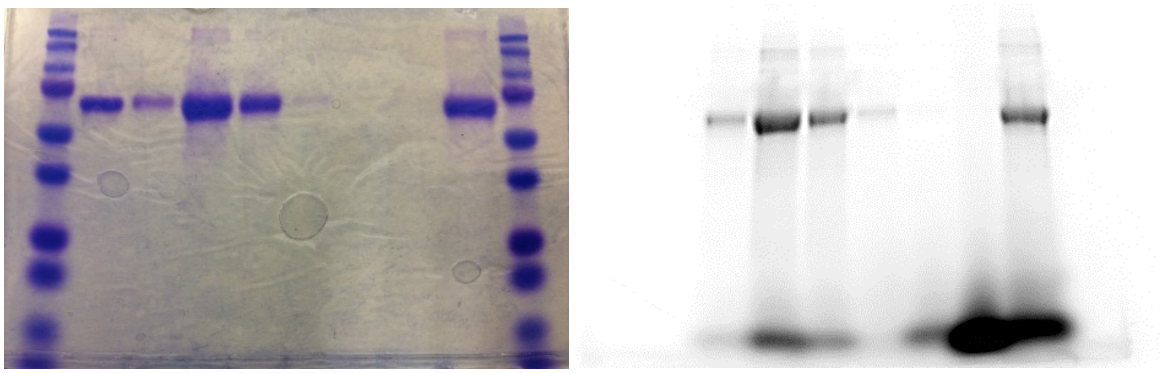

Figure 3.3. SDS-PAGE with coomassie stain and radioactive scan. Lane 1 ladder, lane 2 cold HSA, lanes 3 – 6 radiochemically pure fractions, lanes 7 – 8 ^{64}Cu-labeled *p*-NH_2-Bn-NOTA, lane 9 crude reaction mixture, lane 10 ladder.

Once ^{64}Cu-labeled HSA (**47**) was isolated, a normal BALB/c mouse was injected with 5 MBq of ^{64}Cu-labeled HSA (**47**) in 200 µL of phosphate buffered saline (PBS) and monitored for up to 24 hours post-injection (Figure 3.4). PET studies show significant heart uptake and slow blood pool clearance. Time-activity curves show primarily liver metabolism (Figure 3.5).

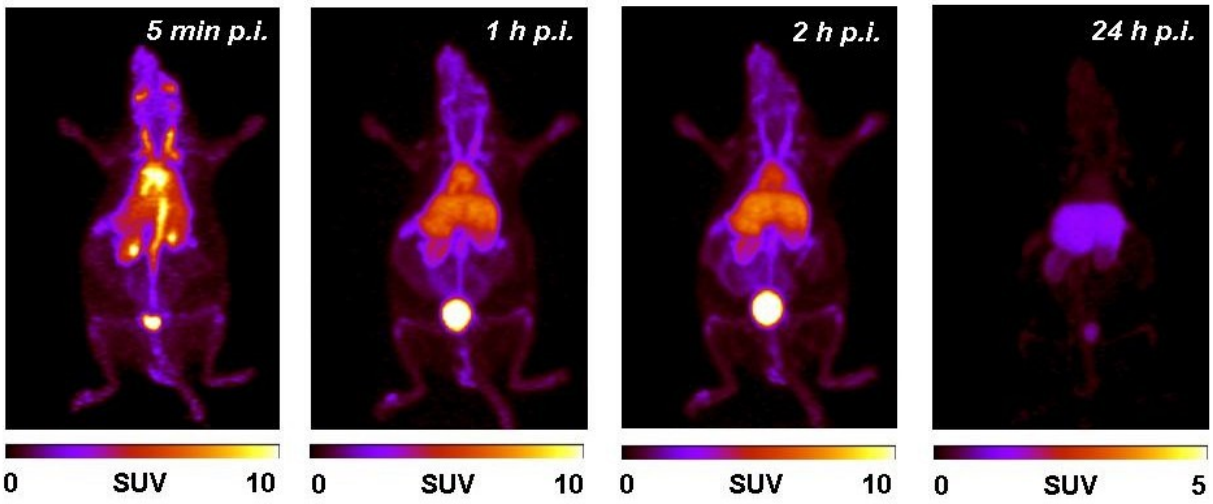

Figure 3.4. Coronal PET images of 5 MBq of ^{64}Cu-labeled HSA in normal BALB/c mouse.

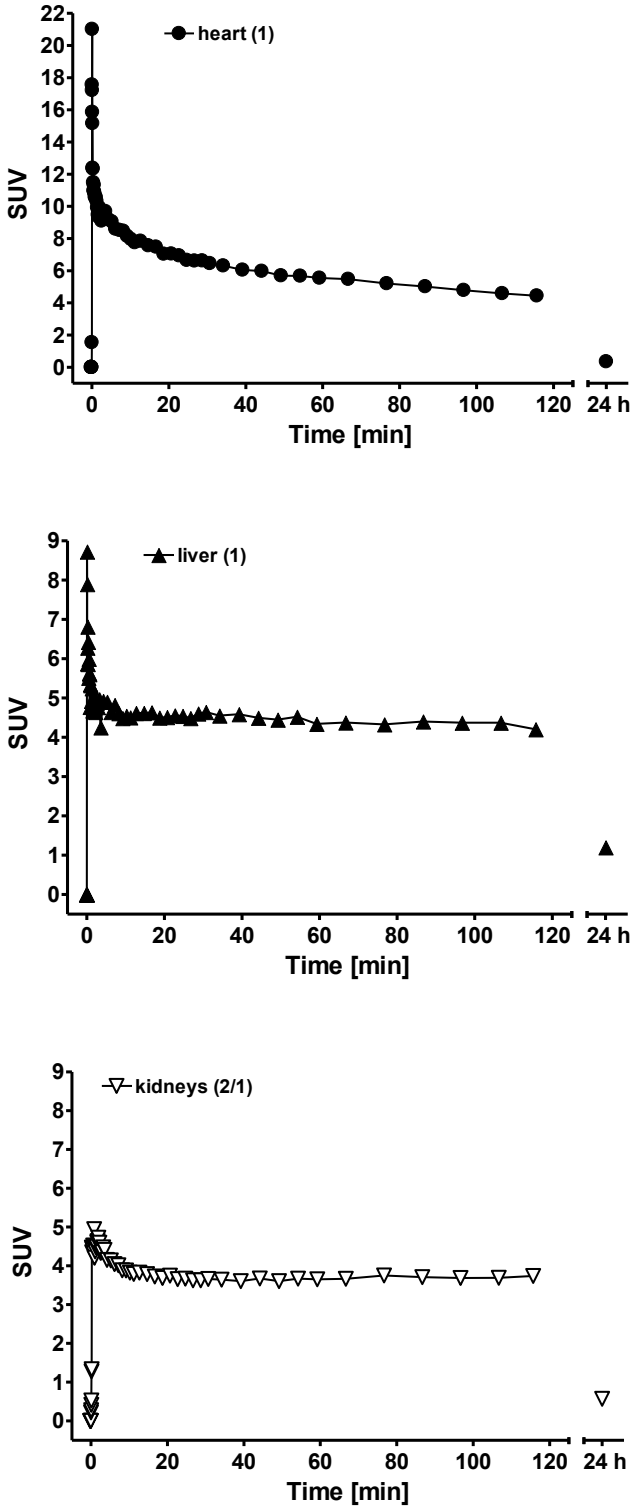

Figure 3.5. Time-activity curves of ^{64}Cu-labeled HSA in the heart, liver and kidneys of normal BALB/c mouse.

Finally, this labeling technique was applied to nanoparticles. ^{64}Cu-labeled compound **41** was used to label tobacco mosaic virus (TMV), a 300 nm rod-shaped virus with a tyrosine-containing protein capsid. Coupling of compound **41** with TMV was carried out at pH 8-9 under mild, aqueous conditions. Following purification by size exclusion chromatography (SEC), compound **48** was obtained in 9% radiochemical yield, and >94% radiochemical purity (Scheme 3.38).

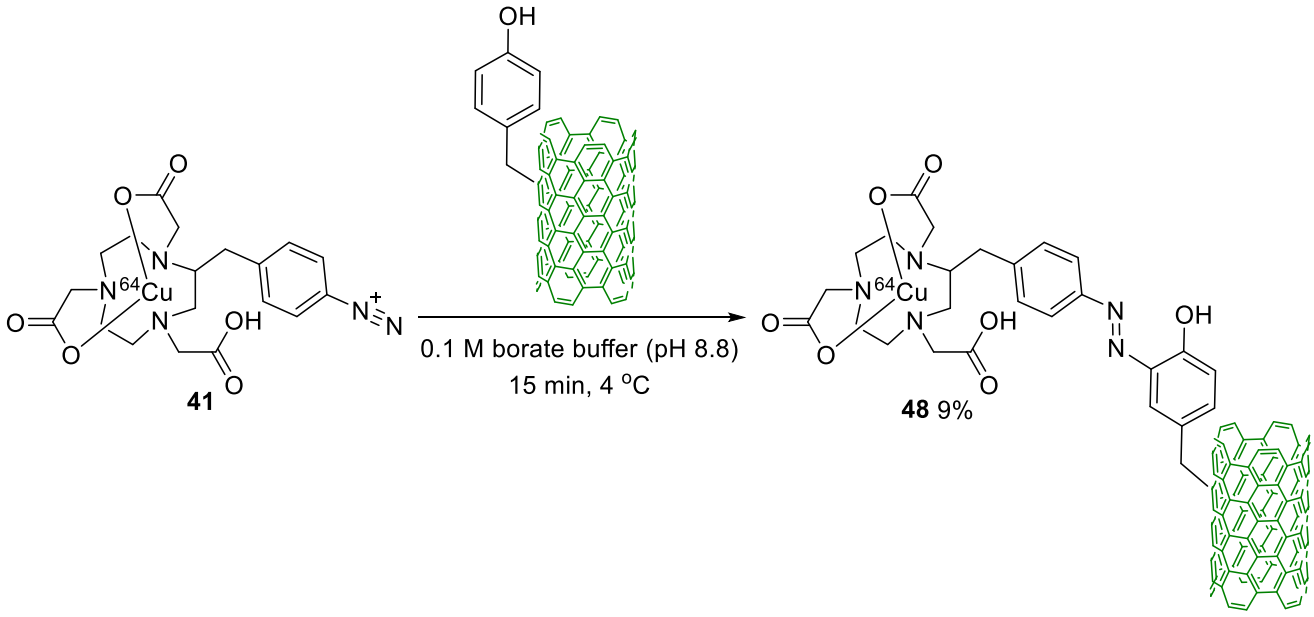

Scheme 3.38. Conjugation of compound **41** with TMV.

4.0 DISSCUSSION

4.1 Stability of cyclic diazodicarboxamides in the tyrosine-click reaction

As strong dienophiles, diazodicarboxamides participate in ene-like reactions with diene derivatives. Cyclic diazodicarboxamides, specifically triazolinediones such as MTAD and PTAD, have recently been reported to participate in a click reaction with the phenol ring of tyrosine [23, 24]. The reactivity of such cyclic diazodicarboxamides can be attributed, in part, to the cis configuration of the azo bond and are typically prepared from urazoles by oxidation of the nitrogen-nitrogen single bond to a double bond [35]. However, their synthesis can be challenging due to the instability of triazolinediones as well as their sensitivity to water, light, heat, acids and bases [36]. Optimization of the oxidation step included nitrogen (IV) oxides and halogens as oxidants, as well as other oxidation methods, which were often carried out immediately before use in the next reaction due to the instability of the oxidized compound [37]. Based on these early examples in literature, the synthesis of a small library of triazolinedione derivatives was attempted for use as cold reference compounds. Unfortunately, the majority of the proposed derivatives, such as compound **5** and compound **7**, could not be formed, or in the case of compound **9** and compound **14**, were formed based on TLC and LCMS analysis of the crude reaction mixture but could not be isolated, as only evidence of degradation was observed following purification of compound **9** by HPLC and multiple side products with retention factors similar to that of compound **14** prevented isolation by both flash column chromatography and preparative TLC. Of the proposed derivatives, compound **10** was successfully isolated and characterized by ^{1}H NMR and MS. However, when conjugation of compound **10** with phenol and L-tyrosine was attempted using a variety of different oxidants, including *N*-bromosuccinimide with pyridine, sodium nitrite with either acetic acid or trifluoroacetic acid and 1,3-dibromo-5,5-dimethylhydantoin, clicked products were obtained in very poor yields (<5%). This is likely due to the instability and inevitable degradation of these compounds shortly after oxidation. Interestingly, when conjugation of compound **10** with tyrosine-containing peptide neurotensin NT(8-13) was attempted, the expected clicked product was not present and only a degradation product was observed, based on MS analysis. However, this degradation product consists of a urazine clicked to neurotensin NT(8-13), which suggests that the cyclic diazodicarboxamide clicked to neurotensin NT(8-13) first and then degraded shortly afterwards, leaving the urazine component of the cyclic

diazodicarboxamide clicked to neurotensin NT(8-13) (Figure 4.1). This result further supports the conclusion that low yields are partially attributable to the instability of the cyclic diazodicarboxamide rather than of the efficiency of the tyrosine-click reaction. Using compound **10** as a cold reference, the ^{18}F-containing compound **19** was synthesized in excellent radiochemical purities (>91%) without purification. Unfortunately, since conjugation of compound **10** with neuroteinsin NT(8-13) was unsuccessful, conjugation of the ^{18}F-containing compound **19** with the tyrosine-containing peptide could not be evaluated, as a cold reference could not be generated. Therefore, tyrosine-click chemistry with triazolinediones is not a feasible approach for the incorporation of ^{18}F into tyrosine-based biomolecules, due to the instability of these compounds.

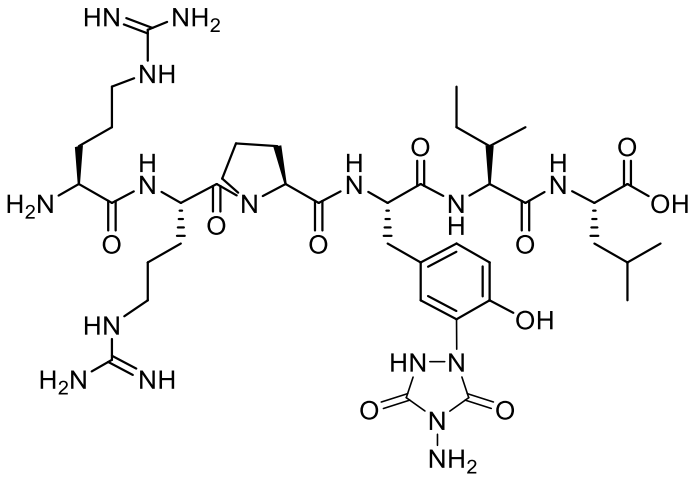

Figure 4.1. Urazine-neurotensin NT(8-13) conjugate.

In contrast, the synthesis of cyclic diazodicarboxamides from luminol derivatives has proven to be less challenging. Luminol derivatives have recently been reported as a more stable alternative to the traditionally used triazolinediones in the tyrosine-click reaction [29]. Their improved stability, which is attributed to their phthalazinedione sub structure, allows for improved chemoselectivity and yields in comparison with the previously used triazolinediones, which degrade to produce an electrophilic isocyanate product. Oxidation can be carried out *in situ* using hydrogen peroxide as an oxidant in the presence of a hemin or horseradish-peroxidase catalyst, in a one pot reaction with tyrosine-containing compounds [38]. Prior to the synthesis of luminol derivatives as cold reference compounds, the effect of *N*-substitution on the reactivity of luminol derivatives was evaluated. Luminol derivatives with either an *N*-phenyl or an *N*-methyl group

were synthesized and their reactivity was compared with that of commercially available phthalhydrazide (Figure 4.2). Following conjugation with *p*-cresol, using the hydrogen peroxide with hemin oxidation system, an overall increase in yield was observed with the *N*-substituted derivatives. Specifically, a 20% increase was observed for the *N*-methyl substituted derivative. These results were consistent with that of the literature, where a 34% increase in yield was reported with *N*-methyl substituted derivatives [29]. Based on these preliminary results, the synthesis of an *N*-methylated luminol derivative was attempted. Following a simple three step synthesis, simple purification by flash column chromatography and characterization by ^{1}H NMR, ^{13}C NMR and LCMS, compound **23** was obtained. The superiority of the hydrogen peroxide with hemin oxidation system was demonstrated by oxidation testing with compound **23** using either *N*-bromosuccinimide with pyridine, 1,3-dibromo-5,5-dimethylhydantoin or hydrogen peroxide with hemin as oxidants in a click reaction with acetyl-L-tyrosine methyl amide. The use of hydrogen peroxide with hemin oxidation system resulted in a 37% increase in yield when compared to the other oxidants. Moving forward, the conjugation of compound **23** with L-tyrosine and acetyl-Ltyrosine methyl amide was attempted. Using the hydrogen peroxide with hemin oxidation system, conjugation with both L-tyrosine and acetyl-L-tyrosine methyl amide was carried out as a one pot reaction. Unfortunately, the tyrosine-click reaction was not successful with L-tyrosine and was only successful when both the N-terminus and C-terminus were protected. Interestingly, literature does not report conjugation of luminol derivatives with L-tyrosine but rather acetyl-L-tyrosine methyl amide or tyrosine-containing angiotensin II [29]. Despite these reports, conjugation of compound **23** with tyrosine-containing peptide neurotensin NT(8-13) was not successful. Further investigation into conjugation of luminol derivatives with other tyrosine-containing peptides was not carried out. Using compound **23** and **25** as cold references, the ^{18}F-containing compound **29** was synthesized and isolated in 48% radiochemical yield, using radio-HPLC. Subsequent conjugation of compound **29** with aectyl-L-tyrosine methyl amide produced the expected conjugate in 27% radiochemical yield, following purification by radio-HPLC. Unfortunately, since conjugation of compound **23** with neuroteinsin NT(8-13) was unsuccessful, conjugation of the ^{18}F-containing compound **29** with the tyrosine-containing peptide could not be evaluated, as a cold reference could not be generated. Therefore, tyrosine-click chemistry with luminol derivatives may be a feasible approach for the incorporation of ^{18}F into tyrosine-based biomolecules, though it requires further optimization.

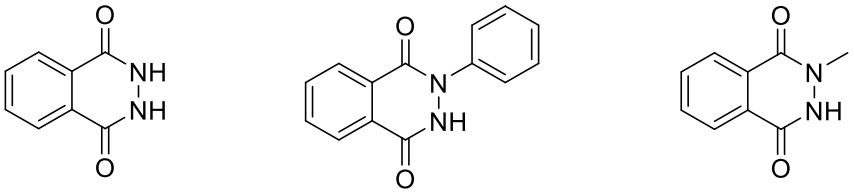

Figure 4.2. *N*-substitution of luminol derivatives; phthalhydrazide and *N*-phenyl and *N*-methyl substituted derivatives.

4.2 A pre-labeling approach to the preparation of radiometal-containing aryl diazonium salts

Aryl diazonium salts are known to undergo an electrophilic aromatic substitution reaction with electron rich aromatic systems, forming a diazo bond [19]. They can therefore act as highly reactive precursors for an azo coupling reaction with the phenol ring of tyrosine and are most reactive near pH 9 [20]. Typically, radiometal-protein conjugates are prepared using a post-labeling approach, in which chelator-containing aryl diazonium salts are first coupled with a tyrosine-containing protein followed by a final chelation step [22]. However, when this strategy was implemented for the synthesis of a NOTA-tyrosine conjugate and a NOTA-peptide conjugate, coupling was not successful. The coupling of *p*-NH_2-Bn-NOTA with L-tyrosine was attempted several times using a variety of different reaction conditions (Table 4.1). Unfortunately, no coupled product was observed based on LCMS analysis of the crude reaction mixture as well as LCMS analysis of peaks collected after HPLC separation. To determine if the charged NOTA starting material or the reaction conditions themselves were responsible for the lack of coupling, the coupling of 3-fluoroaniline with L-tyrosine was attempted using the same reaction conditions (Table 4.2). Surprisingly, coupled products were observed in both attempts. As well, the coupling of *p*-NH_2-Bn-NOTA with neurotensin NT(8-13) was also attempted in 1 x PBS (pH 7.2) and the pH was adjusted to 8 with the addition of a small amount of sodium hydroxide. As expected, no coupled product was observed and only unreacted neurotensin NT(8-13) was present, based on LCMS analysis. Since the only variable that differed between successful and unsuccessful attempts was the starting material, it can be concluded that the NOTA starting material is interfering with the coupling reaction and it was hypothesized that the charge on the carboxyl groups is decreasing the reactivity of the diazonium salt (Figure 4.3).

Attempt	Solvent	pH	Result
1	HCl:NaOH 1:1	8	No coupling
2	HCl:NaOH 1:1	8	No coupling
3	1 x PBS (pH 7.2)	8	No coupling
4	1 x PBS (pH 7.2)	6	No coupling
5	HCl:NaOH 1:1	10	No coupling

Table 4.1. Reaction conditions tested in each attempted coupling of *p*-NH_2-Bn-NOTA with L-tyrosine.

Attempt	Solvent	pH	Result
1	HCl:NaOH 1:1	8	Coupled product
2	HCl:NaOH 1:1	10	Coupled product

Table 4.2. Reaction conditions tested in each attempted coupling of 3-fluoroaniline with L-tyrosine.

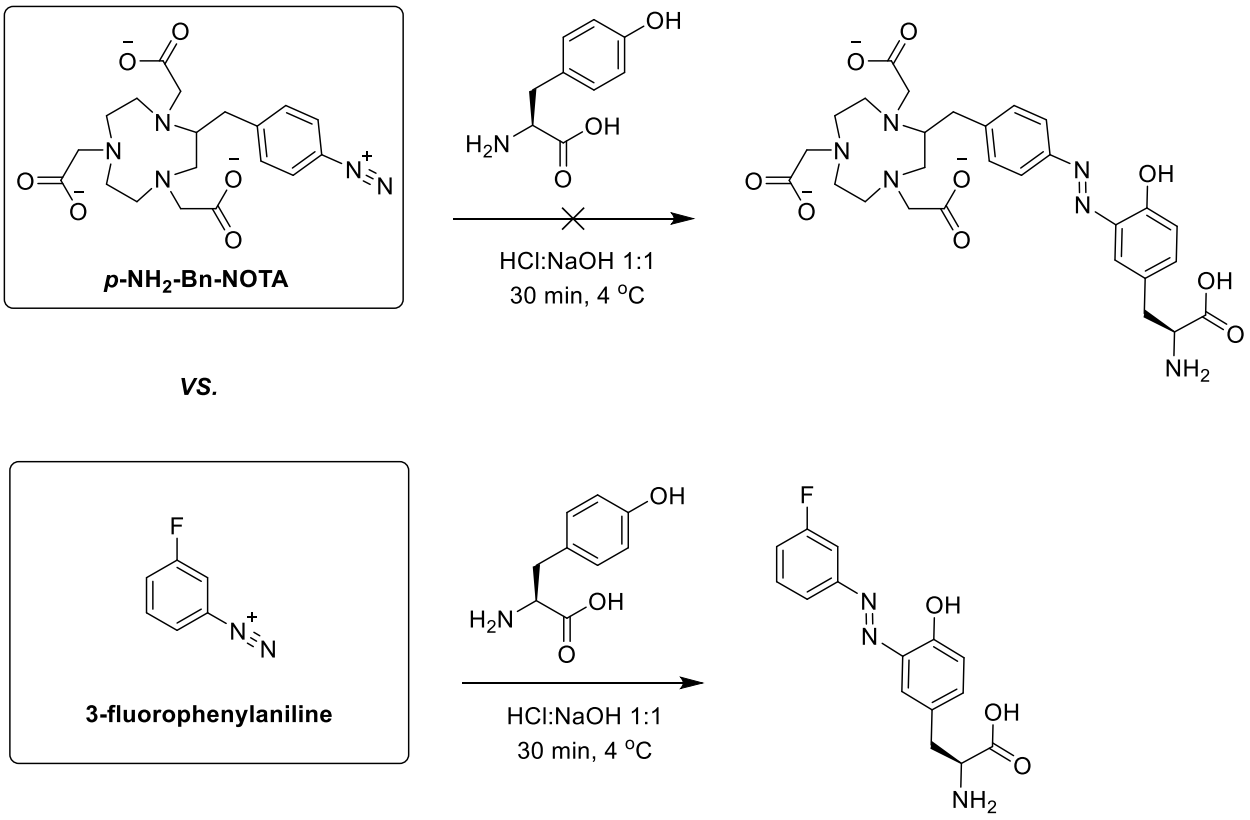

Figure 4.3. Comparison of azo coupling reactions using *p*-NH_2-Bn-NOTA and 3-fluoroaniline starting material.

To test this hypothesis, the pre-labeling approach was implemented for the synthesis of a NOTA-tyrosine conjugate and a NOTA-peptide conjugate. When an initial chelation step was carried out with cold ^{nat}Cu or ^{nat}Ga, thereby reducing or neutralizing the charge on NOTA, coupling with L-tyrosine and neurotensin NT(8-13) was successful and compounds **35**, **36**, **37** and **38** were obtained. The pre-labeling approach also proved successful when applied to radiochemistry. Using compound **35** and compound **36** as cold references, ^{64}Cu- and ^{68}Ga- labeled L-tyrosine was prepared, based on the pre-labeling strategy. The entire synthesis was carried out in under an hour and included three simple steps; pre-labeling with the appropriate radiometal, diazonium salt formation and bioconjugation via azo coupling. No purification was required after the first two steps and only a simple HPLC purification was required after the final bioconjugation step. The final bioconjugation step was carried out under mild, aqueous conditions, making this conjugation strategy applicable to delicate biomolecules, such as proteins. Using compound **37** and compound

38 as cold references, ^{64}Cu- and ^{68}Ga- labeled neurotensin NT(8-13) was also prepared under the same reaction conditions, based on the pre-labeling strategy. Therefore, this pre-labeling approach is key to the use of chelator-containing diazonium salts for introduction of radiometals into tyrosine-containing peptides and proteins.

4.3 The behavior of diazo-conjugates *in vitro* and *in vivo*

Modification of peptides and proteins can affect affinity and receptor binding, which can be problematic when designing targeted tracers or therapeutics. The described bioconjugation technique using radiometal-containing aryl diazonium salts introduces a rather bulky NOTA group which could potentially have a negative impact on receptor binding. To test this, a radiometric competitive binding assay was carried out to determine the IC_{50} values of modified neurotensin NT(8-13) in comparison with unmodified neurotensin NT(8-13). The ^{nat}Cu- and ^{nat}Ga-containing cold reference compounds **37** and **38** were found to have IC_{50} values of 163 pM and 42 pM, respectively. These values are very comparable to that of unmodified neurotensin NT(8-13), which was found to have an IC_{50} value of 33 pM. These results demonstrate that peptide modification did not negatively impact receptor binding, despite the addition of a bulky group. It is also important to note that the introduction of a charged group, ^{nat}Cu-labeled neurotensin NT(8-13) (**37**), did not significantly impact receptor binding (Figure 4.4). Previous attempts in literature to modify neurotensin NT(8-13) included the synthesis of lysine-functionalized and glutamic acid-functionalized monomeric, dimeric and tetrameric peptides [39]. Lysine-functionalized peptides linked at the C-terminus were determined to have IC_{50} values nearly two orders of magnitude greater than that of the unmodified peptide and glutamic acid-functionalized peptides linked at the N-terminus were determined to have IC_{50} values one order of magnitude greater than that of the unmodified peptide, with the exception of the PEGylated tetramer which demonstrated comparable binding kinetics to that of the unmodified peptide. Another attempt to modify neurotensin NT(8-13) included the synthesis of amino-oxyacetic acid-functionalized dimeric and tetrameric peptides where were subsequently labeled with ^{18}F. The dimeric peptide was determined to have an IC_{50} value one order of magnitude greater than that of the unmodified peptide whereas the tetrameric peptide demonstrated comparable binding kinetics to that of the unmodified peptide [40]. Here, the described azo coupling strategy with radiometal-containing aryl diazonium salts resulted in

modified peptides with IC_{50} values comparable to that of the unmodified peptide. It can therefore be concluded that this applied bioconjugation technique is a feasible strategy for the introduction of radiometals into peptides or proteins, without disturbing binding kinetics.

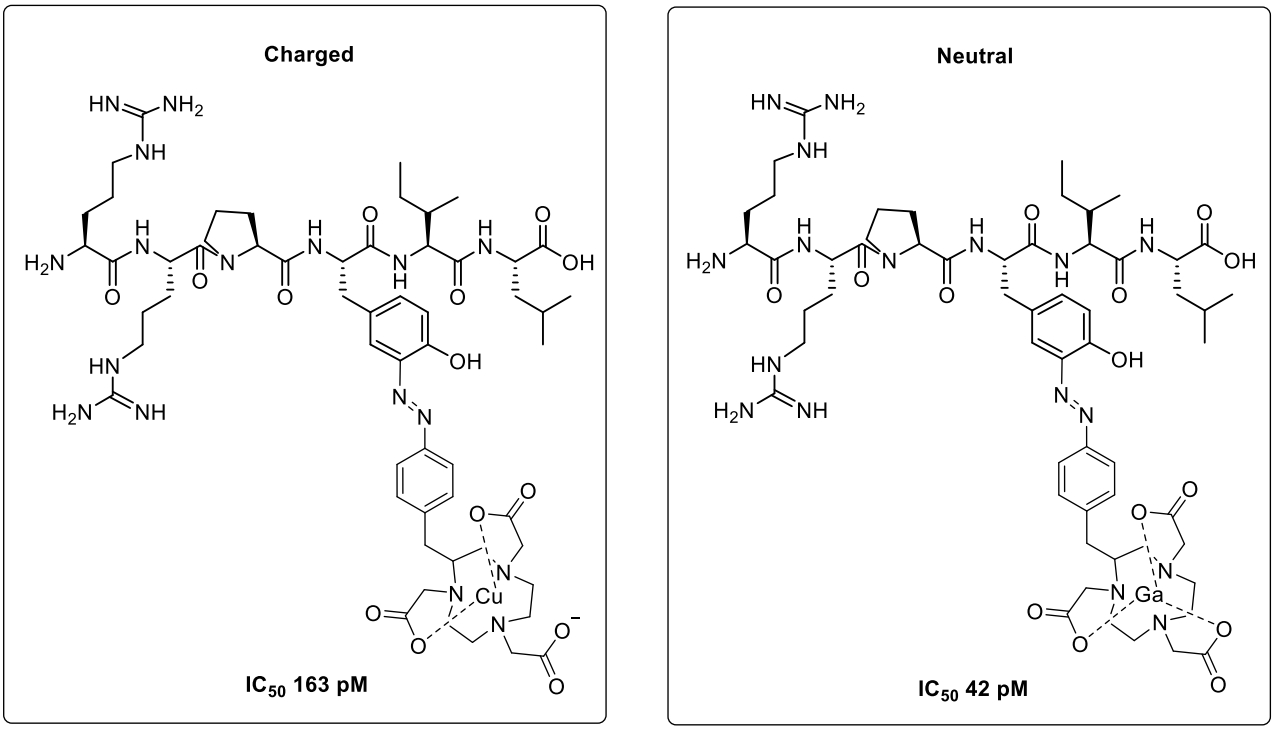

Figure 4.4. Comparison of the effect of charge on receptor binding; charged compound **37** and neutral compound **38**.

With favorable results from *in vitro* binding studies, the *in vivo* behavior and stability of a modified protein was also evaluated. As a well characterized blood pool marker, HSA was used as a model protein for *in vivo* studies. PET imaging of a normal BALB/c mouse injected with 5 MBq of radiochemically pure ^{64}Cu-labeled HSA (**47**) in 200 µL of PBS showed expected biodistribution and metabolic profiles. Significant heart uptake and slow blood pool clearance were observed, characteristic of HSA as a blood pool marker. Primarily liver metabolism was observed, which is characteristic of larger biomolecules. These results are comparable to recent literature, in which RSA and HSA was radiolabeled via lysine or cysteine residues. When ^{18}F-labeled RSA was prepared through conjugation of [^{18}F]2,3,5,6-tetrafluorophenyl 6-fluoronicotinate ([^{18}F]F-Py-TFP) with lysine residues, PET studies showed comparable

biodistribution and metabolic profiles, with the exception of increased muscle uptake and increased kidney metabolism [41]. When ^{64}Cu-labeled HSA was prepared through conjugation of DOTA-NHS ester with lysine or conjugation of DOTA-maleimide with a cysteine residue for post-labeling with ^{64}Cu, PET studies showed comparable biodistribution and metabolic profiles, with the exception of increased kidney metabolism [42]. The favourable *in vivo* profile of ^{64}Cu-labeled HSA, prepared using the described diazonium-based tyrosine labeling method, further demonstrates the feasibility of this strategy for the introduction of radiometals into proteins.

4.4 Diazonium salts: a pH-dependent chemoselectivity for tyrosine?

The chemoselectivity of diazonium salts for tyrosine and histidine has been previously studied [43, 44]. However, attempts to demonstrate the effect of pH on chemoselectivity have provided varying results. Theoretically, histidine which has a pK_a of 6 should be most nucleophilic and therefore most reactive when deprotonated near pH 7 and tyrosine which has a pK_a of 10 should be most reactive near pH 11 [45]. Early studies on the effect of pH on chemoselectivity demonstrated more selectivity for tyrosine at pH 8.5 but increased selectivity for histidine at pH 9.1 and greater [46]. Contrarily, more recent studies demonstrated more selectivity for tyrosine derivatives at pH values ranging from 4 to 10, with a significant increase in selectivity at pH values greater than 7 [47]. The chemoselectivity of radiometal-containing aryl diazonium salts for tyrosine and histidine was investigated over a range of pH values. In a set of 'challenge' style experiment, ^{64}Cu- and ^{68}Ga-labeled diazonium salts in ammonium acetate buffer were reacted with equimolar equivalents of L-tyrosine and L-histidine in borate buffer over a range of pH values (Figure 4.5). The ratio of tyrosine to histidine coupling was determined by HPLC. At pH 7, predominantly ^{64}Cu- and ^{68}Ga-labeled histidine was observed and at pH 8-9, predominantly ^{64}Cu- and ^{68}Ga-labeled tyrosine was observed, specifically 43% tyrosine labeling versus 17% histidine labeling. Interestingly, when sodium acetate buffer was used in place of ammonium acetate buffer only histidine labeling was observed, across all pH values. pH values in the range of 10 or greater were not tested as they are too harsh for protein labeling. A histidine challenge experiment was also carried out using the cold ^{nat}Cu-labeled compound **33** and 64% tyrosine labeling versus 36% histidine labeling was observed at pH 9, which is comparable with the results from the ^{64}Cu and ^{68}Ga experiments. While these results are preliminary and may require further investigation, they

suggest a trend of chemoselectivity for histidine at pH 7 and chemoselectivity for tyrosine at pH 9. Therefore, coupling of radiometal-containing aryl diazonium salts with peptides and proteins should be carried out at pH 9 if tyrosine selectivity is desired.

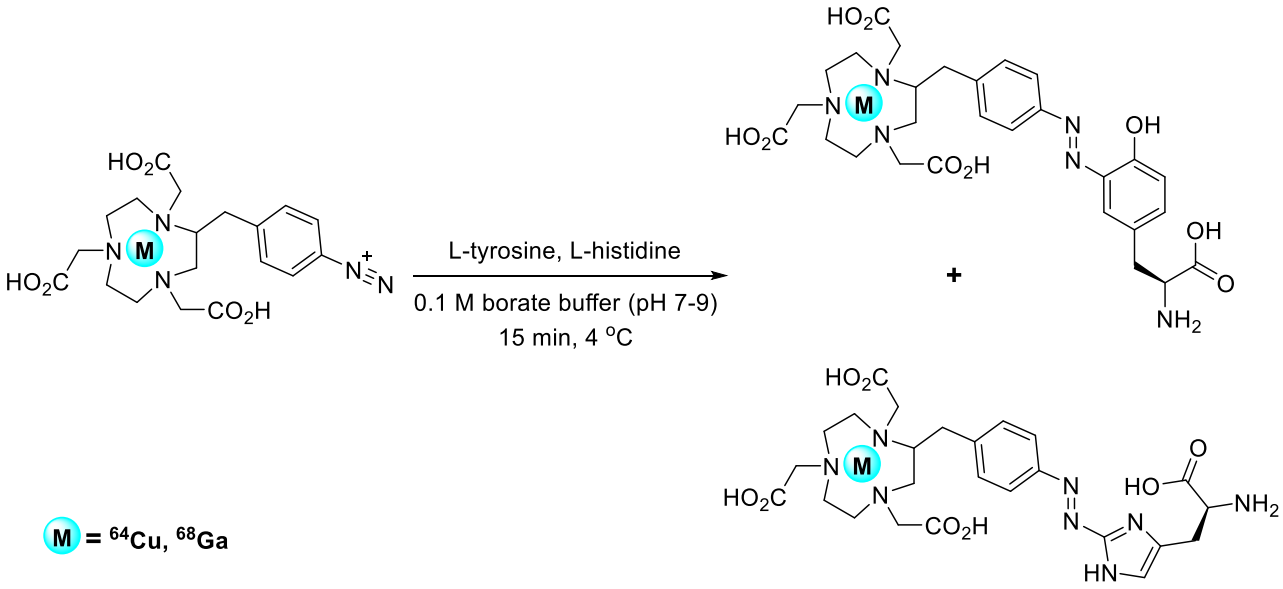

Figure 4.5. Histidine challenge; coupling of ^{64}Cu- and ^{64}Ga-labeled compounds **41** and **42** with L-tyrosine or L-histidine over a range of pH values.

5.0 SUMMARY

This thesis aimed to chemoselectively introduce radionuclides onto tyrosine residues under mild conditions. Bioconjugation techniques that target tyrosine include azo coupling, Mannich-type reactions, tyrosine-click chemistry, Pd-mediated cross-coupling and oxidative coupling (Figure 1.4) [20]. Of these bioconjugation techniques, tyrosine-click chemistry and azo coupling were explored to test the hypothesis that their application to PET radiochemistry would result in the chemoselective bioconjugation of radionuclides with delicate tyrosine-based biomolecules under mild conditions. This hypothesis was verified by:

1) The radiosynthesis of ^{18}F-labeled luminol derivatives followed by tyrosine-click with acetyl-L-tyrosine methyl amide.

2) The preparation of ^{64}Cu- and ^{68}Ga-labeled diazonium salts and their subsequent azo coupling with L-tyrosine, neurotensin NT(8-13), HSA and TMV.

^{18}F-labeled luminol derivative *N*-(4-[^{18}F]fluorobenzyl)-2-methyl-1,4-dioxo-1,2,3,4-tetrahydrophthalazine-6-carboxamide (**29**) was prepared from [^{18}F]fluorobenzylamine (**28**) and an acid chloride starting material. Subsequent oxidation and bioconjugation with acetyl-L-tyrosine methyl amide in a one-pot reaction afforded the expected conjugate in 27% radiochemical yield. Oxidation using hydrogen peroxide as an oxidizing agent in the presence of hemin as a catalyst demonstrated improved oxidation when compared with other oxidizing agents, such as 1,3-dibromo-5,5-dimethylhydantoin, *N*-bromosuccinimide, 1,3,4,6-tetrachloro-3α,6α-diphenyl-glucoluril coated iodination tubes and *N*-chloro-benzenesulfonamide coated iodination beads. Bioconjugation was carried out under mild aqueous conditions and the entire radiosynthesis, including bioconjugation, was carried out within 60 minutes.

^{64}Cu- and ^{68}Ga-labeled diazonium salts were prepared using [^{64}Cu]copper chloride and [^{68}Ga]gallium chloride for chelation with *p*-NH_2-Bn-NOTA, followed by *in situ* diazotization. Bioconjugation of ^{64}Cu-labled compound **41** with L-tyrosine and neurotensin NT(8-13) afforded

the expected conjugates in 56% and 19% radiochemical yield, respectively. Similarly, bioconjugation of ^{68}Ga-labeled compound **42** with L-tyrosine and neurotensin NT(8-13) afforded the expected conjugates in 80% and 45% radiochemical yield, respectively. IC_{50} determination using the corresponding ^{nat}Cu- and ^{nat}Ga-labeled neurotensin NT(8-13) cold reference compounds showed comparable binding affinity to that of the unmodified peptide in neurotensin receptor 1 expressing HT-29 cells, with IC_{50} values in the picomolar range. Moreover, bioconjugation of ^{64}Cu-labled compound **41** with HSA and TMV afforded the expected conjugates in 20% and 9% radiochemical yield, respectively. PET studies carried out using 5 MBq of ^{64}Cu-labled HSA (**47**) showed the expected biodistribution and metabolic profile in a normal BALB/c mouse. In all cases, bioconjugation was carried out under mild aqueous conditions and the entire radiosynthesis, including bioconjugation, was carried out within 60 minutes.

In summary, these results demonstrate the utility of the described luminol-based tyrosine-click chemistry technique and azo coupling technique for application in PET radiochemistry.

6.0 CONCLUSION AND FUTURE WORK

It can be concluded that luminol-based tyrosine-click and azo coupling are both feasible approaches for PET radiochemistry. Radiolabeled luminol derivatives provide a potentially promising strategy for the incorporation of radionuclides into tyrosine-containing compounds but further optimization of the oxidation chemistry may be necessary. Radiometal-containing aryl diazonium salts provide a more promising strategy for the incorporation of radiometals into tyrosine-containing biomolecules. This strategy has been applied on the amino acid, peptide, protein and nanoparticle level and bioconjugation was carried out under mild aqueous conditions within 60 minutes. The applied mild reaction conditions make this strategy compatible with delicate biomolecules and the reasonable time frame of 60 minutes allows application of this strategy to a variety of short-lived positron emitters.

Future work on the luminol-based tyrosine-click approach should focus on further optimization of the oxidation chemistry and the labeling of tyrosine-containing peptides. This approach may also be expanded to include other radionuclides. Future work on the azo coupling approach may include radiolabeling higher molecular weight tyrosine-containing biomolecules, such as antibodies and liposomes.

REFERENCES

[1] Beierwaltes WH. The history of the use of radioactive iodine. Seminars in Nuclear Medicine 1979;9:151-5.

[2] Seidlin SM, Marinelli LD, and Oshry E. Radioactive iodine therapy: effect on functioning metastases of adenocarcinoma of the thyroid. Journal of the American Medical Associaction 1946;132:838-47.

[3] Moore GE, Hunter SW, and Hubbard TB. Clinical and experimental studies of fluorescein dyes with special reference to their use for the diagnosis of central nervous system tumors. Annals of surgery 1949;130:637-42.

[4] Tape GF. Beta-spectra of iodine. Physical Review 1939;56:965-71.

[5] Hamilton JG and Soley MH. Studies in iodine metabolism of the thyroid gland in situ by the use of radio-iodine in normal subjects and in patients with various types of goiter. American Journal of Physiology 1940;131:135-43.

[6] Keston AS, Robert PLL, Frantz KV, and Palmer WW. Storage of radioactive iodine in a metastasis from thyroid carcinoma. Science 1942;95:362-3.

[7] Stöcklin G. Bromine-77 and iodine-123 radiopharmaceuticals. The International Journal of Applied Radiation and Isotopes 1977;28:131-48.

[8] Schwarz SB, Thon N, Nikolajek K, Niyazi M, Tonn J, Belka C, et al. Iodine-125 brachytherapy for brain tumours-a review. Radiation Oncology 2012;7:1-28.

[9] Mundinger F, Ostertag CB, Birg W, and Weigel K. Stereotactic Treatment of Brain Lesions. Stereotactic and Functional Neurosurgery 1980;43:198-204.

[10] Fine J and Seligman A. Traumatic shock. VII. A study of the problem of the “lost plasma” in hemorrhagic, tourniquet, and burn shock by the use of radioactive iodo-plasma protein. Journal of Clinical Investigation 1944;23:720-30.

[11] Hughes Jr WL and Straessle R. Preparation and Properties of Serum and Plasma Proteins. XXIV. Iodination of Human Serum Albumin. Journal of the American Chemical Association 1950;72:452-7.

[12] Crispell KR, Porter B, and Nieset RT. Studies of plasma volume using human serum albumin tagged with radioactive iodine131. Journal of Clinical Investigation 1950;29:513-6.

[13] Yalow RS and Berson SA. Immunoassay of endogenous plasma insulin in man. Journal of Clinical Investigation 1960;39:1157-1175.

[14] Landon J and Moffat AC. The radioimmunoassay of drugs. A review. Analyst 1976;101:225-43.

[15] Cole EL, Stewart MN, Littich R, Hoareau R, and Scott PJH. Radiosyntheses using fluorine-18: the art and science of late stage fluorination. Current Topics in Medicinal Chemistry 2014;14:875-900.

[16] Kuhnast B and Dollé F. The challenge of labeling macromolecules with fluorine-18: Three decades of research. Current Radiopharmaceuticals 2010;3:174-201.

[17] Lattuada L, Barge A, Cravotto G, Giovenzanac GB, and Teid L. The synthesis and application of polyamino polycarboxylic bifunctional chelating agents. Chemical Society Reviews 2011;40:3019-49.

[18] Price EW and Orvig C. Matching chelators to radiometals for radiopharmaceuticals. Chemical Society Reviews 2014;43:260-90.

[19] McKay CS and Finn MG. Click chemistry in complex mixtures: bioorthogonal bioconjugation. Chemistry & biology 2014;21:1075-101.

[20] Trader DJ and Carlson EE. Chemoselective hydroxyl group transformation: an elusive target. Molecular BioSystems 2012;8:2484-93.

[21] Sundberg MW, Meares CF, Goodwin DA, and Diamanti CI. Selective binding of metal ions to macromolecules using bifunctional analogs of EDTA. Journal of medicinal Chemistry 1974;17:1304-7.

[22] Hruby M, Kucka J, Novakova M, Mackova H, and Vetrik M. New coupling strategy for radionuclide labeling of synthetic polymers. Applied Radiation and Isotopes 2010;68:334-9.

[23] Ban H, Gavrilyuk J, and Barbas CF. Tyrosine Bioconjugation through Aqueous Ene-Type Reactions: A Click-Like Reaction for Tyrosine. Journal of the American Chemical Society 2010;132:1523-5.

[24] Ban H, Nagano M, Gavrilyuk J, Hakamata W, Inokuma T, and Barbas CF. Facile and Stabile Linkages through Tyrosine: Bioconjugation Strategies with the Tyrosine-Click Reaction. Bioconjugate Chemistry 2013;24:520-32.

[25] Jessica F, Corentin W, Sylvestre D, Christian L, and André L. Synthesis of [18 F]4-(4-fluorophenyl)-1,2,4-triazole-3,5-dione: an agent for specific radiolabelling of tyrosine. RSC Advances 2013;3:24936-40.

[26] Al-Momani E, Israel I, Buck AK, and Samnick S. Improved synthesis of [18F]FS-PTAD as a new tyrosine-specific prosthetic group for radiofluorination of biomolecules. Applied Radiation and Isotopes 2015;104:136-42.

[27] Khan P, Idrees D, Moxley MA, Corbett JA, Ahmad F, von Figura G, et al. Luminol-Based Chemiluminescent Signals: Clinical and Non-clinical Application and Future Uses. Applied Biochemistry and Biotechnology 2014;173:333-55.

[28] Merenyi G, Lind J and Eriksen T. Luminol chemiluminescence: chemistry, excitation, emitter. Journal of Bioluminescence and Chemiluminescence. 1990;5:53-56.

[29] Sato S, Nakamura K, and Nakamura H. Tyrosine-Specific Chemical Modification with in Situ Hemin-Activated Luminol Derivatives. ACS Chemical Biology 2015;10:2633-40.

[30] Way J and Wuest F. Fully automated synthesis of 4-[18F]fluorobenzylamine based on borohydride/NiCl2 reduction. Nuclear Medicine and Biology 2013;40:430-6.

[31] Keana JFW, Guzikowski AP, Ward DD, Morat C, and Faith LVN. Potent hydrophilic dienophiles. Synthesis and aqueous stability of several 4-aryl-and sulfonated 4-aryl-1, 2, 4-triazoline-3, 5-diones and their immobilization on silica gel. The Journal of Organic Chemistry 1983;48:2654-60.

[32] Zolfigolo M and Mallakpour SE. A Convenient Method for the Oxidation of Urazoles to Their Corresponding Triazolinediones Under Mild and Heterogeneous Conditions with Sodium Nitrite and Oxalic Dihydrate. Synthetic Communications 1999;29:4061-9.

[33] Zolfigol M, Nasr-Isfahani H, Mallakpour S, and Safaiee M. Oxidation of Urazoles with 1,3-Dihalo-5,5-dimethylhydantoin, both in Solution and under Solvent-Free Conditions. Synlett 2005:761-4.

[34] Gleu VK and Pfannstiel K. Über 3-Aminophthalsäure-hydrazid. Journal für praktische Chemie 1936;146:137-50.

[35] Cookson RC, Gilani SSH, and Stevens IDR. 4-Phenyl-1, 2, 4-triazolin-3, 5-dione: a powerful dienophile. Tetrahedron Letters 1962;14:615-8.

[36] Moriarty RM, Prakash I, and Penrnasta R. An improved synthesis of ethyl azodicarboxylate and 1, 2, 4-triazoline-3, 5-diones using hypervalent iodine oxidation. Synthetic Communications 1987;17:409-13.

[37] De Bruycker K, Billiet S, Houck HA, Chattopadhyay S, Winne JM, and Du Prez FE. Triazolinediones as highly enabling synthetic tools. Chemical Reviews 2016;116:3919-74.

[38] Sato S, Nakamura K, and Nakamura H. Horseradish-Peroxidase-Catalyzed Tyrosine Click Reaction. ChemBioChem 2017;18:475-8.

[39] Hultsch C, Pawelke B, Bergmann R, and Wuest F. Synthesis and evaluation of novel multimeric neurotensin(8-13) analogs. Bioorganic & medicinal chemistry 2006;14:5913-20.

[40] Hultsch C, Berndt M, Bergmann R, and Wuest F. Radiolabeling of multimeric neurotensin(8-13) analogs with the short-lived positron emitter fluorine-18. Applied radiation and isotopes :

including data, instrumentation and methods for use in agriculture, industry and medicine 2007;65:818-26.

[41] Basuli F, Li C, Xu B, Williams M, Wong K, Coble VL, et al. Synthesis of fluorine-18 radio-labeled serum albumins for PET blood pool imaging. Nuclear Medicine and Biology 2015;42:219-25.

[42] Kang C, Kim H, Koo H-J, Park J, An G, Choi J, et al. Catabolism of 64Cu and Cy5.5-labeled human serum albumin in a tumor xenograft model. Amino Acids 2016;48:1667-75.

[43] Tracey BM and Shuker DEG. Characterization of Azo Coupling Adducts of Benzenediazonium Ions with Aromatic Amino Acids in Peptides and Proteins. Chemical Research in Toxicology 1997;10:1378-86.

[44] Sheremet'ev SV, Lonshakov DV, Korovkin SA, Belosludtseva EM, Kacelnik AV, Semchenko AV, et al. Synthesis and Pharmacological Properties of Linear Poly (Ethylene Glycol) s Conjugated to Interferon α-2b by Azo Coupling. Pharmaceutical Chemistry Journal 2017;50:788-93.

[45] Jones MW, Mantovani G, Blindauer CA, Ryan SM, Wang X, Brayden DJ, et al. Direct Peptide Bioconjugation/PEGylation at Tyrosine with Linear and Branched Polymeric Diazonium Salts. Journal of the American Chemical Society;134:7406-13.

[46] Paik CH, Eckelman WC, and Reba RC. Reactivity of amino acids in the azo coupling reaction: I. Dependence of their reactivity on pH. Bioorganic Chemistry 1979;8:25-34.

[47] Curreli N, Oliva S, Rescigno A, Rinaldi AC, Sollai F, and Sanjust E. Novel diazonium-functionalized support for immobilization experiments. Journal of Applied Polymer Science 1997;66:1433-8.

APPENDIX

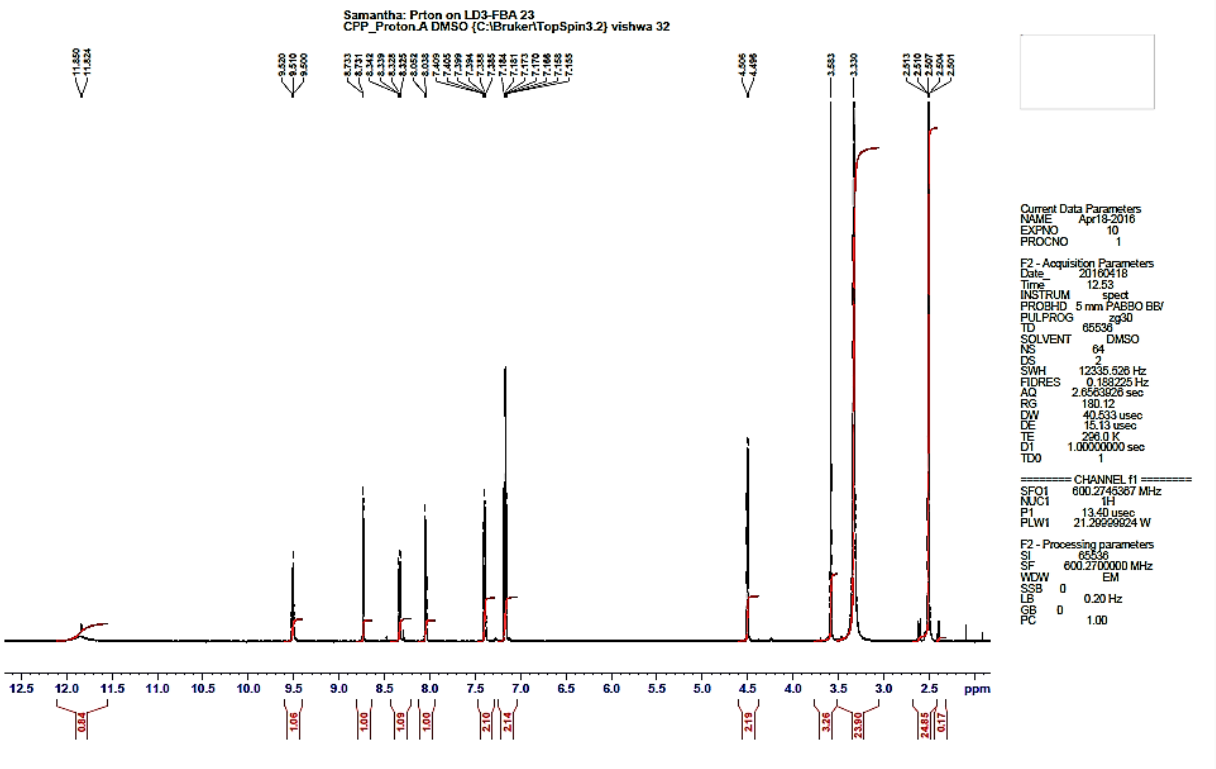

^{1}H NMR of cold reference compound *N*-(4-fluorobenzyl)-2-methyl-1,4-dioxo-1,2,3,4-tetrahydrophthalazine-6-carboxamide (**23**).

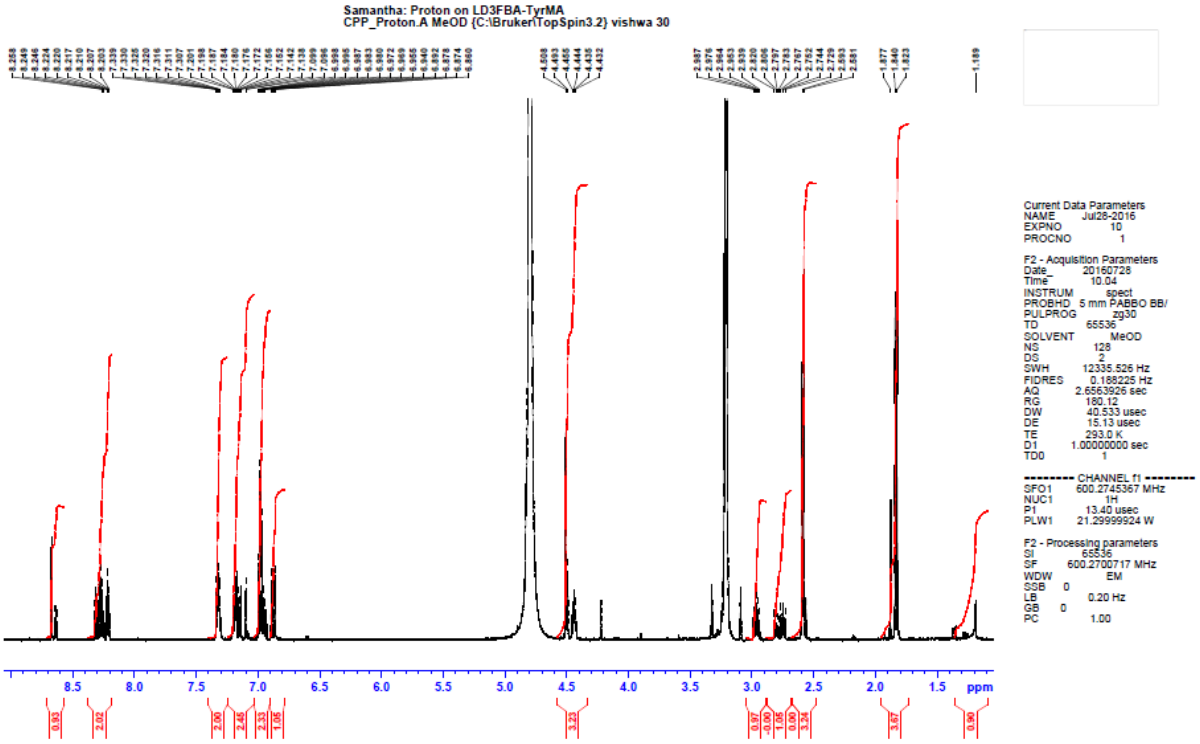

^{1}H NMR of cold reference compound **29** clicked with acetyl-L-tyrosine methyl amide (**30**).

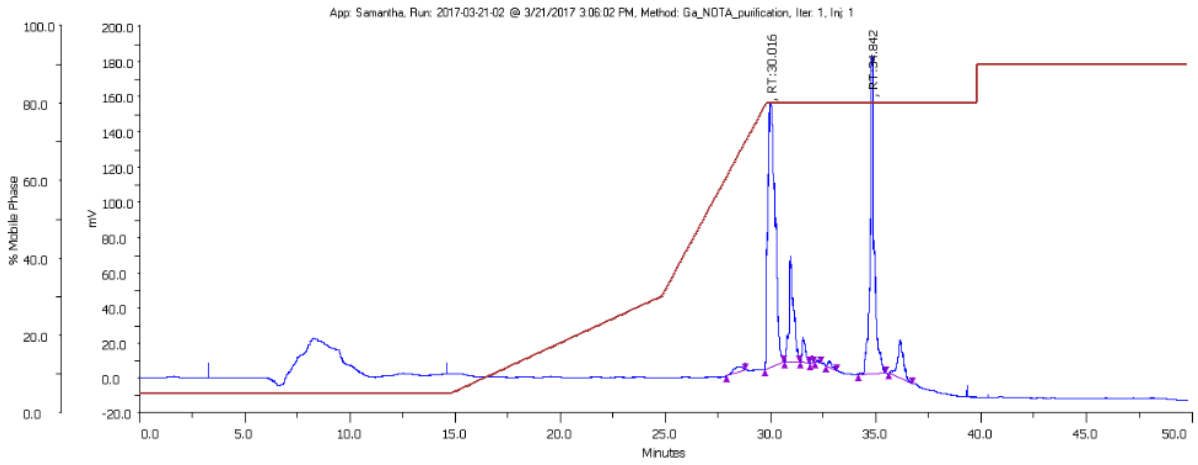

HPLC trace of histidine challenge experiment with cold ^{nat}Cu-labeled diazonium salt and equimolar equivalents of L-tyrosine and L-histidine at pH 9; ^{nat}Cu-labeled L-histidine (retention time 30 minutes) and ^{nat}Cu-labeled L-tyrosine (retention time 35 minutes).

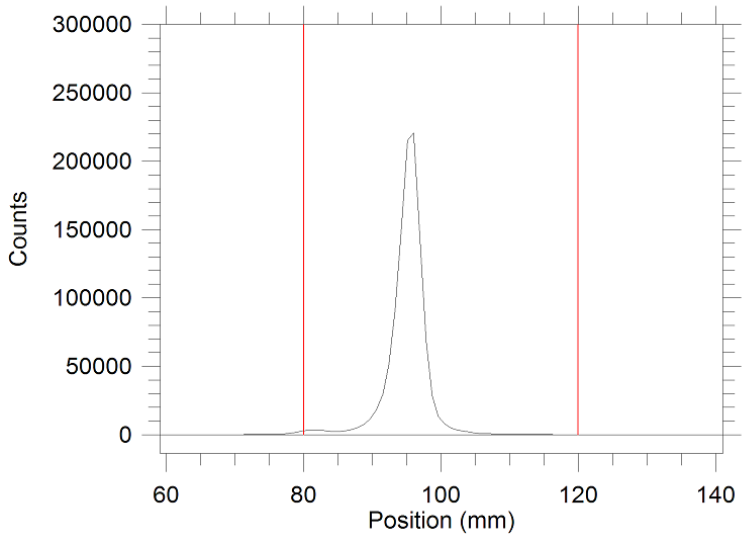

Radio-TLC analysis of ^{64}Cu-labeled *p*-NH_2-Bn-NOTA chelate (**39**); reverse phase TLC plate and a 10% 1 M ammonium acetate in methanol solvent system.

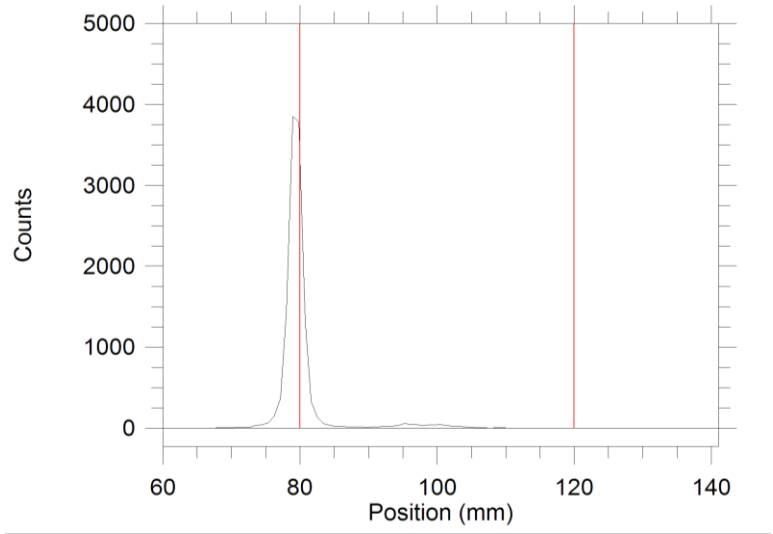

Radio-TLC analysis of ^{64}Cu-labeled HSA (**47**); reverse phase TLC plate and a 10% 1 M ammonium acetate in methanol solvent system.